TOBB UNIVERSITY OF ECONOMICS AND TECHNOLOGY GRADUATE SCHOOL OF NATURAL AND APPLIED SCIENCES

A SUSTAINABLE LIGHTWEIGHT MASONRY UNIT: A BIOPLASTIC, BIODEGRADABLE, MODULAR PROPOSAL WITH INTERLOCKING QUALITIES

MASTER OF SCIENCE IN ARCHITECTURE

Erdem BAZ

Department of Architecture

Supervisor: Assoc. Prof. Dr. Elif MIHÇIOĞLU

08.2023

DECLARATION OF THESIS

I hereby declare that all information in this document has been obtained and presented in accordance with academic rules and ethical conduct. I also declare that, as required by these rules and conduct, I have fully cited and referenced all material and results that are not original to this work. Also, this document has been prepared following the thesis writing rules of TOBB ETU Graduate School of Natural and Applied Sciences.

Erdem BAZ

ABSTRACT

Master of Science in Architecture

A SUSTAINABLE LIGHTWEIGHT MASONRY UNIT:
A BIOPLASTIC, BIODEGRADABLE, MODULAR PROPOSAL
WITH INTERLOCKING QUALITIES

Erdem BAZ

TOBB University of Economics and Technology
Institute of Natural and Applied Sciences
Graduate Program in Architecture

Supervisor: Assoc. Prof. Dr. Elif MIHÇIOĞLU
Co-supervisor: Doç. Dr. M. Recep GÖRGÜLÜARSLAN

Date: August 3rd, 2023

After the study of the materials widely used in the construction industry and the development of sustainability, the examination of existing materials in terms of sustainability revealed the necessity of a sustainable alternative. In this context, it is aimed to present an alternative lightweight masonry unit that aims to make a significant contribution to waste reduction and energy efficiency in the construction field, that is recyclable and completely biodegradable, offering a completely innovative design and a new material.

The raw materials of both aerated concrete and tuff-based construction blocks are cement-based and not suitable for recycling. The debris accumulated after the demolition of the structures built with these lightweight masonry blocks is transported to places away from the habited areas and stored there. This situation creates significant environmental health problems in the long run. Since the cement is used as an additive in such wastes and the materials are not suitable

for recycling, their dissolution time in the environment is quite long. Similar to demolition processes, the production processes of existing aerated concrete and standard lightweight masonry units do not have an environmentally friendly and/or positive aspect in terms of waste reduction and sustainability.

The alternative lightweight masonry unit, in other terms ‘construction block’, is the subject of this interdisciplinary study, and provides significant contributions to the environment in terms of both production and post-dissolution processes, waste reduction, and sustainability. When aerated concrete and tuff-based construction blocks are examined, it is known that these products produce some harmful substances such as aluminum, silicate, and radon gas. This situation carries significant risks for both human health and the environment.

Within the scope of this study, the alternative construction block developed as a solution to these problems is obtained from bioplastic raw materials that are completely biodegradable. Bioplastics are completely environment-friendly and sustainable raw materials that are produced because of the recycling of starch and cellulose-based wastes. Another important feature of the developed construction block is its original design. The developed block is not monolithic like aerated concrete and other construction blocks. It has a completely modular and self-interlocking, clamping system and a design that allows horizontal and vertical installation transitions. The developed construction block provides significant advantages in terms of transportation and storage space, as it is lighter than the existing ones and occupies less space as it consists of six separate modular parts. The modular individual parts can be stacked and therefore create small volumes, thus significantly reducing transportation and storage costs compared to others. Compared to the construction blocks in current use which occupy the same volume logistically, an average of 4 times more area can be built with the developed alternative product, and while a standard construction block of the same dimensions is approximately 8 kg and an aerated concrete is about 5 kg, the proposed bioplastic alternative construction block is about 3 kg.

During the product development process, simulations were carried out with dead loads, live loads, and earthquake loads on it, using the NX software, which offers simulation opportunities. In addition, lignocellulosic materials and graphene oxide are used as

strength-increasing additives to find the right additives and the best combination to provide sustainability and the strongest and lightest biodegradable prototype. The experiments carried out with the construction offer advantages in many ways compared to the existing alternatives widely used in the construction industry and developed as eco-friendly, proving that it provides the same average strength values as the widely used current blocks.

Keywords: Lightweight masonry units, sustainable construction technology, biodegradability, modularity, interlocking system.

ÖZET

Mimarlık Yüksek Lisans Tezi

SÜRDÜRÜLEBİLİRBİR YAPI MALZEMESİ BLOĞU:
BİYOPLASTİKTEN, BİYOLOJİK OLARAK BOZUNABİLİR, MODÜLER,
KENET SİSTEMLİ BİR ÖNERİ

Erdem BAZ

TOBB Ekonomi ve Teknoloji Üniversitesi
Fen Bilimleri Enstitüsü
Mimarlık Anabilim Dalı
Mimarlık Yüksek Lisans Programı

Danışman: Doç. Dr. Elif MIHÇIOĞLU
İkinci Danışman: Doç. Dr. M. Recep GÖRGÜLÜARSLAN

Tarih: 3 Ağustos 2023

İnşaat sektöründe yaygın olarak kullanılan malzemeler ve sürdürülebilirliğin gelişimi üzerine yapılan araştırma sonrasında, mevcut malzemelerin sürdürülebilirlik açısından incelenmesi, sürdürülebilir bir alternatifin gerekliliğini ortaya koymuştur. Bu kapsamda, yapı blokları alanında atık azaltma ve enerji verimliliği konularına önemli bir katkı sağlamayı hedefleyen, geri dönüşümlü ve doğada tamamen çözünebilen, tamamen yenilikçi tasarım ve malzeme önerisi sunan bir alternatif yapı bloğu ortaya koymak hedeflenmiştir.

Hem gazbeton hem de tüf bazlı yapı malzemesi bloklarının hammaddeleri çimento bazlı olup geri dönüşüme uygun değildir. Bu bloklarla inşa edilen yapıların yıkımından sonra oluşan enkazlar uzak yerlere taşınarak buralarda depolanmaktadır. Bu durum, uzun vadede çevre sağlığı için önemli sorunlar yaratmaktadır. Bu tür atıklarda katkı maddesi olarak çimento kullanılması ve malzemelerin geri dönüşüme uygun olmaması

nedeniyle çevrede çözünme süreleri gibi oldukça uzundur. Yıkım süreçlerine benzer şekilde, mevcut gazbeton ve standart yapı bloklarının üretim süreçlerinin de atık azaltımı ve sürdürülebilirlik konularında çevreye duyarlı ve/veya olumlu yönü bulunmamaktadır.

Bu disiplinlerarası çalışmaya konu olan alternatif yapı malzemesi bloğunun hem üretim hem de yıkım sonrası süreci, atık azaltımı ve sürdürülebilirlik konularında çevreye önemli katkılar sunmaktadır. Gazbeton ve tüf bazlı yapı malzemesi blokları incelendiğinde, bu ürünlerin alüminyum, silikat ve radon gazı gibi bazı zararlı maddeler ortaya çıkardıkları bilinmektedir. Bu durum, gerek insan sağlığı, gerekse de çevre için önemli riskler taşımaktadır.

Yapılan çalışma kapsamında, bu sorunlara çözüm niteliğinde geliştirilen alternatif yapı bloğu tamamen doğada çözünebilen biyoplastik hammaddeden elde edilmektedir. Biyoplastikler özellikle nişasta ve selüloz bazlı atıkların geri dönüştürülerek kullanılması sonucunda ortaya çıkan tamamen çevreci ve sürdürülebilir hammaddelerdir. Geliştirilen yapı bloğunun bir diğer önemli özelliği özgün tasarımıdır. Geliştirilen blok, gazbeton ve diğer yapı malzeme blokları gibi yekpare değildir. Tamamen modüler ve kendi içinde birbirine geçmeli, kenet sistemli ve içinde yatay ve düşey tesisat geçişine olanak tanıyan bir tasarıma sahiptir. Geliştirilen yapı malzeme bloğu, mevcut alternatiflerinden daha hafif olması ve modüler altı ayrı parçadan oluşması nedeniyle az yer kapladığı için taşıma ve depolama alanı açısından önemli avantajlar sağlamaktadır. Modüler ayrı parçalar üst üste paketlenebilmekte ve bu nedenle küçük hacimler oluşturmakta, dolayısıyla nakliye ve depolama maliyetlerini diğerleriyle kıyaslandığında önemli ölçüde düşürmektedir. Lojistik olarak aynı hacim kaplayan genel kullanımdaki yapı malzemesi bloklarına göre, geliştirilen alternatif ürünle ortalama 4 kat daha fazla alan inşa edilebilmektedir ve aynı ölçülerdeki bir standart yapı malzemesi bloğu ortalama 8 kg ve bir gazbeton yaklaşık 5 kg iken, önerilen biyoplastik alternatif yapı bloğu yaklaşık 3 kg'dır.

Ürün geliştirme sürecinde, simülasyon imkânı sunan NX yazılımı kullanılarak, üzerine binen sabit ve hareketli yükler ile simülasyonlar yapılmıştır. Ayrıca, sürdürülebilirlik ve biyolojik olarak doğada çözünebilir en güçlü ve en hafif prototipi sağlayacak en doğru katkı malzemeleri ile en iyi bileşimi bulmak amacıyla, mukavemet artırıcı katkı maddesi olarak lignoselülozik maddeler ve grafenoxide kullanılmaktadır. Yapı inşaat sektöründe yaygın olarak kullanılan mevcut alternatiflerine kıyasla pek çok yönden avantajlar sunan ve çevre dostu olarak geliştirilen yapı malzemesi bloğu ile

gerçekleştirilen deneyler, diğer bloklarla ortalama aynı mukavemet değerlerini sağladığını kanıtlamaktadır.

Anahtar Kelimeler: İnşaat blokları, sürdürülebilir inşaat teknolojisi, biyolojik olarak parçalanabilirlik, modülerlik, birbirine geçmeli sistem.

ACKNOWLEDGEMENTS

I would like to express my deepest appreciation to my supervisor Assoc. Prof. Dr. Elif Mıhçıoğlu who guided me with her continuous encouragement and contributions throughout my studies, for her patience, knowledge, and her kindness. Then, I would like to extend my sincere gratitude to my co-supervisor Assoc. Prof. Dr. M. Recep Görgülüarslan for his valuable contributions to my thesis. I am also deeply indebted to my thesis committee for their invaluable comments and contributions, as well as to the faculty of TOBB ETU Department of Architecture, who shared their valuable knowledge and experience that I have highly benefited from during my graduate studies. Last but not least, I am extremely grateful to my family and my friends who have always stood by me with their support.

CONTENT

LIST OF FIGURES

Page

LIST OF TABLES

Page

ABBREVIATION

AAC: Aerated Autoclaved Concrete
SPB: Standard Pumice Blocks

INTRODUCTION

1.1 Sustainability and Green Technology Products

Green technology is a technology, that aims all technological devices, systems, and products to be sustainable and eco-friendly, reducing the carbon footprint and pollution all over the world. By implying the need for technology, human beings can live together without providing threats to each other. Sustainability is a requirement for a valid green technology. It must be valid and alive without giving hazardous impacts on the world, for the whole future (Özdemir & Özkan, 2021). If a system or product meets those requirements, then it can be called a green technology product.

Sustainability and elaboration of green technology have arisen due to recent additional requirements and a new understanding of developing technology. The occasion to produce nature-friendly products and metallurgical exploration has been carried out in numerous sectors. As a result of these studies, high-strength, long-life products are manufactured. Occasions to produce durable and more functional products have raised and begun to be used in areas where it is demanded. According to their technology, nanotechnological and compounded materials are started to be used. New-generation products have also contributed a great deal to energy and time savings in the area they are used (Drazal et al., 2022). New investments are made every day and new goods are produced with this aim. In this environment, those products reduce energy consumption, they are durable, easier to shape, of better quality, and high-functioned. Incorporating digital outfits into those products and outfits used in the defense industry became more practical to use. The defense industry mostly uses these sustainable products for uniforms because of new studies in cloth technology, becoming more combustible, leakproof, and heat resistant. Fabrics with minimum transfer and their use in affiliated sectors have increased. The machine industry also uses sustainable products for almost every sector where machine parkour is required for manufacturing processes (Özdemir & Özkan, 2021). Like other sectors which have mentioned above

in the construction industry, in line with the requirements arising in the product rouse of structures, new products have been used and developed every day.

1.2 Concepts of Renewable Energy and Waste Reduction in the Construction Industry

Blocks of construction, such as pumice blocks and AACs, play a crucial role in the constructed environment. It is essential to evaluate their environmental impact even though they provide structural integrity and durability.

The extraction of concrete block raw materials, such as sand and aggregate, frequently results in habitat devastation and ecosystem degradation. (Mboya et al., 2011)

Grasser and Minke imply that the production of concrete necessitates significant energy consumption, which contributes to greenhouse gas emissions and climate change. The commonly used blocks tend to consume higher energy as mentioned in many researches (Grasser & Minke, 1990). "Because traditional pumice block production necessitates high energy consumption and extensive use of nonrenewable resources, it is imperative to seek out more environmentally friendly alternatives."(Url-1) That is the reason why the hazardous effects are high, additionally this situation results in pollution in the air because of the oscillations of the gasses released from traditional blocks.

The firing of clay bricks emits pollutants into the atmosphere, degrading air quality and contributing to environmental degradation. (Caldas et al., 2021)

For the manufacturing processes, the commonly used bricks release hazardous material not just into the air but also pollute the soil, which results in wide ecological pollution. Grasser and Minke justified that the production of clay bricks at a large scale could lead to land degradation and soil erosion, negatively impacting local ecologies. (Grasser & Minke, 1990)

What are the most sustainable innovations and solutions?

a. "Exploring alternative materials, such as recycled aggregates, fly ash, and geopolymer, shows promise in reducing the environmental impact of construction blocks." (Url-2)

b. "Adopting energy-efficient manufacturing techniques and utilizing renewable energy sources can significantly reduce the production of construction blocks' carbon footprint." (Url-3)

c. "Encouraging the use of locally sourced and ethically extracted raw materials can reduce transportation-related emissions and stimulate regional economies." (Url-3)

Life cycle assessment's significance:

Life cycle assessments (LCA) provide a comprehensive understanding of the environmental impact of construction blocks, enabling informed decision-making for sustainable building practices. It is possible to select environmentally friendly construction materials considering embodied energy, carbon emissions, and end-of-life options through LCAs. (Souza et al., 2016)

In sustainable construction, the environmental impacts of commonly used building materials, such as concrete and clay pavers, are essential considerations. LCAs also play a role in circular economy by helping to identify chances for recycling, reuse, and responsible disposal of construction blocks. (Huarachi et al., 2019)

Although these materials provide structural benefits, their production processes and resource extraction may cause environmental degradation. By adopting innovative alternatives, implementing sustainable practices, and undertaking life cycle assessments, the construction industry can reduce the environmental impact of building blocks, thereby promoting an eco-friendlier built environment.

Due to technology, the future of sustainable construction is promising. Attaining sustainability does not bear the industry to fully annihilate adverse environmental impacts, but element analyzing them to a reasonable level will make life conducive for humans, shops, and creatures. Construction materials have different environmental and potential impacts as listed in Table 1 (Majdalani et al., 2005).

Table 1: Environmental Impacts of Construction Materials (Majdalani et al., 2005)

Environmental impacts	Description	Potential Impacts on		
		Air	Water	Soils and land cover
Extracting raw materials	Sand and gravel	Particulate emissions	Water courses near quarries are altered	Landscape degradation
Manufacturing building materials	Cement production	Particulate emissions CO, Sox and NOx	–	Deposition of dust
Constructing buildings	Transporting materials	NO_x and CO_2 emissions	–	Taking up new areas of land
	Building sites	Noise, particulate emissions	–	–
Using buildings	Energy consumption	CO_2 emissions	–	–
	Water consumption	–	Wastewater discharges containing detergents and organic matter	–
	Wear and tear of materials	Asbestos fibres, indoor radon emissions	–	–
Demolishing buildings		Noise, particulate emissions	–	Demolitions waste to be land filled or reused for sea reclamation

Source: Adapted from *The Environment in France*. French Institute for the Environment (IFEN, 1999).

In this regard, the construction sector in cooperation with cement companies must ultimately replace old systems, like the use of ready-blend concrete with ultramodern practices. These old practices have little regard for environmental safety. Important effort must be given to make sustainability one of the primary aspects, using this emphasis for any construction. Thus, a good place to start would be with the birth of nature-based raw materials (Zabihi et al., 2012). Although builders, concrete suppliers, and masterminds have little influence over the birth of natural reserves, the government can help discourage this exertion by demanding more recycled materials, more mineral reserves, and more effective use of energy.

1.3 Lightweight Masonry Unit Technology

Many different construction materials are used for different parts of a building. However, a building is composed of two main parts; load-bearing and non-load bearing. This thesis study aims to focus on an alternative construction material for the non-load-bearing parts of a building. For these parts of a building, two different types of construction material products are used mostly. The first one is the plate-type products that are produced by wood or cement-based materials. They are plates that have to be applied by some steel, aluminum beams, or chips for durability. The other

type of product for the partition walls is the lightweight masonry units or construction blocks. This thesis study aims to provide an alternative solution for those commonly used construction blocks. With this scope, some comparisons will be made between these commonly used materials and the proposed construction material.

When the commonly used lightweight masonry units are examined, their main raw material is a type of sand with the additional main materials of cement and water. One type that is quite widespread today is the autoclaved aerated concrete (AAC) blocks (Figure 1) which contain the raw materials of quartz, cement, lime, and water. Another type is the pumice-based concrete blocks (Figure 2) also known as BİMS blocks in Turkey with its brand name (Zabihi et al., 2012).

Figure 1: AAC blocks, widely known as Ytong with the brand name (Url-4)

Figure 2: Concrete blocks, known as BİMS with the brand name (Url-5)

The raw materials, of both the AACs and the pumice blocks, are sand based, which is not suitable for recycling. After the demolition of the buildings constructed with these types of lightweight masonry units, debris is carried away to a location far from the habited area and left to the environment hazardously. This debris has no chance to dissolve in the environment, as they are not degradable materials, and materials with cement additives become inappropriate for recycling (Gironi & Piemonte, 2011).

The manufacturing processes of these current lightweight masonry units are not cooperative with nature and do not implement a positive effect on the environment. Positive manufacturing processes decrease pollution in the environment, which also decreases the emission rates, hazardous oscillation of gasses, or the pollution of materials in the environment by using them in the process itself, which results in cleaner environments and can be called 'eco-friendly' or 'eco-supporting' manufacturing process. When the manufacturing processes of lightweight concrete and pumice lightweight masonry units are examined, there are no significant environmentally positive aspects. On the contrary, they expose aluminum, silicate, and radon in the manufacturing process of the AACs, which are highly harmful to the

human respiratory system and damage the lungs severely, causing cancer (Sofiah et al., 2018).

The common lightweight masonry units' dimensions vary, but mostly used dimensions are 20 cm by 40 cm by 20 cm. With these dimensions, there are about 12 units in 1 sqm and the capacity of a truck is about 100 m3. It can be said that a 9 sqm wall can be built with the capacity of one full truck. Pumice-based concrete block weighs about 8 kg and AAC block weighs about 5 kg (depending on the density of the pumice-based concrete block is 500 kg/m3, AAC is 350 kg/ m3) (Amri, Ekawati, et al., 2018). A truck with a volume of 1.4 m3, weighs about 700 kg when full of pumice-based concrete blocks and weighs about 400 kg when full of AAC blocks.

1.4 Problem Statement

The main problems in the construction industry can be collected under two topics. The first one is sustainability and being environmentally friendly. The second one is the design problem which also includes weight and logistic issues.

Today, construction materials that are used at inner and outer walls for separation are mainly pumice blocks and aerated autoclaved concretes. Either of them is not sustainable or eco-friendly, and on the contrary, they have many hazardous effects. Sometimes standard construction blocks are used for load-bearing parts of the building. (Smyrou, 2016) On the other hand, the proposed construction block developed through this study is necessary to be used in partition walls, but not in a load-bearing wall.

Another problem is the design of the commonly used construction blocks and their quite heavy weights. Both pumice blocks and AAC blocks are rigid blocks that can be carried by their fixed forms after their manufacturing processes. The fixed forms of these masonry units cause many problems due to their size and heavy weight. This causes difficulty in logistics, as well as health-threatening problems in disasters, in case they fall from a height on people, the weight issue gets more dramatic and hazardous.

1.5 The Objective of the Study and Hypothesis

The objective of this study is to search for and develop a sustainable alternative to commonly used lightweight masonry units. To achieve this, the proposed alternative should meet the following requirements:

1) It should be environmentally friendly, and made of recycled biodegradable materials, thus being safer for health.

2) It should be providing a much smaller storage volume, resulting in financial advantage as storage areas bring remarkable expenses today.

3) Its weight should be approximately half of the standard blocks with the same dimensions to be advantageous.

4) It should be designed in a modular way with interlocking qualities that are also industry-applicable, providing advantages in transportation as well as in the site.

The lightweight masonry unit proposal is planned to be produced from entirely biodegradable bioplastic material, reducing pollution as obtained from waste. Bioplastics are plastics derived from renewable biomass sources such as vegetable oil sand fats, cornstarch, straw bale, woodchips, and food scraps. Bioplastic can also be obtained from agricultural by-products, as well as from used plastic bottles and microorganisms. In addition, compared to aerated concrete, it is almost half as light (Amri, Ekawati, et al., 2018). For this reason, it provides clear advantages in disasters (Yılmaz & Bakış, 2015). In addition, this product offers sustainability and fills a gap in the construction industry where sustainability has great importance (Sofiah et al., 2018).

The proposed lightweight masonry unit is specifically planned to use starch and cellulose-based bioplastics.

The type of raw material additive for strengthening the proposed lightweight masonry unit will be examined and tested as a hypothesis of this study. To find the best additive, firstly, graphene oxide will be examined as it is found to strengthen the bioplastics

remarkably depending on literature research. Hence, the other aspects will be also examined like the application and economic issues to understand if it is feasible or not.

Secondly, lignocellulose will be examined as a more recent additive material found in the literature. It is a material derived from organic materials such as plants. The application and derivation issues will be examined elaborately.

1.6 Methodology and Content of the Study

After a literature survey on sustainability, green technology, renewable energy, waste reduction in the construction industry, and lightweight masonry unit technology, the problem statement, the objective of the study, hypotheses, methodology, and content of the study are defined.

In this thesis, both qualitative and quantitative research methods are used. In the sequential phases of analysis, evaluation, and conclusion, an analysis of the commonly used lightweight masonry units are made. Then, a sustainable alternative is searched, proposed, and tested digitally through simulations in comparison to the commonly used lightweight masonry units and newly proposed sustainable alternatives with different additives. Manufacturing a prototype is not practical and efficient because the requirements of many different data have to be checked. The reason why finite element analysis simulations are used is that.

In two analysis parts, the available lightweight masonry units and the proposed product are examined focusing on two aspects as 'design' and 'material' to reach the best possible alternative as the best sustainable, biodegradable, and modular version.

In the evaluation section, the design alternatives and the possible chemical compound options for the bioplastic raw material will be discussed mutually. Depending on this, the manufacturing process, the applicability to the construction industry, and the economic issues will be reviewed.

Consequently, the summary and conclusion parts are included in the final.

1.7 Finite Element Analysis

1.7.1 General Formulation

The finite element analysis method also provides the ability to change data during testing. This is a critical issue as the test prototype must be repeatedly recreated for each part of the test. This is a huge effort and costs for real-world testing. On the other hand, with the finite element method, it is very easy to perform many different tests by simply changing the parameters. Also, in practice, the manufactured prototype may need to be tested for different dimensions, which means that the prototype must be manufactured again and again for each desired dimension. This is also not so practical and feasible.

The finite element analysis method is used for many various engineering problems to be able to make observations without manufacturing a prototype. The finite element is the analysis of a product with high-level software where all the properties are the same in real life and also all conditions in real life are monetized and the analyses have been made under all of those variables similar to real life.

There are many industries and sectors which are using finite element analysis methods, but the most common ones are the construction, aviation, and automotive industries because many times manufacturing prototypes for every single alternative is too expensive and difficult. So, this analysis provides observation for prototype behaviors under many different conditions. This analysis also brings the ease of changing the parameters rapidly however in real life while testing a prototype changing test parameters or conditions, can be very difficult (Url-6).

The aviation industry is one of the remarkable industries which use the finite element analysis method frequently. As seen in Figure 3 a private jet general Falcon 7X finite element analyses have been made (Meyeret al., 2016). This provides the behavior of the load-bearing parts of the aircraft under forces due to the vibrations that the aircraft encounters while flying. For these analyses the boundary conditions are, the body of the flight is not fixed anywhere, but the wings are fixed to the vibrators just from one point each, close to the tires. And finite element analyses have been made by considering the vibrating forces which are encountered by the flight during turbulence.

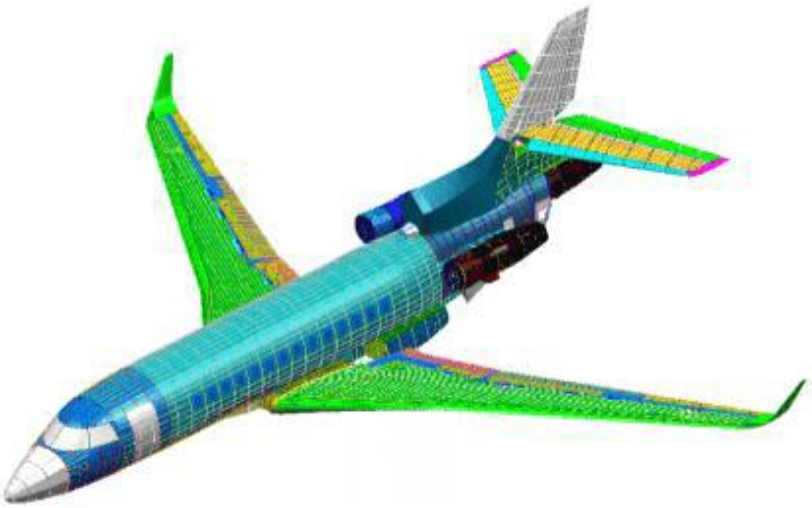

Figure 3A: Finite element model (Meyer et al., 2016)

Figure 3B: Actual aircraft in real life (Meyer et al., 2016)

Finite element analysis is used for simulating different physics such as static analysis to simulate the deformation behavior and identify the stresses of a structure under a static load, vibration analysis to identify natural frequencies of a structure, heat transfer analysis to simulate the temperature change on a structure for a certain heat flux (Reddy, 2019).

Because the deformations and stresses on the construction blocks under certain static loads are of interest in this study, the finite element analysis under static loads is explained in this thesis.

In a finite element analysis, the following six-step procedure is applied (Kattan, 2008, pp. 12-13)

1) **Discretize the domain** which involves subdividing the domain into elements and nodes. For discrete systems, as the system is already discretized, the step is not so important where the answers obtained are exact. On the other hand,

for continuous systems, this step is very crucial where the answers obtained are only approximate. The discretization used determined the accuracy of the solution.

2) **Write the element stiffness matrices** for each element in the domain**.**
3) **Assemble the global stiffness matrix** with a direct stiffness approach.
4) **Apply the boundary conditions** as in supports and applied loads and displacements.
5) **Solve the equations** by partitioning the global stiffness matrix and solve the equations using Gaussian elimination.
6) **Post-process** to obtain additional information possible as the reactions and element forces and stresses.

Static finite element analysis assumes that there is no time-dependent change in the loading applied to a structure. Then, the following equation is solved to simulate the deformation behavior of a structure under applied static loads.

$$\mathbf{F} = \mathbf{KU} \quad (1)$$

Here, **F** is the global nodal force vector, which includes forces applied on each node on the finite element model, and **U** is the global displacement vector which has the displacement values of each node corresponding to the degree of freedom of the used finite element type. The application of the known displacement values on the finite element model is called applying the boundary conditions (BCs) while the application of the known force values on the model is called applying the loading conditions (LCs).

K is called the global stiffness matrix, which defines the linear elastic material properties of each element in the finite element model. **K** is also called the assembly stiffness matrix because it is formed by combining the elemental stiffness matrices k_i (i = 1,2,3,…, e) where e is the total number of finite elements in the finite element model. The number of nodes (n) in the discretized domain and the corresponding degrees of freedom (k) for each node determines the size of the stiffness matrix. For instance, for the linear three-dimensional (3D) tetrahedral solid elements used in this study, there are k=3 degrees of freedom for each node. Hence, the size of **K** is defined as 3nx3n since there are 3 degrees of freedom at each node.

The linear tetrahedral solid element used in this study is a 3D finite element, which is characterized by linear shape functions and linear elastic material properties. The material is assumed to be isotropic (i.e., the deformation behavior is the same in all directions); therefore, this element requires only the modulus of elasticity € and Poisson's ratio (ν). Each tetrahedron element has four nodes as shown in Figure 4 with three degrees of freedom at each node: the displacements in three main directions. Further details of this element type and finite element formulations are skipped for brevity and can be found in Matlab Guide to Finite Elements (Kattan, 2008, pp. 337).

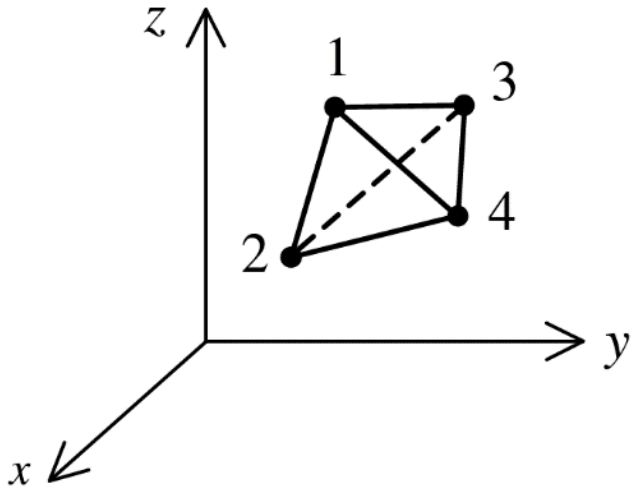

Figure 4: Linear tetrahedral solid element (Kattan, 2008)

Once the finite element model is generated using the chosen element type and all the BCs and LCs are defined, Eq. (1) is solved by partitioning and Gaussian elimination to calculate the unknown displacements and reaction forces.

An example of using linear tetrahedron elements for static finite element analysis is given from the aviation industry where the deformation behavior of an aircraft wing is simulated under lifting forces assumed as static loadings on the wing (Meyer et al., 2016). The linear tetrahedron elements and the displacement results of the static finite element analysis obtained by (Meyer, et al., 2016) are shown in Figure 5. The color bar from blue to red shows the increase of the displacements as a distribution on the model based on the displacements calculated for each node in the model. It is seen that the maximum displacements are obtained on the nodes at the wing tip because the load

is applied at this region while the displacements are zero on the other side because all the degrees of freedom of the nodes on that side are fixed.

For the aviation industry as shown in Figure 5, more specific analysis can be made for some parts of the aircraft. One of the most scientific parts of an airplane is the wings. The wings are the parts that provide the lifting force for airplanes. That is why the analysis of the wings is so important and must be made elaborately. Even for the analysis of the critical parts of an aircraft the finite element analysis method is used. In this test, the boundary condition is that the large part of the wing which is connected to the body of the aircraft is fixed and the upward and downward forces are applied considering the possible forces encountered while landing and taking off.

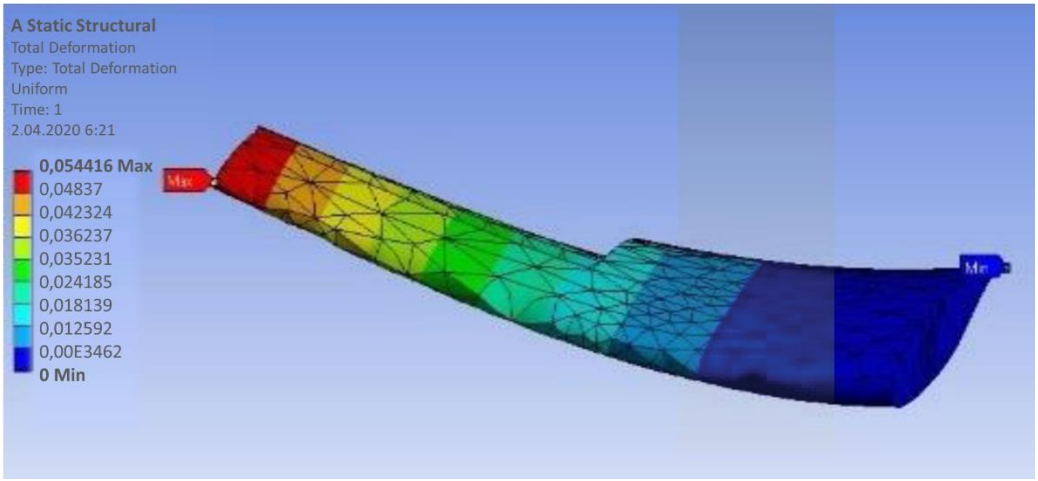

Figure 5: Finite element Analysis of wings of an aircraft (Kaya et al., 2020)

For the construction industry, which is the subject of this thesis, finite element analysis is used to predict the deformation behavior and safety of the building components. For instance, finite element analysis is used widely for bridge constructions (Wu et al., 2018) modeling the entire bridge made of metallic material with individual components as shown in Figure 6. The exact locations for the load-bearing joints were chosen based on the finite element analysis results. The reason for using finite element analysis in the construction industry is that the load-bearing locations of a body are significantly important for strength. The assumptions made during the design for the exact locations of the load-bearing components have to be corrected by the finite element analysis results. Otherwise, the structure will be weak and will lead to many remarkable load-bearing problems.

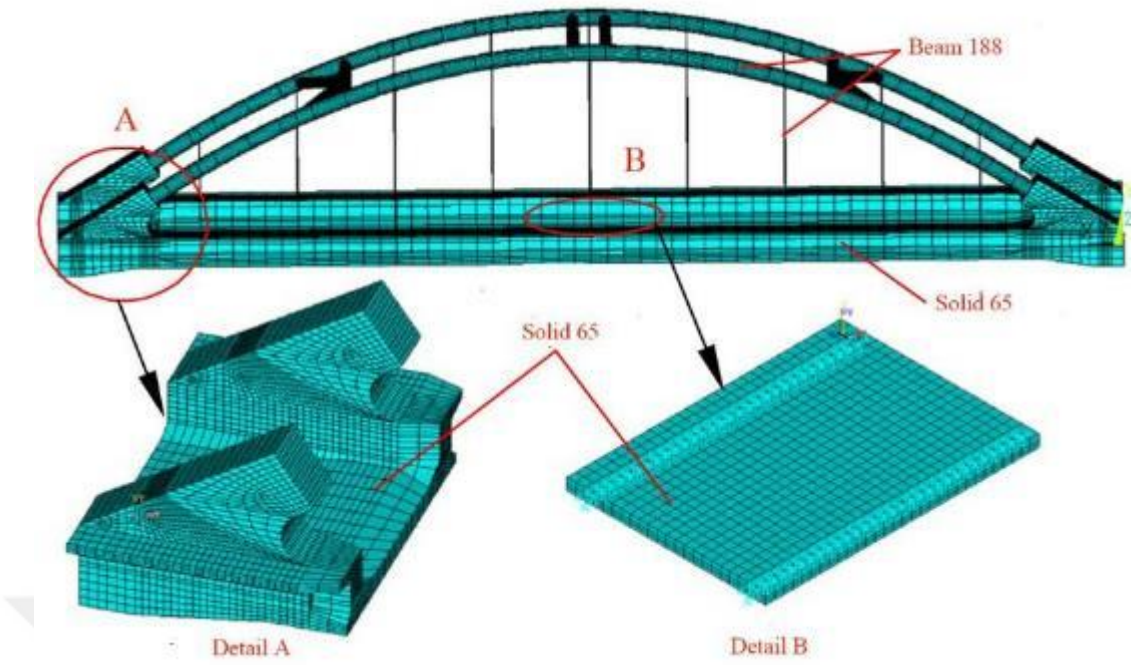

Figure 6: Finite element analysis of parts of a bridge (Wuet al., 2018)

In another example, Zimmermann, (2012) studied the strength of the leg of another bridge from the aspect of different located downward forces because of its shape. In Figure 6, the weak parts of the leg were analyzed if it is adequate for load bearing or if it bends under the load it has to carry. For this purpose, the von Mises stresses are calculated by the finite element analysis at each element based on the calculated reaction forces when Eq. (1) is solved. The von Mises stress, which is also called the equivalent stress, is calculated based on the maximum distortion energy theory. Details of calculating the von Mises stress are skipped for brevity and can be found in (Hibbeler, 2014, pp. 526).

As seen in Figure 7B, a distribution of the von Mises stresses can be obtained from the finite element analysis. Then, the region which has the highest von Mises stress can be determined. In Figure 7B, for instance, the maximum stress values were on the red regions which have sharp transitions of geometry. If the maximum stress values are lower than the yield strength of the material, then the design is assumed to be safe. Otherwise, some design changes should be made to reduce the maximum von Mises stress until it is lower than the yield strength.

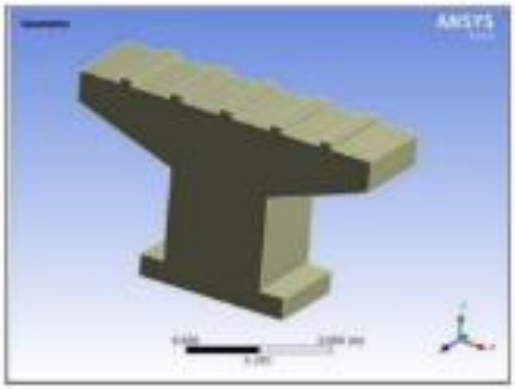

Figure 7A: Finite element analysis of the legs of an arch bridge (Zimmermann, 2012)

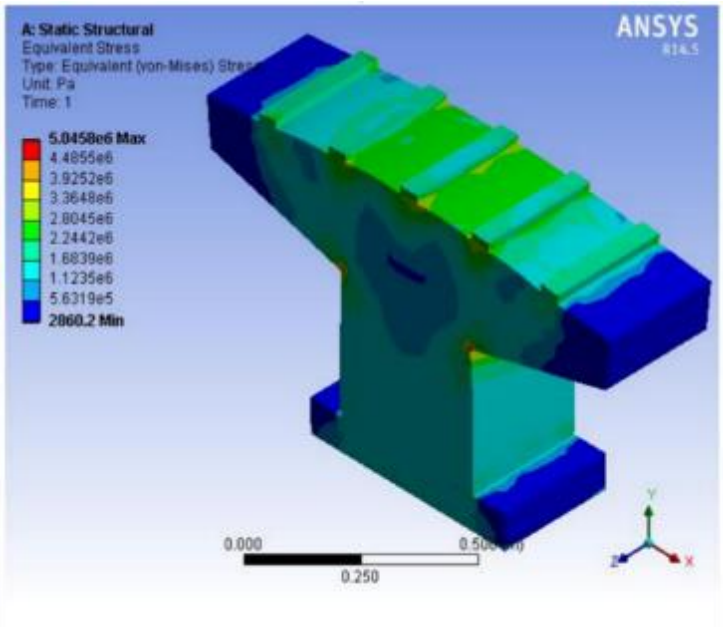

Figure 7B: Finite element analysis of the legs of an arch bridge (Zimmermann, 2012)

In this thesis study, finite element analysis is used to evaluate the performance of the proposed construction block. The finite element analysis has already been used for different construction blocks in the literature. Some examples from the literature with applied boundary and loading conditions and certain assumptions are explained in the following sub-section.

1.7.2 Literature Review for Finite Element Analysis of Construction Blocks

Finite element analysis for the construction industry is also important and especially for the construction blocks finite element analysis is frequently made for predicting the behaviors of the blocks under different conditions, in real life.

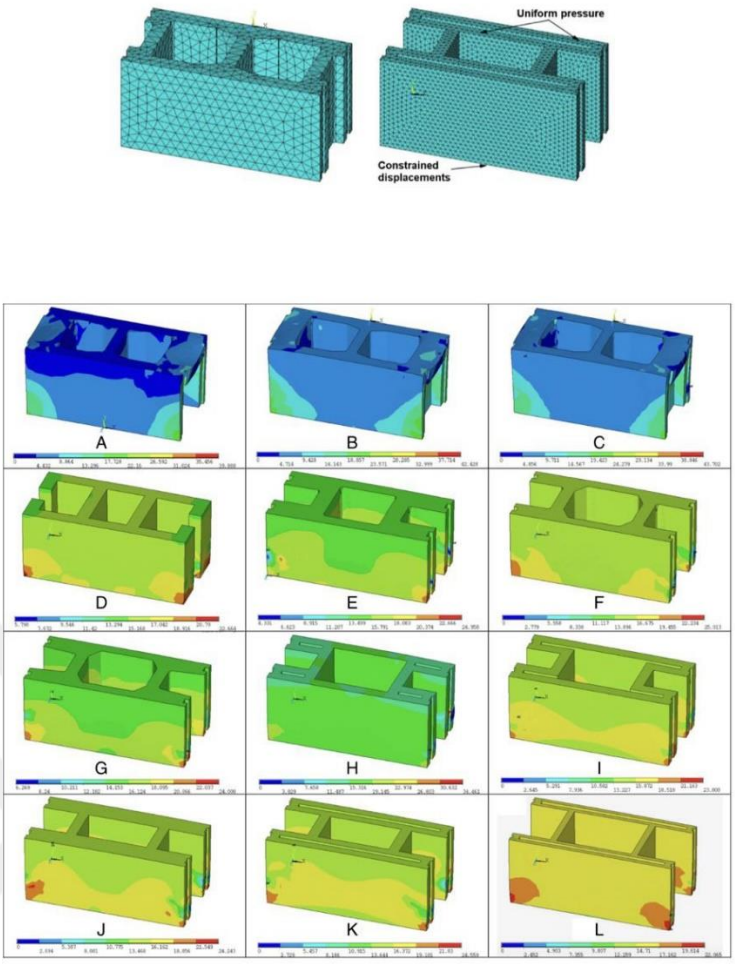

Figure 8: Finite element analysis of different raw material construction blocks (Diaz et al., 2011).

The mesh refinement and finite element analysis has been used by various construction block analysis. Finite element analysis of different materials pumice blocks is implemented in Figure 8. The mechanical properties of the material are defined in the software. In the boundary condition, the block is fixed in all directions for displacement, and 16 MPa pressure is applied from the top for this analysis (Diaz et al., 2011).

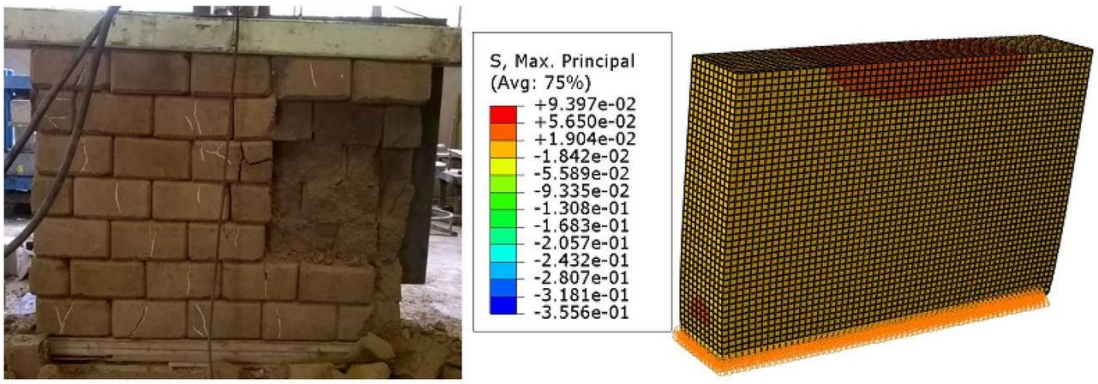

a Failure mode of experimental wall (LSW1) b Maximum principal stress distribution

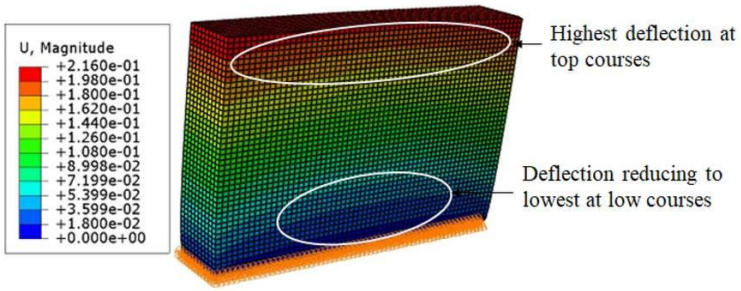

c Finite element wall displacement

Figure 9: Finite element analysis of s stone-based construction block wall (Fundi et al., 2021)

For the finite element analysis of another pumice block shown in Figure 9, the boundary condition is that the bottom surface of the wall is fixed and 0.94 Mpa pressure is applied from upward. The mechanical properties for that pumice block are defined in the finite element analysis software (Fundi et al., 2021).

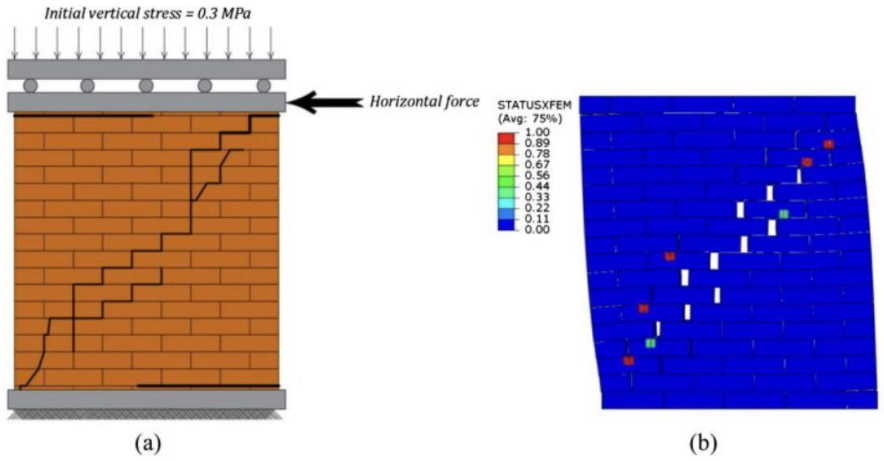

Figure 10: Finite element analysis of another type of construction block (Abdulla et al., 2017)

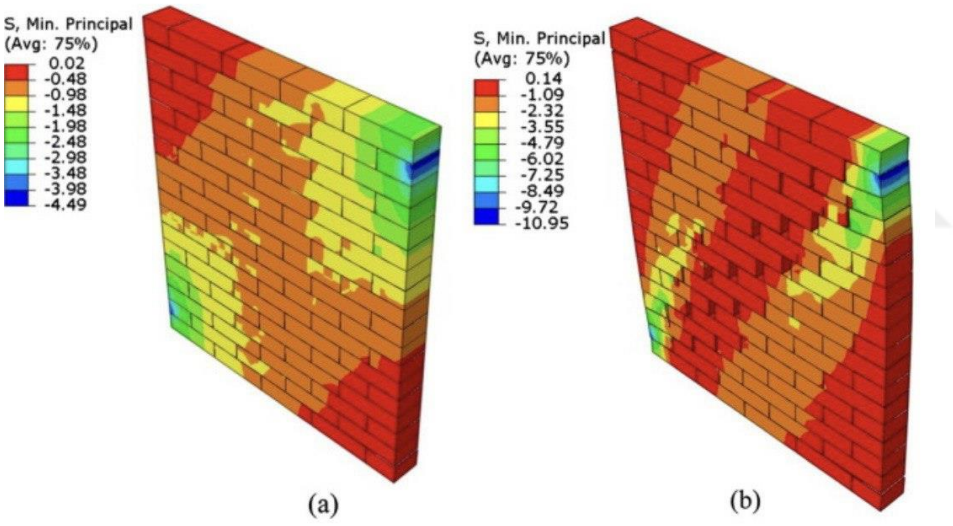

Figure 11: Finite element analysis of a cement-based construction block wall (Abdulla et al., 2017)

In Figures 10 and 11, 0.3 Mpa pressure is applied from upward to the wall generated by pumice blocks. The mechanical properties are defined in the finite element analysis software. The boundary condition is defined, the bottom surface of the wall is fixed, and the results are obtained under those conditions (Abdulla et al., 2017).

Properties	*Concrete Masonry Units*	Cement Mortar
Modulus of Elasticity MPa	7200	1500
Poisson's ratio	0.15	0.2

Table 2: Inelastic properties of mortar

Angle of friction φ	*Flow stress ratio k*	*Dilation angle ψ*
37°	0.8	20°

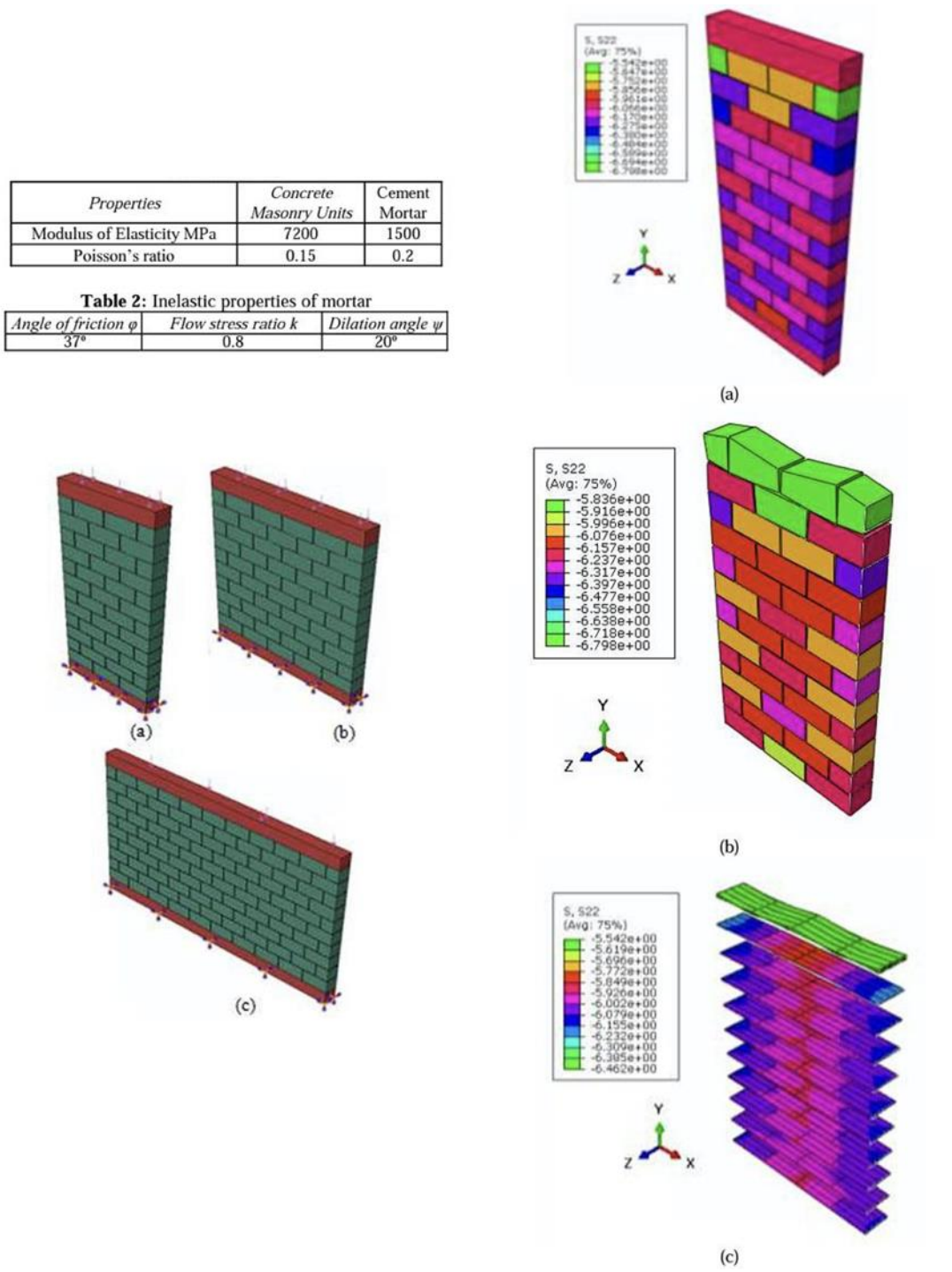

Figure 12: Finite element analysis of another type of stone-based construction block (Zuhairi et al., 2018).

In Figure 12, the finite element analysis of another wall generated by another type of construction block has been made. The bottom surface of the wall is fixed and 6N/mm^2 pressure is applied from upward and the results are obtained and shown above (Zuhairi et al., 2018).

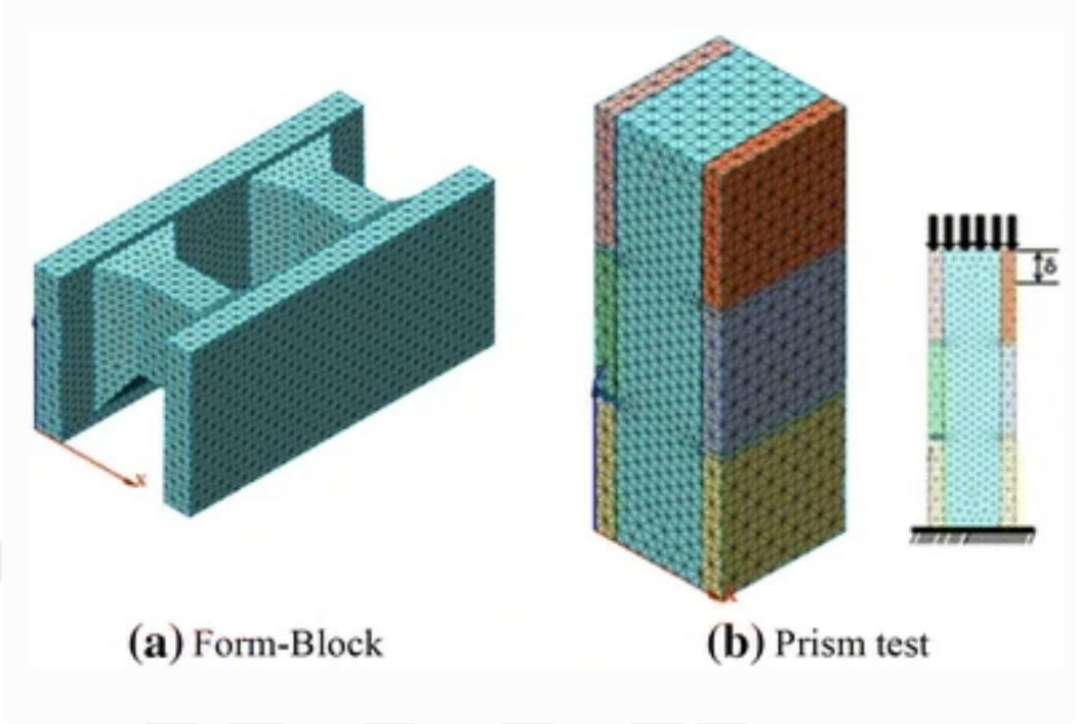

Figure 13: Finite element analysis of another type of construction block with a different design (Seo et al., 2015)

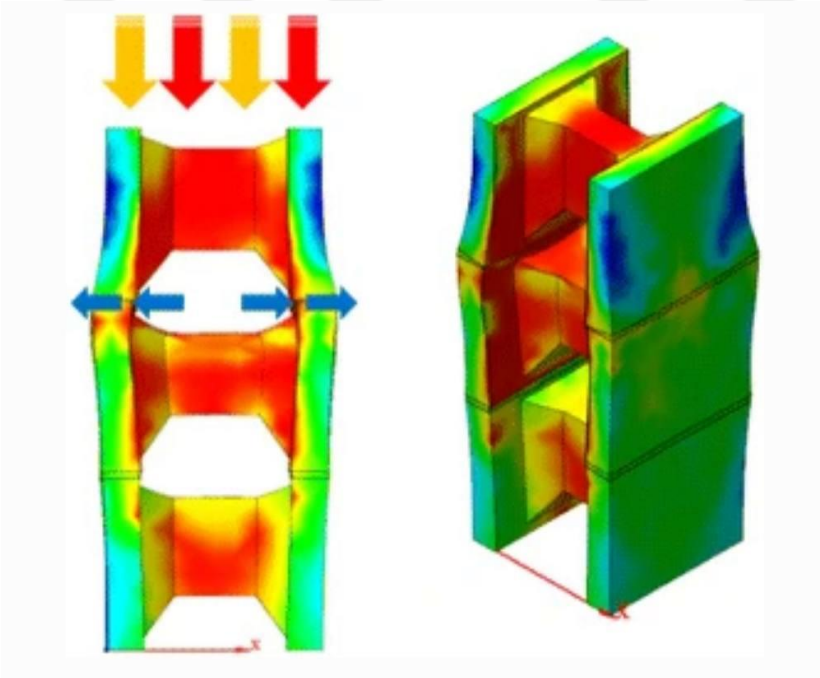

Figure 14: Finite element analysis of another type of construction block with a different design 2(Seo et al., 2015)

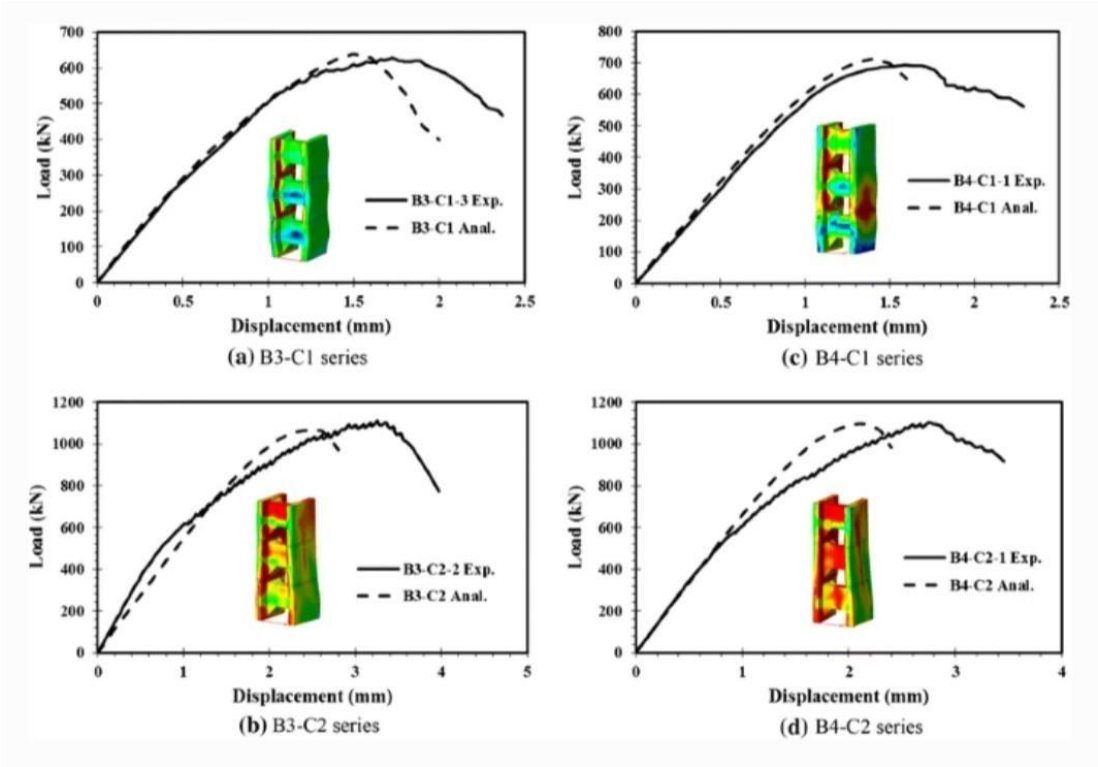

Figure 15: Finite element analysis of another type of construction block with a different design (Seo et al., 2015)

In Figures 13, 14, and 15, another type of construction block is examined. As a boundary condition, the bottom of the wall generated by this construction unit is fixed and various distributed force is applied from upward changes between 800- 1200 kN, and the results are implemented by graphics (Seo et al., 2015).

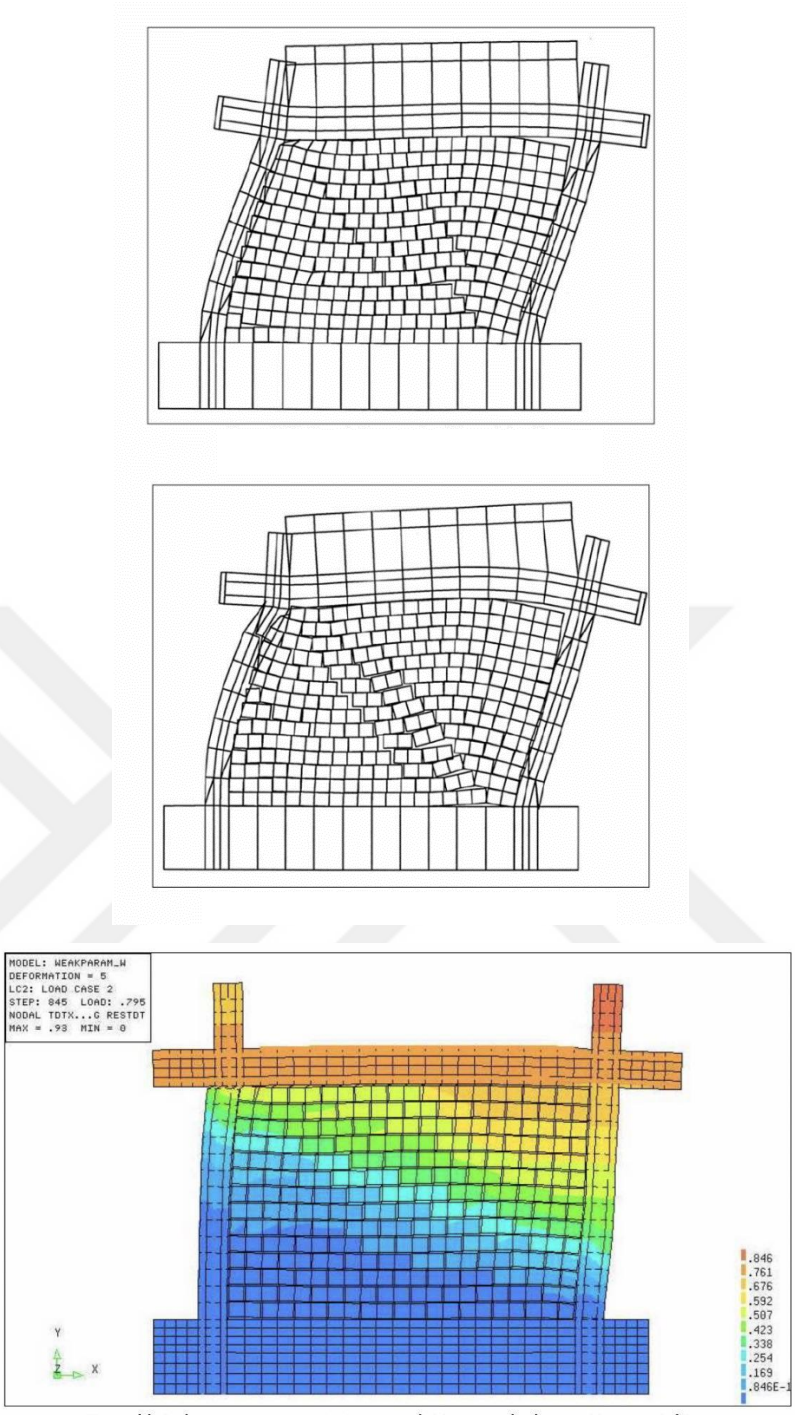

Figure 16: Finite element analysis of another type of construction block wall with different applications (Seo et al., 2015)

In Figure 16, another construction block is analyzed the boundary condition is the bottom surface of the wall is fixed and 22 kips pressure is applied from upward the results are observed (Al-Chaar et al., 2008).

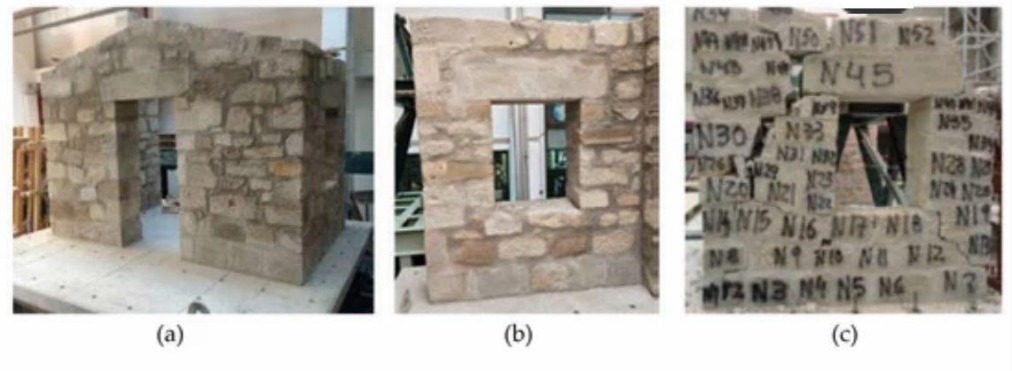

Figure 17: Finite element analysis of another type of construction block (Lemos, 2019)

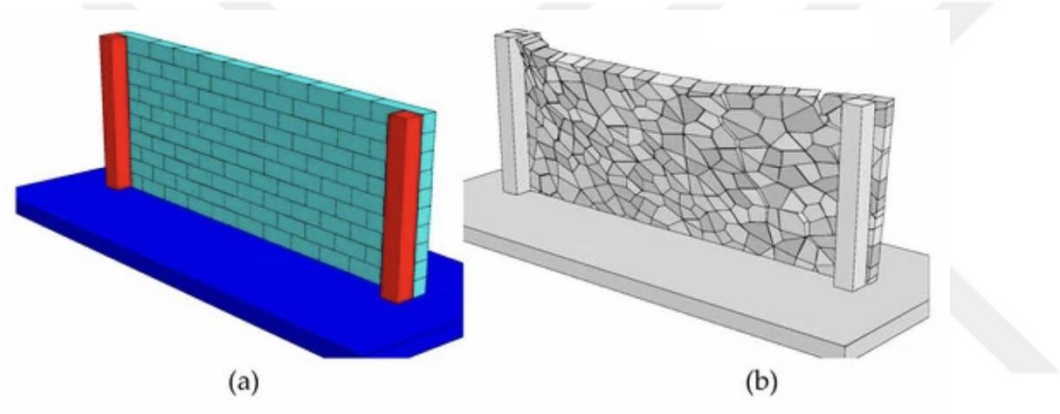

Figure 18: Finite element analysis of another stone based on a construction block in a different wall type (Lemos, 2019)

In Figure 17 and Figure 18 the stone blocks are analyzed; by the finite element analysis method and the boundary condition is the bottom surface of the wall is fixed and 0.32Mpa pressure is applied upward, and the analysis results are obtained (Lemos, 2019).

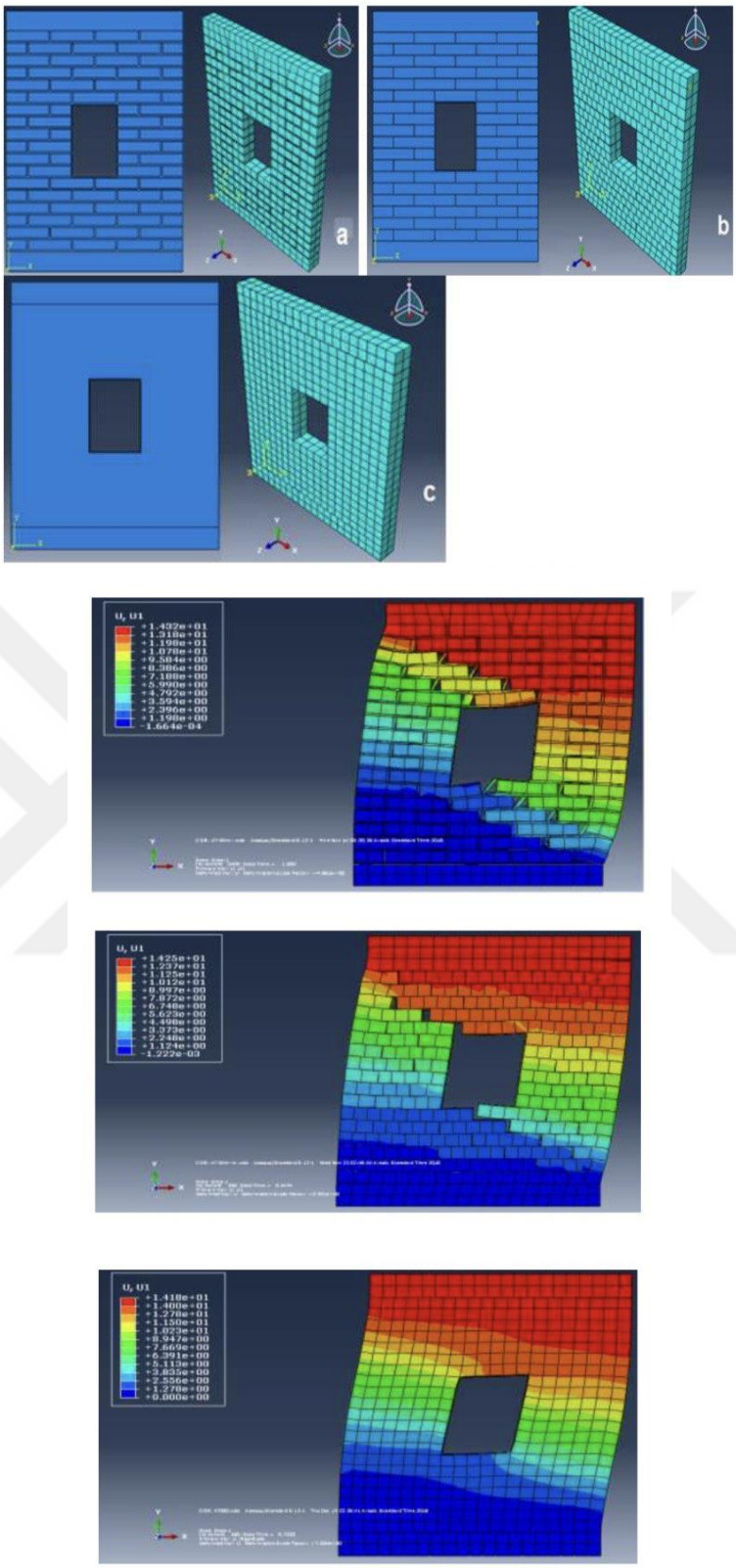

Figure 19: Finite element analysis of another type of a construction block wall with a window (Abbas et al., 2017)

Figure 19 demonstrates another construction block wall under 0.3 N/mm2 pressure applied with the boundary condition the bottom surface is fixed to the ground and the results of the analysis are obtained (Abbas et al., 2017).

1.7.3 Why Siemens NX as Finite Element Analysis Software

Numerous software is based on finite element analysis, but Siemens NX was chosen for the analysis due to the software's remarkable advantage and dependability for construction materials.

The use of NX increases efficiency, profitability, and consistency in the processes, as well as the quantity and quality of the planning.

Obermeyer's Head of Special Section BIM for Civil Engineering is Markus Hochmuth.

The Obermeyer Corporate Group (Obermeyer) is an independent engineering firm that provides technical and integrated planning for nearly all disciplines of construction planning, such as buildings, transportation infrastructure, energy, and the environment. As part of its range of offerings, the company provides project management and object tracking. Obermeyer was founded in 1958 in Munich, Germany, where its headquarters are located. It has over 1,200 employees globally. (Url-7)

Due to the extremely complex planning processes and calculations required by Obermeyer for its projects, the company must employ a variety of specialized information technology (IT) solutions. Markus Hochmuth, head of the special section of building information modeling (BIM) for Civil Engineering at Obermeyer, explains they must unify the IT environment and establish a consistent and integrated planning process, including the BIM process, which is gaining importance in the construction industry BIM is a technique for optimizing the design, construction, and operation of structures. Using software tools, Obermeyer Construction Engineering Firm improves its efficiency and profitability with NX. The BIM process is based on an object-oriented 3D model that enables firms to utilize and integrate a variety of data in subsequent processes. (Url-7)

The existing Cologne railway viaduct needs renovation. Copywritten material explains that: the topography of the surrounding area must be considered when designing roads, railway lines, bridges, and other transportation projects. They frequently adhere to intricate curves and organic surfaces. To better support the BIM process with 3D

modeling, Obermeyer sought out a 3D computer-aided design (CAD) system suitable for use with traffic structures and bridges. Professionals imply that specific processes can often be parameterized when designing a bridge. The goal was to optimize the planning processes with software that enables the execution of tasks more efficiently and with higher quality, which was challenging with existing planning tools. Using 2D CAD, the representation of the transverse section, longitudinal section, and gradient is very time-consuming and error-prone, especially when variants or modifications must be investigated. (Url-7)

In addition, they note that the use of 3D CAD for product design is widespread throughout the manufacturing industry. As most architectural CAD solutions are concentrated on the definition of planes and verticals, software systems used in these industries are evaluated. (Url-7)

The selection process included several leading 3D-based CAD systems. The software was evaluated using the example of a bridge design to see if the tested solutions could support standardization and optimization of the processes and how that would improve profitability, efficiency, and quality. Furthermore, a new solution is needed to allow the integration of existing planning processes and procedures, such as specialized software for route surveying and solutions for the bidding process. (Url-7)

The selection process requires remarkable achievements about usage areas of the software to illustrate this specific usage areas Figure 20, 21, 22, 23 and 24 demonstrates, for the bridge strengthen alternatives in which loadbearing issues are significantly important.

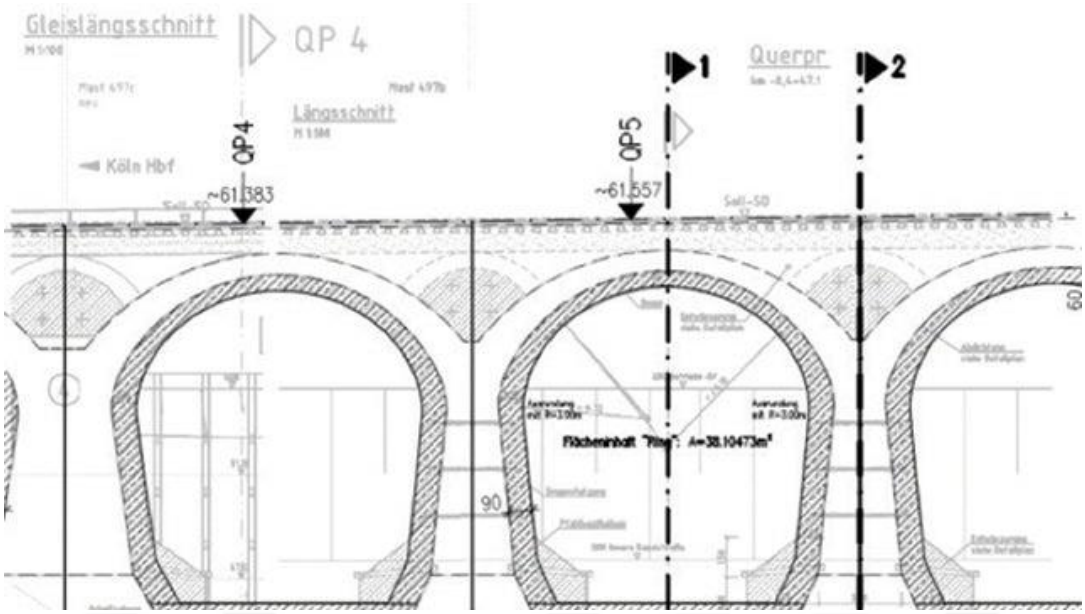

Figure 20: Alternative proposal by Obermeyer and Falkenhahn Bau now being implemented (Hochmuth, 2023)

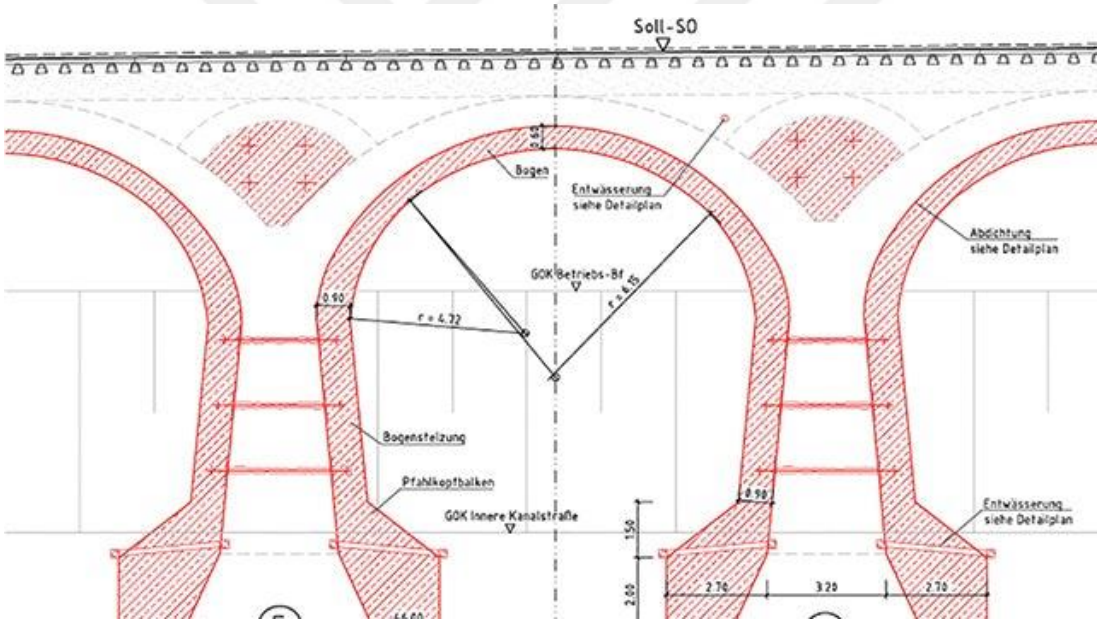

Figure 21: Original plan of the contractor (Hochmuth, 2023)

About the selection process, Hochmuth explains that Siemens Digital Industries Software's NX has been chosen as it provided the best opportunity for integration with existing planning processes and as it anticipated the greatest output from the 3D model in terms of the derived 2D construction plans. Although this could have been achieved with all tested systems, NX provided the most comprehensive and effective tools. Even more significant was Siemens' partnership with NeoApps, which develops a variety of construction-specific applications (Url-7)

As in other industries, 3D modeling offers many advantages, but for Obermeyer, it is only expedient. Industry-certified, approved 2D construction plans are produced before the realization of building projects. (Url-7)

In addition, it is crucial for us to quickly generate 2D plans directly from the 3D model, not with separate, time-consuming downstream solutions or by transferring the data to a 2D system, which would break the design chain, especially because making changes would require a great deal of effort and could result in errors. (Url-7)

Obermeyer avoids such problems by using NX and the NeoApps drafting solution. The models and 2D drawings created using NX are associative. Architectural, engineering, and construction (AEC) industry requirements are reflected in the NeoApps solution AEC Drafting. Therefore, any changes to the model are updated automatically and by industry standards. (Url-7)

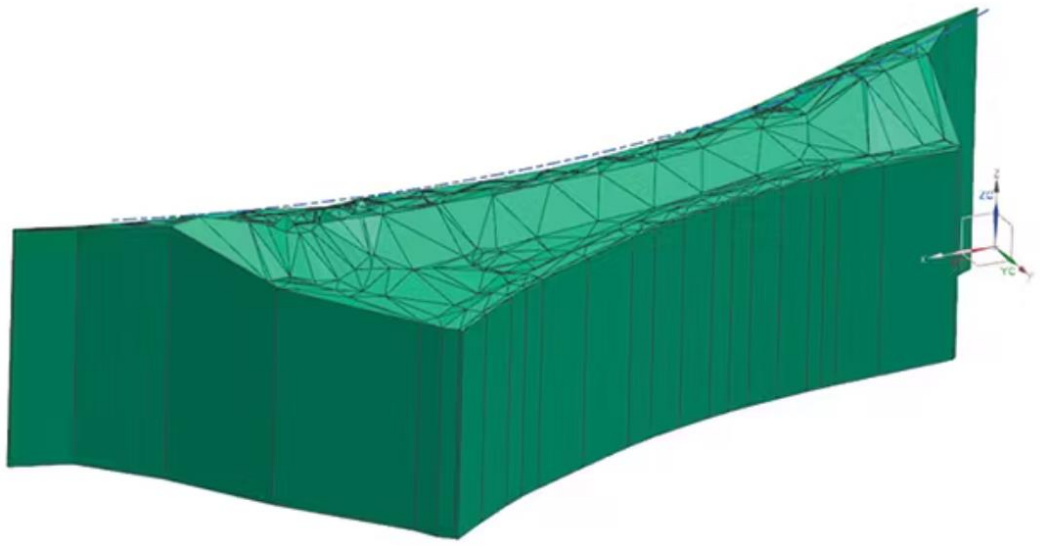

Figure 22: Triangle terrain model created with ProVI software imported into NX (Hochmuth, 2023)

The renovation of a railway bridge in Cologne, Germany, is an excellent example of the efficiency that results from using NX. Due to the impossibility of rerouting the line and its location between a very busy road and a goods yard facility, the stabilization work must be conducted during active rail traffic. (Url-7)

Deutsche Bahn (German Railway) intended to renovate a viaduct constructed in 1912, a vaulted bridge with 12 arches and a length of approximately 200 meters. The purpose

of the undertaking was to stabilize the existing structure with new shells of reinforced concrete.

Obermeyer collaborated with the construction company Falkenhahn Bau to develop an acceptable alternative proposal. Instead of a deep foundation, the new arches are constructed with base plates that are rigidly connected to the imposts. (Url-7)

The combination of the arch shape and the weight of the geographical environment resulted in complex geometric conditions. For the modeling of the new concrete shells, defined points on the extant arches were measured and used to define NX freeform surfaces. The design of the new arches was based on these freeform surfaces. (Url-7)

In addition, a digital terrain model, which included the location of the railway, was constructed based on measurements taken on-site. (Url-7)

To ensure that the NX-defined splines and freeform surfaces precisely suit the existing stone arches, one arch was scanned in 3D. The variance between the results and the created surfaces from a small number of measuring sites was within tolerance and, thus, acceptable.

The 3D model was also used to generate certified 2D plans and to calculate the required cubic capacity, which will be utilized by the construction contractors. (Url-7)

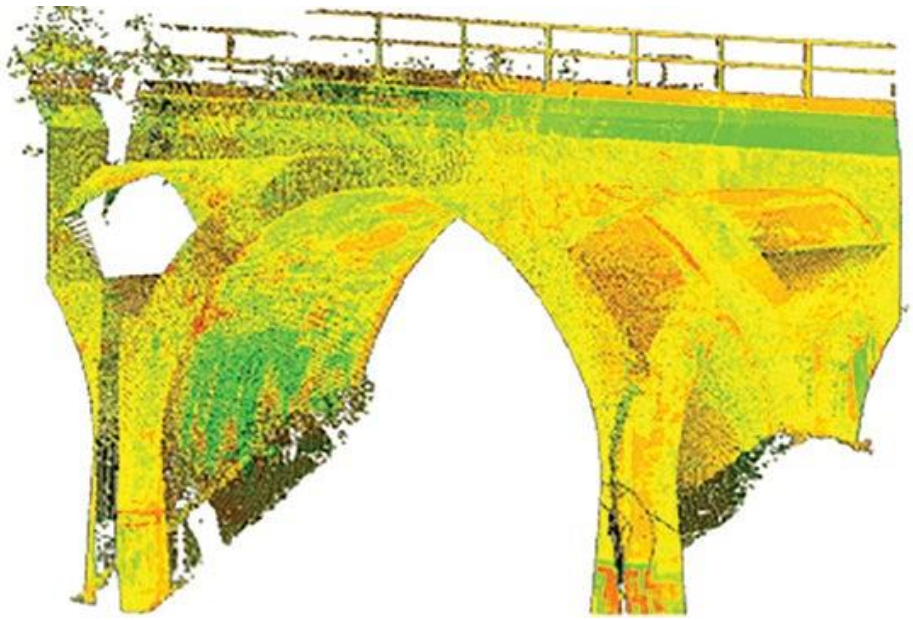

Figure 23: 3D scan of one arch. Copyright: Ingenieurbüro Dr. Sauermann – Orlicek – Rohen GmbH (Hochmuth, 2023)

A distinct advantage of using NX is Hochmuth asserts that the use of NX results in increased productivity, profitability, and consistency in processes, as well as greater quantity and quality in planning. It is just beginning to use NX, it can be already told that it is a highly productive instrument that will meet the quality, transparency, cost, and delivery date requirements.

Hochmuth notes that additional benefits of utilizing NX include parameterized models and enhanced customer transparency through virtual, easily modifiable visualizations that can incorporate the surrounding environment. The fact that model data can be reused for subsequent procedures is an additional benefit.

Only 3D object models can contain the necessary information for processes such as the construction of 2D drawings, finite element modeling (FEM), and cost estimation.

According to Hochmuth, the widespread adoption of 3D planning tools is anticipated to persist. Obermeyer currently employs BIM methods for building construction and has co-created the BIM guideline for Germany with AEC3, which is published by the Federal Institute for Research on Building, Urban Affairs, and Spatial Planning (BBSR).

Nevertheless, 3D CAD is not the only tool used for global planning in the construction industry. Hochmuth is confident that the connectivity of the various software tools will become even more crucial in the future.

In addition to enhancing the use of 3D CAD, it will be essential to establish a comprehensive data management tool that can be used to manage the ever-increasing digital data, and governing processes, and leverage all software tools involved. As an illustration, he notes that all the data for a bridge structure should be preserved digitally with all the necessary information, from the initial concept through the planning process, construction, utilization, and maintenance, to its eventual decommissioning.

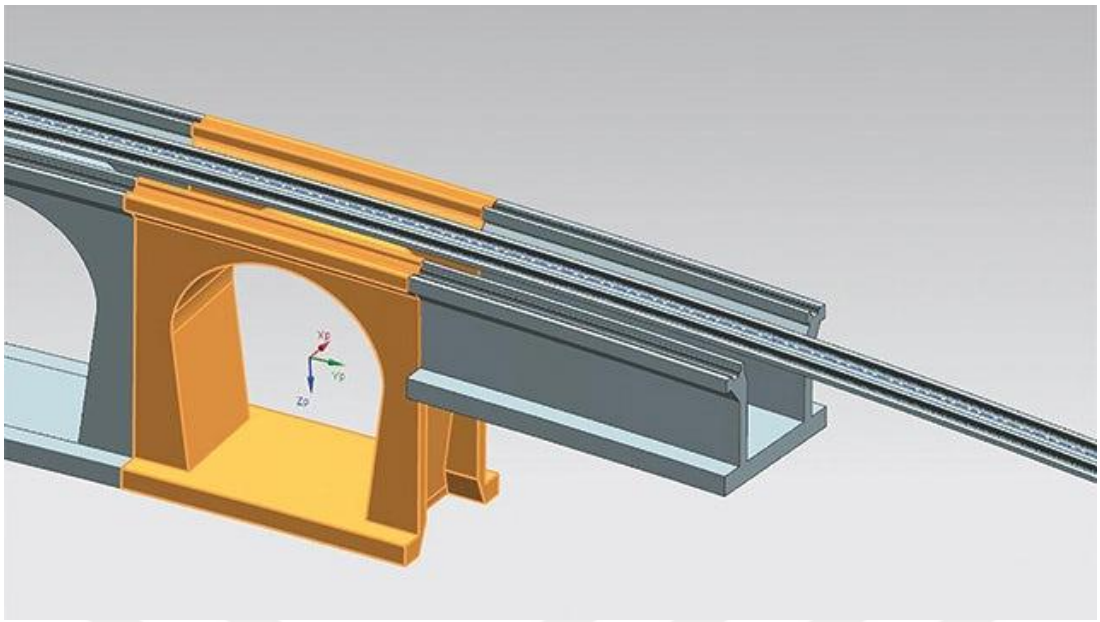

Figure 24: Using NX to produce a mass calculation (Hochmuth, 2023)

It is early in the use of NX, but it can already be assumed that it is a highly productive tool that will satisfy quality, transparency, cost, and delivery date requirements. Numerous finite element analysis-based software exist, but Siemens NX was chosen for the analysis due to its exceptional advantage and dependability for construction materials.

2. ANALYSIS OF THE COMMONLY USED LIGHTWEIGHT MASONRY UNITS

2.1 Sustainability Aspects

Both for the concrete blocks and the AACs, the raw materials are sand-based, and they are not suitable for recycling. Also, after the demolishing of a building constructed with those blocks, debris is carried somewhere far from the city and will be discharged into the environment. There is no option to dissolve them in the environment because they are not degradable materials. When cement is used then materials become inappropriate for recycling.

Manufacturing processes of construction blocks are not cooperating with the environment, because they are not implementing a positive effect on the world. To illustrate, positive manufacturing processes give decrease pollution for the environment, it can be decreasing the emission rates or hazardous gasses oscillation, or it can decrease the pollution materials on the environment by using them in the process itself, then this results in the cleaning of the environment, and it can be called as an eco-friendly or eco-supporting manufacturing process. On the other hand, when these are checked, it is observed that there are not any significant points as mentioned before which can be called environmentally positive. Additionally, in the manufacturing process of the AACs, aluminum, silicate, and radon are exposed. These gasses are very hazardous to human lungs. Table 2 shows the risk of lung cancer death due to radon exposure as an example. So, it can be said that the manufacturing process of AACs harms both human health and the environment (Url-8).

Table 2: Lifetime Risk of Lung Cancer Death from Radon (Url-9)

Radon Level [a]	Lifetime Risk of Lung Cancer Death (per person) from Radon Exposure in Homes [b]		
pCi/L	Never Smokers	Current Smokers [c]	General Population
20	36 out of 1,000	26 out of 100	11 out of 100
10	18 out of 1,000	15 out of 100	56 out of 1,000
8	15 out of 1,000	12 out of 100	45 out of 1,000
4	73 out of 10,000	62 out of 1,000	23 out of 1,000
2	37 out of 10,000	32 out of 1,000	12 out of 1,000
1.25	23 out of 10,000	20 out of 1,000	73 out of 10,000
0.4	73 out of 100,000	64 out of 10,000	23 out of 10,000

a Assumes constant lifetime exposure in homes at these levels.
b Estimates are subject to uncertainties as discussed in Chapter VIII of the risk assessment.
c Note: BEIR VI did not specify excess relative risks for current smokers.

As an example, in Istanbul after an AAC factory demolition, the neighborhood close to that area, was affected very negatively by the oscillation of the radon gasses from the factory to the environment during the demolition process. This is implemented on news for a long time in 2019 (T24 news agency broadcast on 6/06/2019, reachable on the web).

When examining environmental issues for commonly used concrete blocks, environmentally friendly issues are not logical almost totally for the pumice blocks, which are a kind of concrete blocks. The pumice blocks do not provide any positive aspects except the fact that they are lighter than standard concrete blocks. They are about 40% lighter than those. Because of that, it provides a decrease in gasoline consumption during the shipping phase and a decrease in the labor force due to its advantages in logistics. Also, it provides more heat insulation compared with standard concrete blocks and this can be named as an eco-friendly side.

Another issue with the commonly used masonry units, pumice blocks, and AACs is that they consist of silicate, aluminum, and also the most important one is radon gas. Van Der Pal (2004, p.?) says "Health risks of radon exposure to high concentrations of radon and its progeny in air leads to increased risk of lung cancer". The latest report of the World Health Organization (WHO) on the biological effects of alpha radiation, Bear VI, estimates the radiation dose due to construction products, will reach high levels in the future and cause cancers remarkably in his article titled "Radon Transport in Autoclaved Aerated Concrete" (Url-9). Also, the EPA, the United States Environmental Protection Agency on its website under its article called "What is Radon Gas? Is it Dangerous?" claims "Breathing radon over time increases your risk of lung cancer. Radon is the second leading cause of lung cancer in the United States. Nationally, the EPA estimates that about 21,000 people die each year from radon-related lung cancer. Only smoking causes more lung cancer deaths." (Url-9) This study also claims that the radon gas in autoclaved aerated concrete is remarkably hazardous. Moreover, the final report (Url-9) published in 2003 about the application of some hazardous materials indicates that it must be cut to adjust dimensions and there occurs oscillation of gasses. The negative effects of aluminum silicate and radon can be very hazardous for humans, so workers must be very careful when working with these products.

Moreover, the small pieces of AACs can continue to oscillate those hazardous gasses even after the application process is completed. Those gasses can transfer through the coating or the plaster, and it is risky for the building residents. Additionally, after the demolition of these buildings, those oscillations are exposed.

Today, there are some general aspects of being environmental, it can be simplified to two main issues, one is zero-emission and gas oscillation, and the second one is sustainability.

For the first, today almost every product is examined from the view of energy consumption and emissions all over the world. So, the construction materials and products also must be elaborately examined, the construction blocks are to be studied about the levels of emissions and gas oscillations. For the standard concrete blocks, its CO_2 oscillation is the highest one, and after that AACs have almost a %50 less CO_2oscillation.

From the sustainability aspect, both are not sustainable. Firstly, their materials are not sustainable. They cannot be recycled, and their rubble is hazardous and cannot be dissolved in the environment in a short time.

Consequently, standard concrete blocks and the AACs both require an additive material for the application. They must be used as a mixture which is derived from the cement, to come together and provide a structure that can keep them standing.

This mixture is almost the same for both and as it's a cement-based material, it also has similar negative effects on the environment.

2.2 Finite Element Analysis of the Pumice Block

When Finite element analysis approach described in Section 1.5 is implemented in this study first for the existing pumice block for comparison purposes. Siemens NX software was used for the static finite element analysis in this study.

There are SPB units with various dimensions in the market. In this study, it has taken the dimensions of the unit which are suitable for comparison with the other blocks which are examined in this study. The long edge through the X direction is 40 cm and the short edges are some dimensioned through Y and Z directions 20 cm. There are 2 holes in the middle of the unit throughout the Z direction having dimensions of 36 cm by 7 cm as shown in Figure 25.

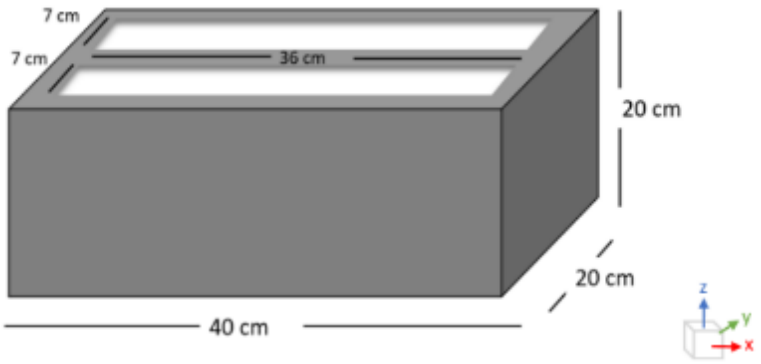

Figure 25: Dimensions of the standard pumice block used in this study (Baz, 2023)

An isotropic linear elastic material property is assumed for the pumice block finite element analysis. The concrete used to make the pumice block is assumed to have a modulus of elasticity of 30GPa and Poisson's ratio of 0.2 in the finite element analysis (Guo, 2014).

In the finite element analysis, a distributed load of 300 N was applied on the top surface of the one-unit pumice block. The square side surfaces of the blocks are fixed in all degrees of freedom as the boundary condition.

This shows the simulation for the load-bearing block which carries the other blocks, located on it. The ceiling height can be higher or lower, but the height of the ceiling is assumed as 3m on average. When an average ceiling with a height of 3 meters is regarded, it means the load-bearing block will carry 14 blocks on it. Because each block has a mass of 2,16 kg, then, for 14 blocks, the total mass of the one-unit block is 30,24 kg. When the gravity is assumed to be 9,8 m/s2, the total load carried by the unit block is 296,352 N. It is rounded to 300 N to apply in the finite element analysis on the top surface of the unit block as a distributed force.

In addition, a mesh refinement study is required to determine the appropriate mesh size for the discretization of the domain mentioned in Section 1.5. For this purpose, different mesh sizes such as 10 mm, 8 mm, 6 mm, and 4 mm have been used to generate the mesh with 3D tetrahedral solid elements. The results of these for different mesh sizes are shown in Figures 26 to 29.

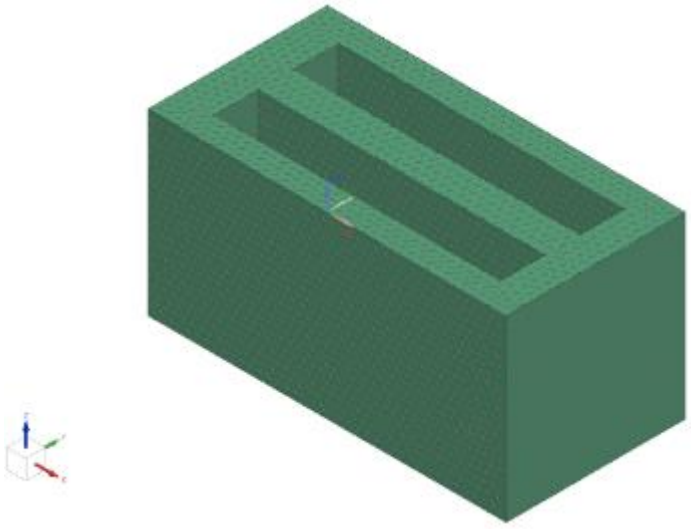

Figure 26A: Finite element analysis with 10 mm mesh size displacements and von Mises stresses (Baz, 2023)

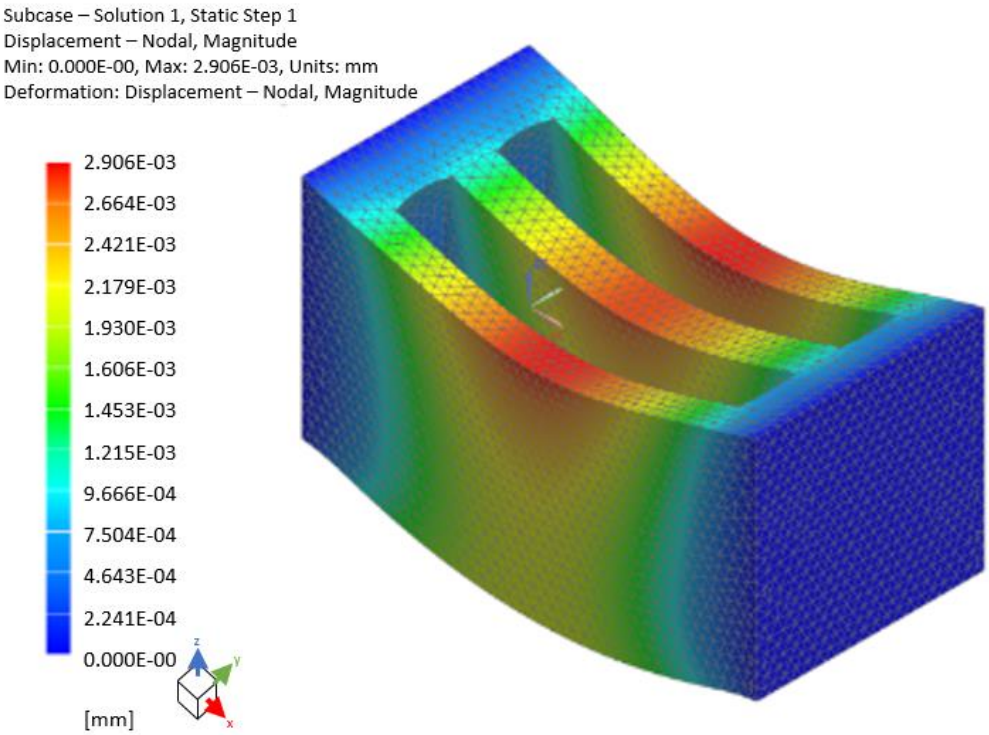

Figure 26B: Finite element analysis with 10 mm mesh size displacements (Baz, 2023)

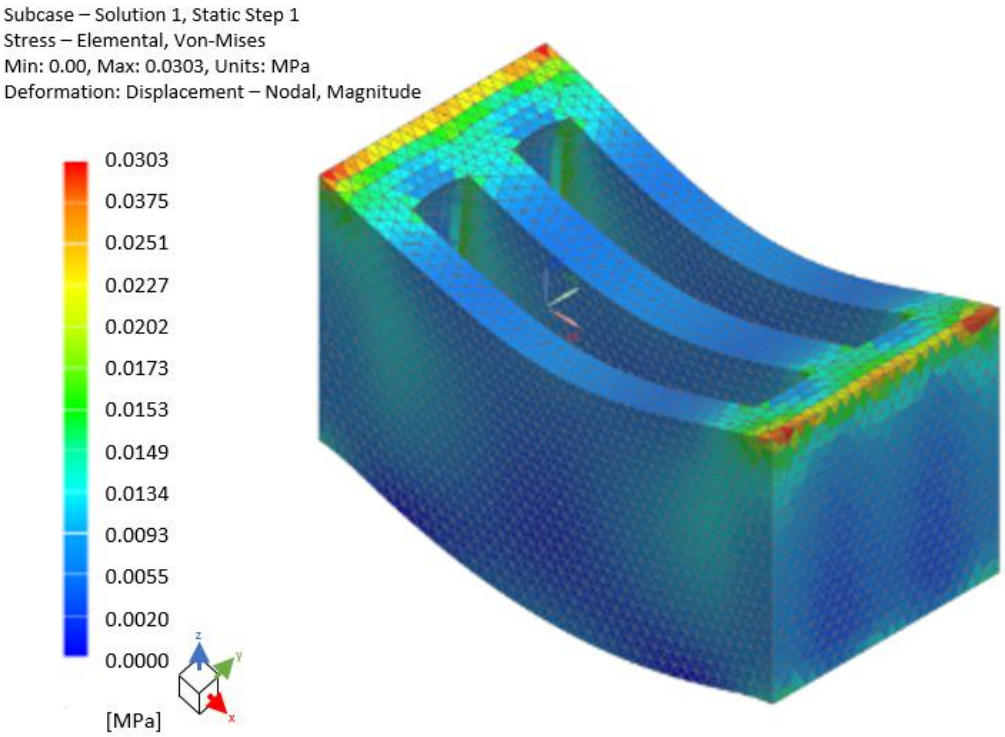

Figure 26C: Finite element analysis with 10 mm mesh size von Mises stresses (Baz, 2023)

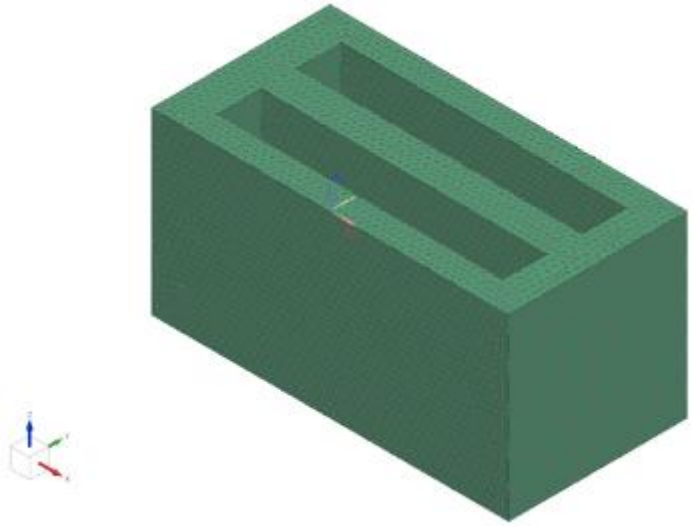

Figure 27A: Finite element analysis with8 mm mesh size displacements and von Mises stresses (Baz, 2023)

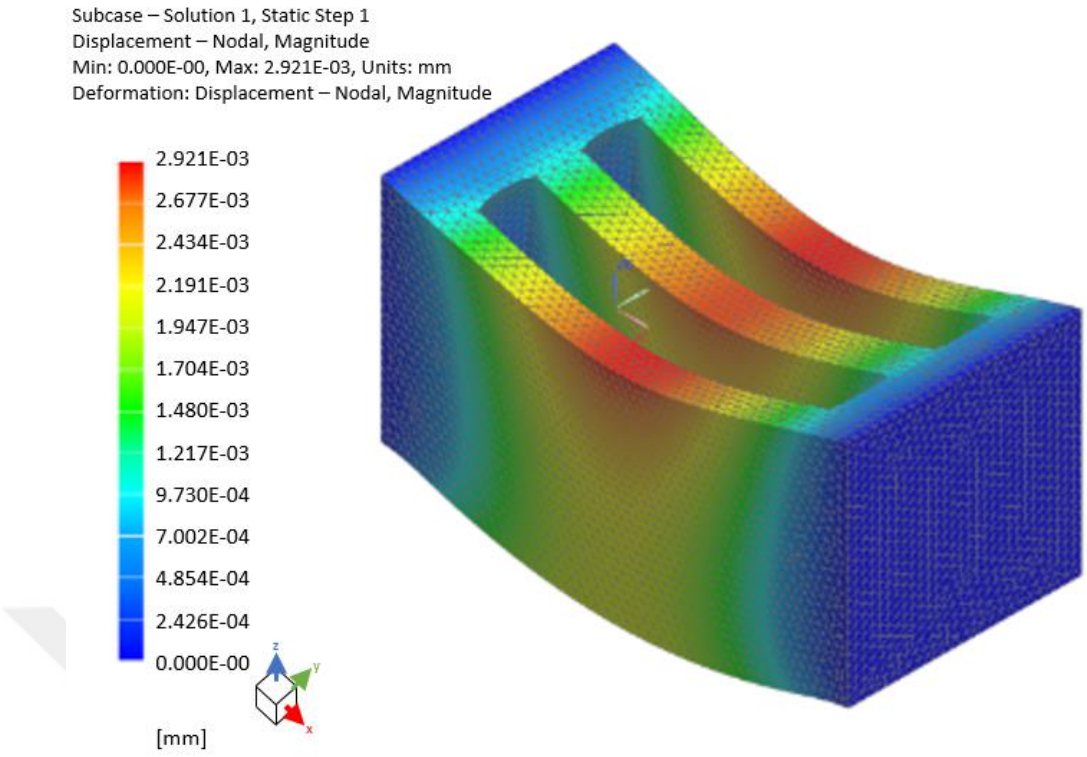

Figure 27B: Finite element analysis with8 mm mesh size displacements (Baz, 2023)

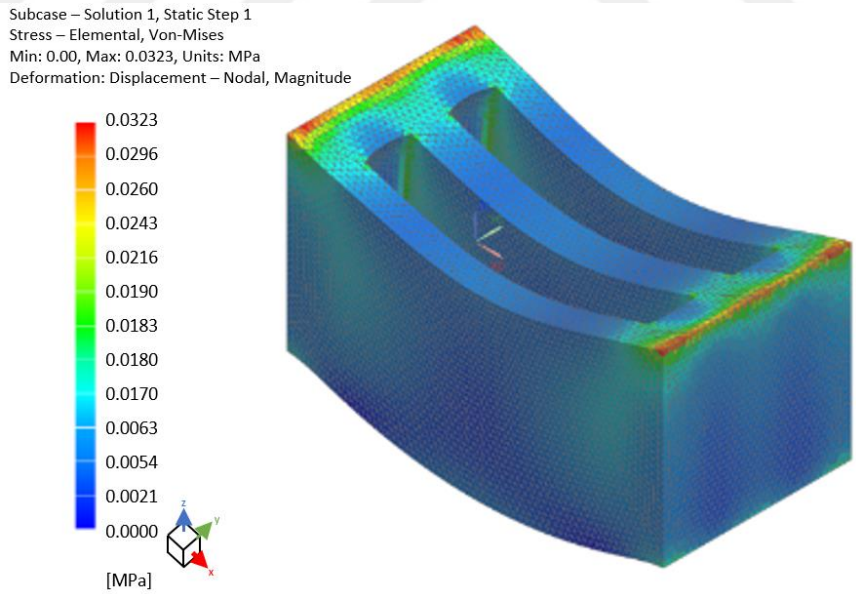

Figure 27C: Finite element analysis with8 mm mesh size von Mises stresses (Baz, 2023)

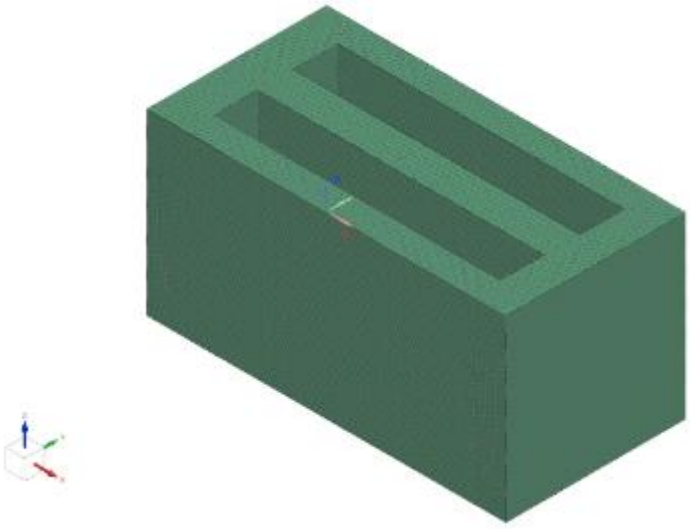

Figure 28A: Finite element analysis with6 mm mesh size displacements and von Mises stresses (Baz, 2023)

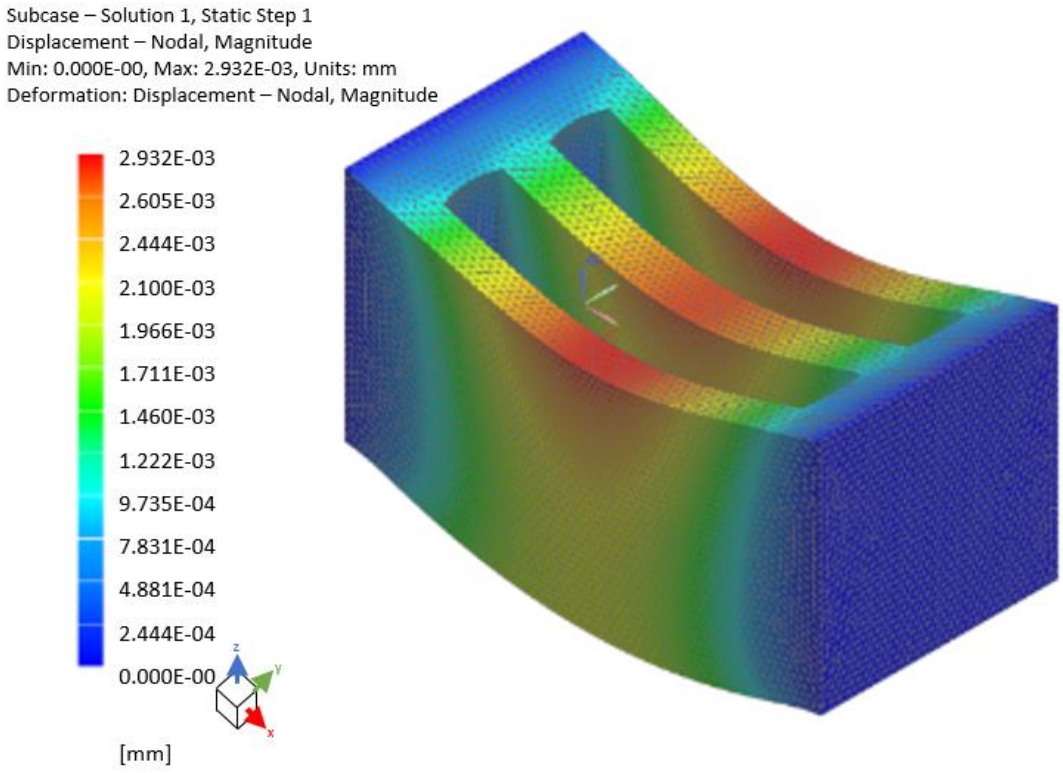

Figure 28B: Finite element analysis with6 mm mesh size displacements (Baz, 2023)

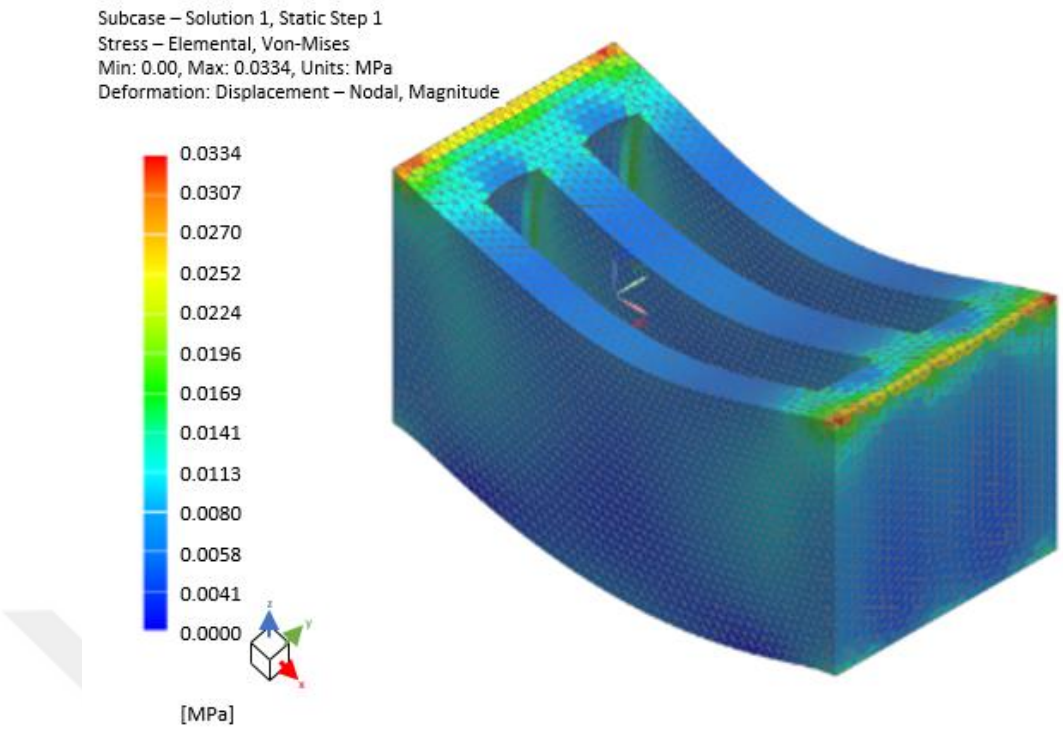

Figure 28C: Finite element analysis with 6 mm mesh size von Mises stresses (Baz, 2023)

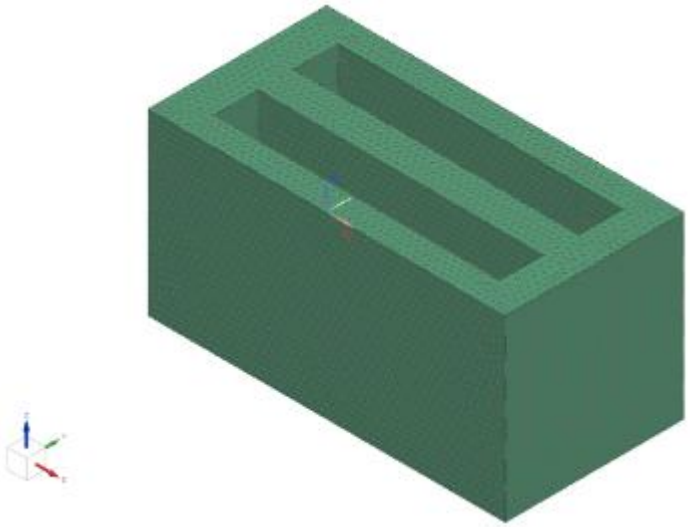

Figure 29A: Finite element analysis with 4 mm mesh size displacements and von Mises stresses (Baz, 2023)

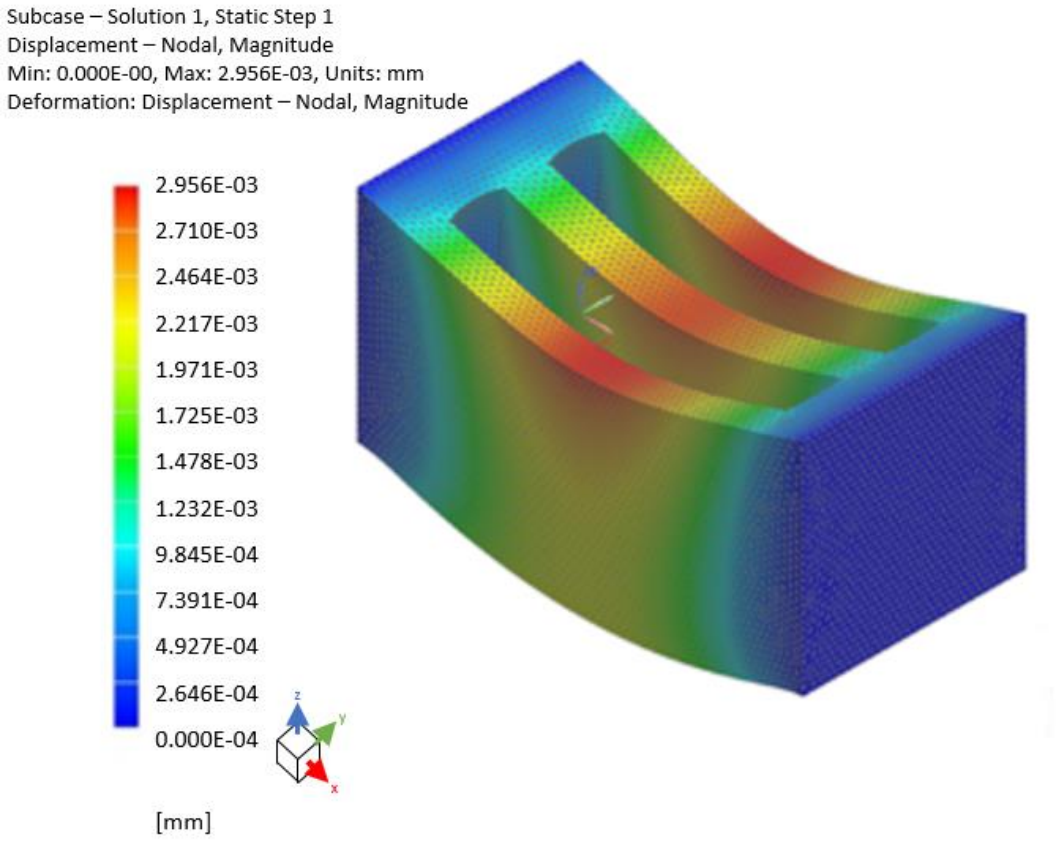

Figure 29B: Finite element analysis with 4 mm mesh size displacements (Baz, 2023)

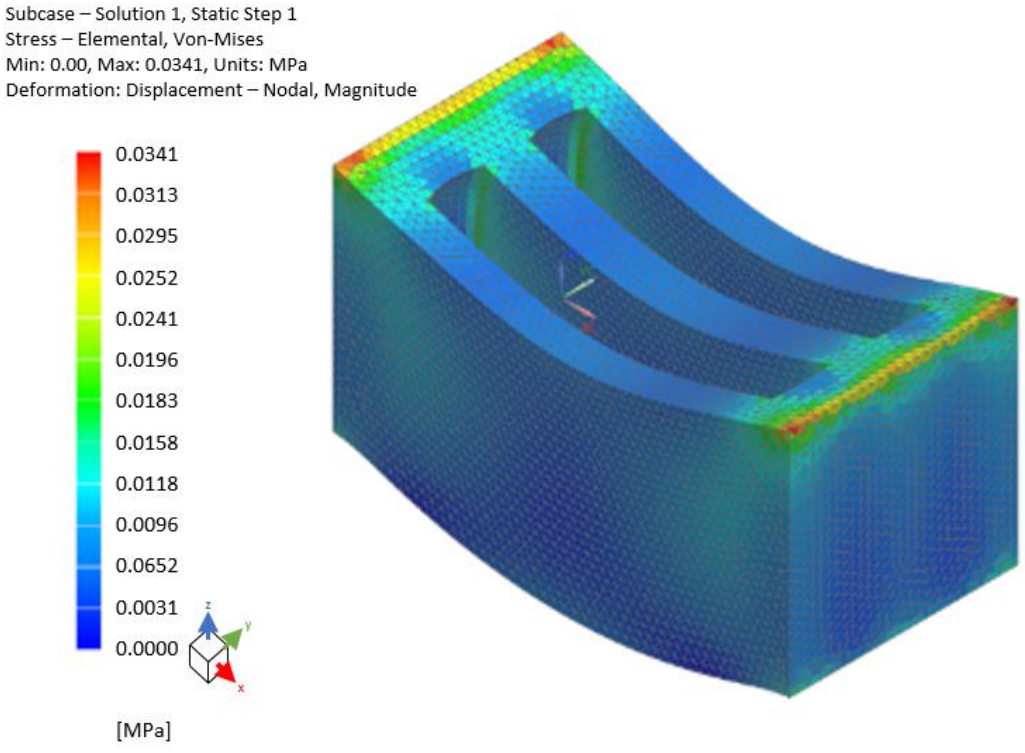

Figure 29C: Finite element analysis with 4 mm mesh size von Mises stresses (Baz, 2023)

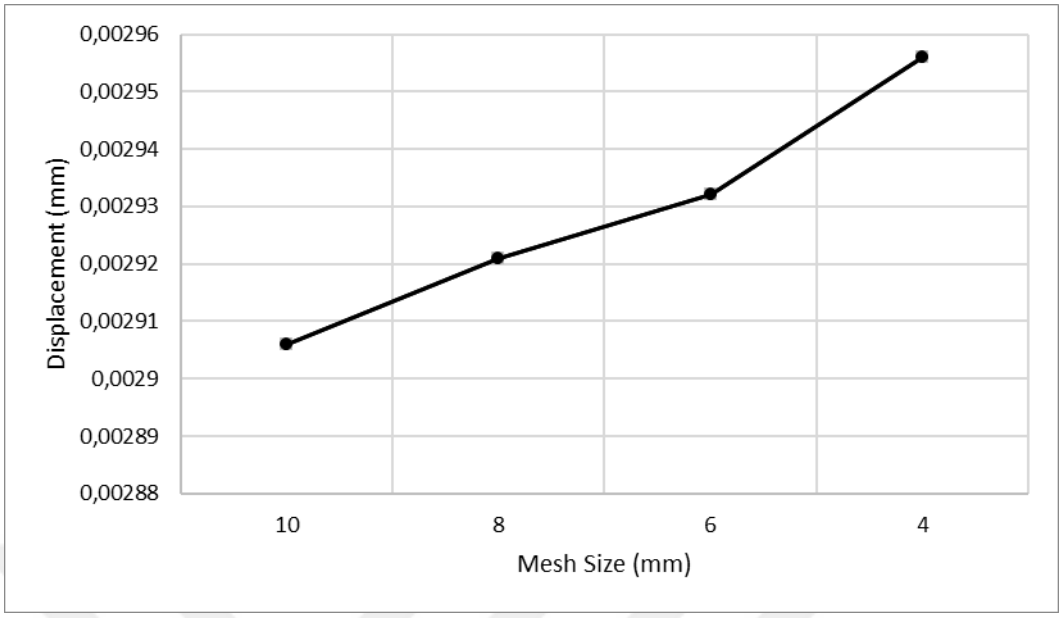

Figure 30: Graph of mesh size vs maximum displacement of Pumice Block (Baz, 2023)

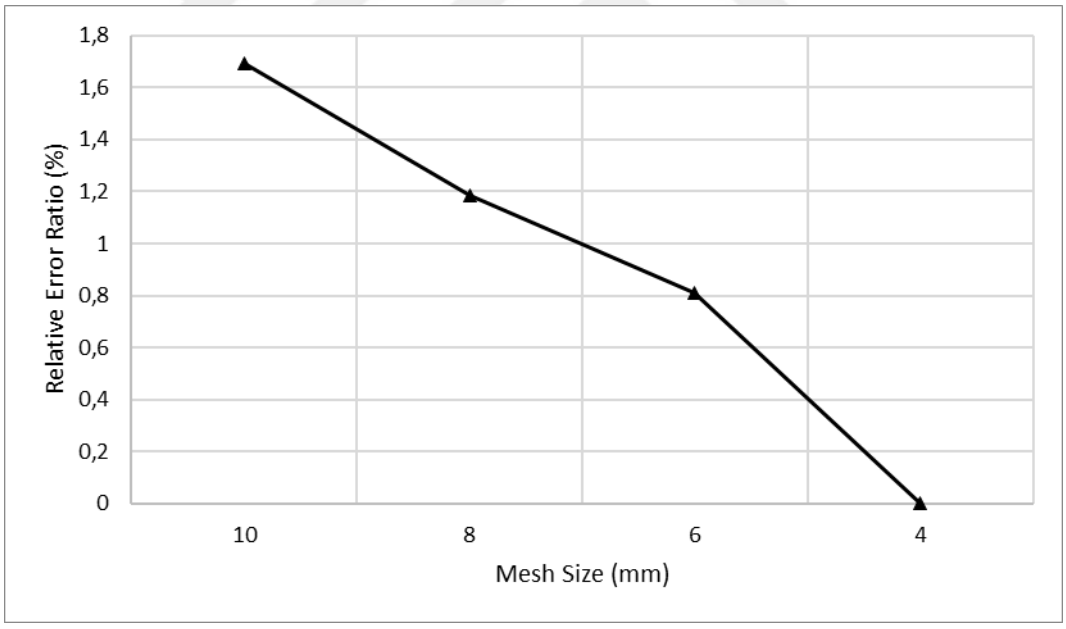

Figure 31: Graph of mesh size vs relative error ratio (%) for the displacement of Pumice Block (Baz, 2023)

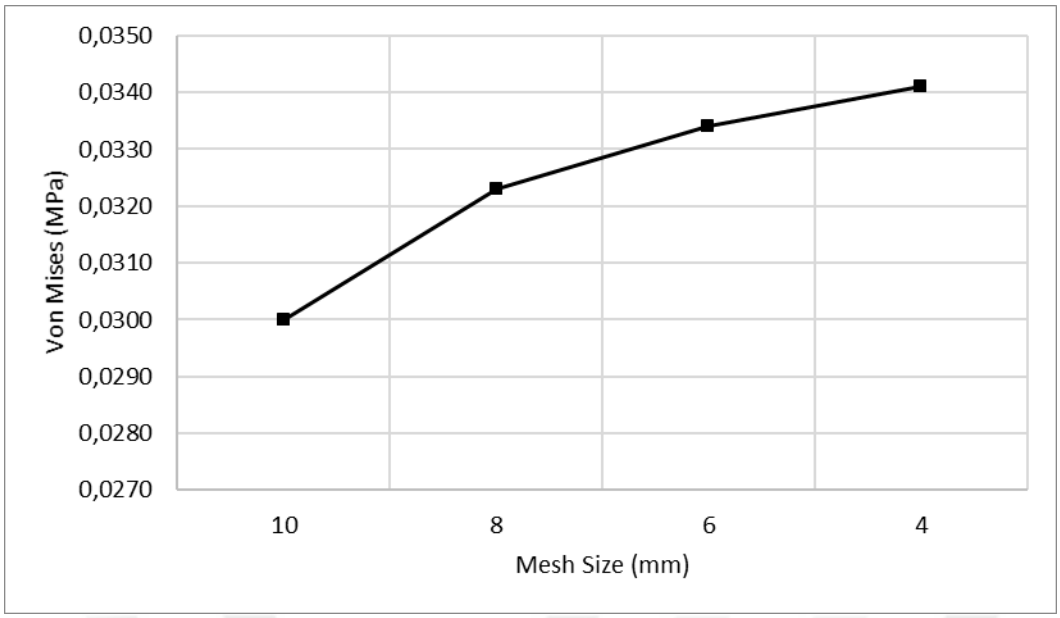

Figure 32: Graph of mesh size vs maximum von Mises of Pumice Block (Baz, 2023)

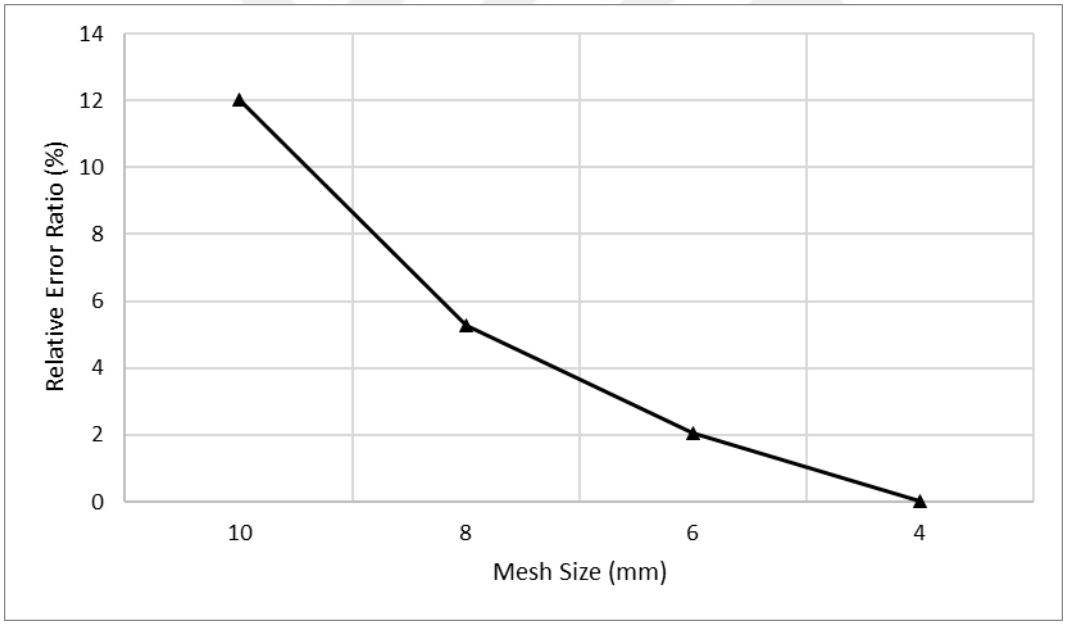

Figure 33: Graph of mesh size vs relative error ratio (%) for von Mises of Pumice Block (Baz, 2023)

Displacement results of the finite element analysis on the pumice block are shown in Figure 34 when the bottom surface is fixed to the ground and a distributed load of 300 N is applied on the top surface. The boundary condition is different for this analysis because this analysis for testing the behavior under carrying the other blocks when the

applicant puts them exactly linear on top of each other. The entire top surface is deflected equally with a maximum deformation of $1.59x10^{-3}$ mm. This is expected because the load is assumed to be evenly distributed on the top surface for this analysis. The maximum deformation value is very small which shows the pumice block does not have large deflections under this loading condition.

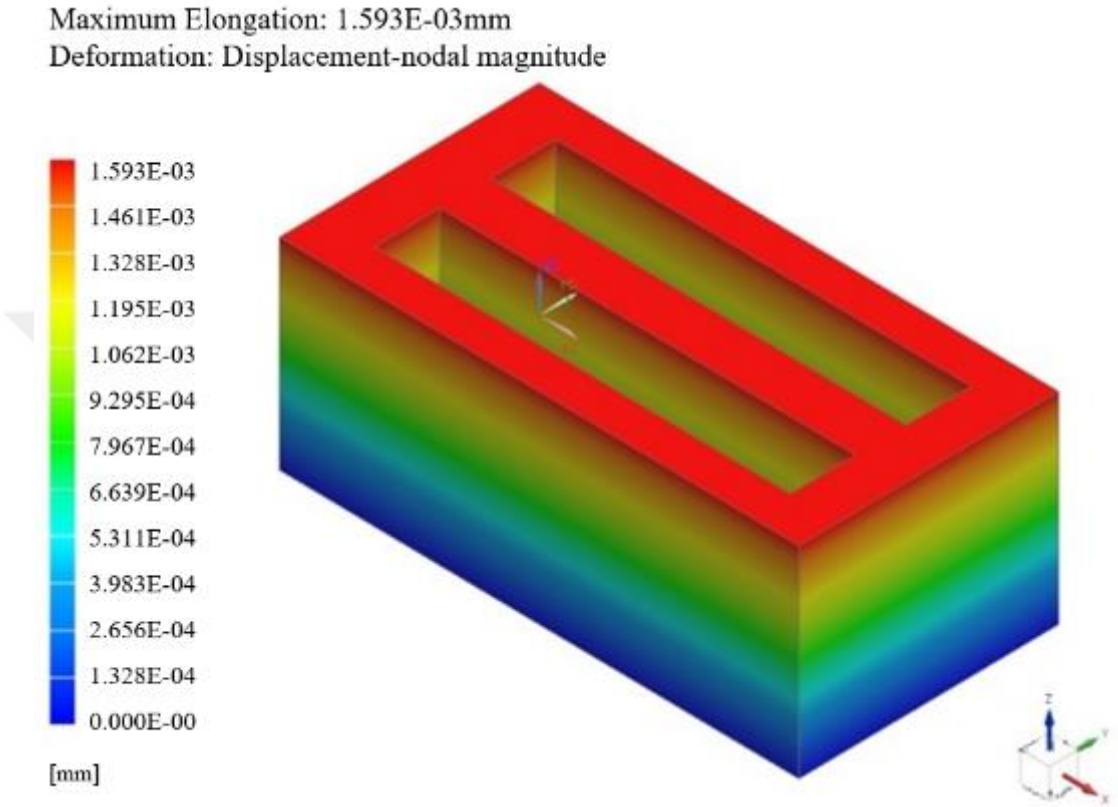

Figure 34: Displacement results of the Standard Pumice Block's Simulation Under 300N Distributed Force from the Top (Baz, 2022)

As an alternative loading condition, distributed downward load through the negative Z-direction at the center of the block was applied in another simulation. This case was considered for examining the possible problems when a certain point load is exerted on the block instead of a distributed load. This loading condition can occur because in practical use many times the applier changes the shapes of the blocks by dividing them into pieces and the edges of some parts will come to the center of the other unit randomly, so the load-bearing part of the block becomes the center heterogeneously so for those kinds of applications, the analysis has to be made. Displacement results of the finite element analysis on the pumice block are shown in Figure 34 when the square

side surfaces are fixed and a distributed load is applied on the top surface, the maximum deformation occurred at the center of the top region as expected. The maximum deformation is $2{,}956 \times 10^{-3}$ mm as seen in Figure 35 which means a very small deformation occurs on the pumice block for the considered loading condition.

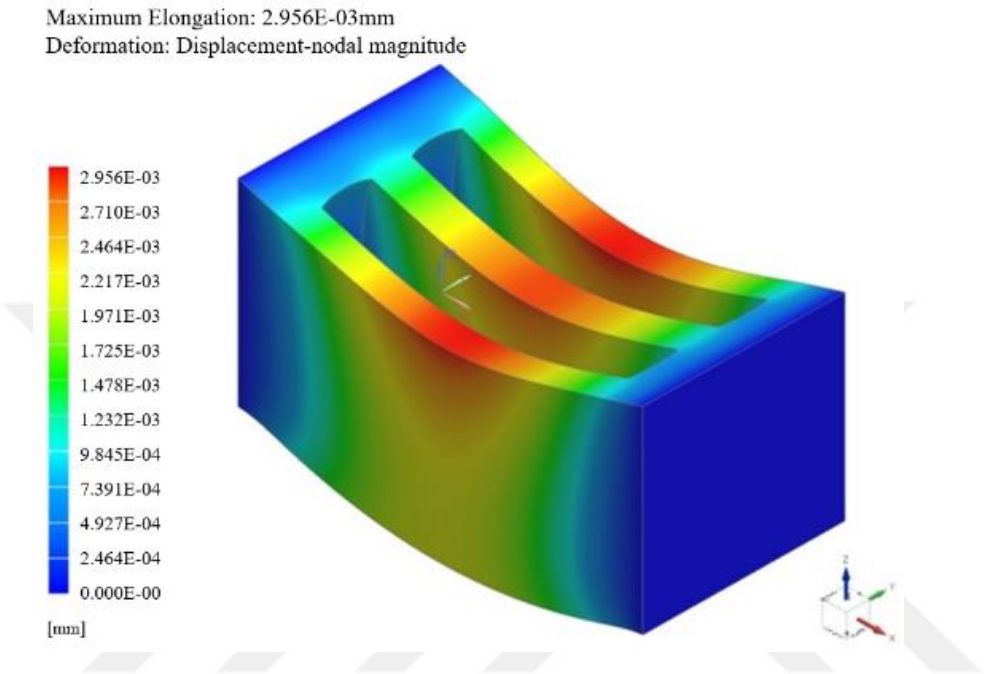

Figure 35: Displacement results of the Standard Pumice Block's Simulation Under 300N Distributed Force from Top-Middle (Baz, 2022)

2.3 Finite Element Analysis of the Autoclaved Aerated Concrete (AAC)

Finite element analysis was also performed for another existing construction block type, which is called the AAC block. Its dimensions, thickness values, minimum compressive strength, and dry density properties are shown in Table 3.

Table 3: Standard AAC's Properties (Url-10)

Properties of AAC Block	Specifications
General Size	625 mm * 240 mm * (75-300) mm
Thickness	50,75,100,125,150,200,225
Minimum Compressive Strength	3 to 4.5 N/mm^2 (IS 2185)
Minimum Dry density	450 to 650 Kg/m^3

The dimensions used in the finite element analysis for an AAC block are 62,5cm by 24 cm by 5 cm as shown in Figure 36. According to the basic principles of physics, it is clear that when the long side of a rigid, prismatic body gets shorter and the short sides of it get longer, the block becomes more durable and more rigid. Hence, it can be said that the simulations with those dimensions are enough to make comparisons with the others.

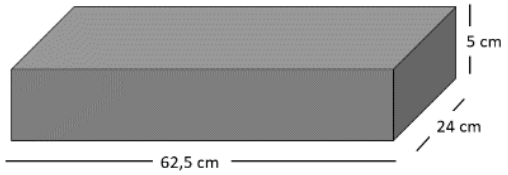

Figure 36: Dimensions of AAC Blocks (Baz, 2023)

The material of the AAC block is also considered to be isotropic, similar to the assumption made for the pumice block in Section 2.3. Then, in the finite element analysis, a linear elastic material is used with a modulus of elasticity of 1.226GPa and a Poisson's ratio of 0,2 (Guo, 2014).

A mesh refinement study was also conducted for the AAC finite element model. Rectangular side surfaces are fixed, and 300 N distributed force is applied from the top. Different mesh sizes of 10 mm, 8 mm, 6 mm, and 4 mm have been used in the mesh refinement study. The meshed geometries and the displacement and von Mises distribution results are shown in Figures 37-40. Maximum displacement and von Mises results for different mesh sizes are plotted in Figure 41 and Figure 43, respectively. A 4mm mesh size has been chosen.

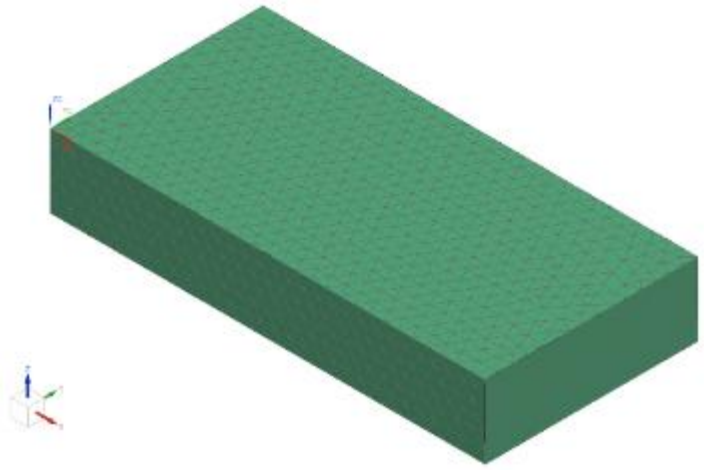

Figure 37A: Finite element analysis with 10 mm mesh size displacements and von Mises stresses for AAC Blocks (Baz, 2023)

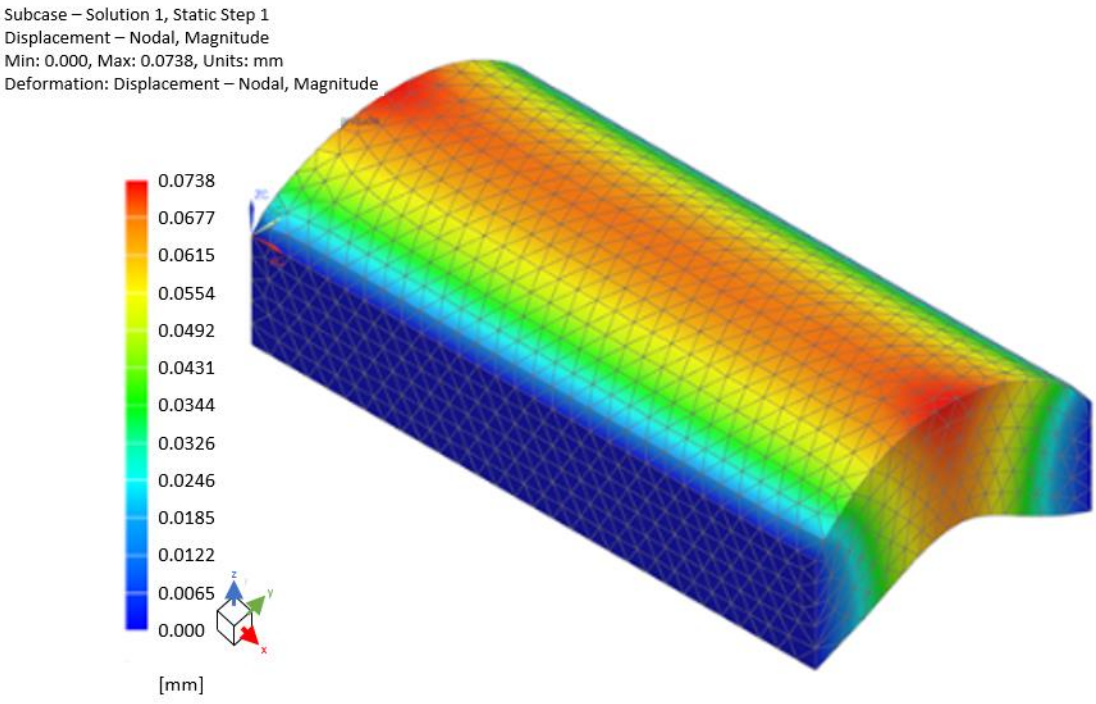

Figure 37B: Finite element analysis with 10 mm mesh size displacements for AAC Blocks (Baz, 2023)

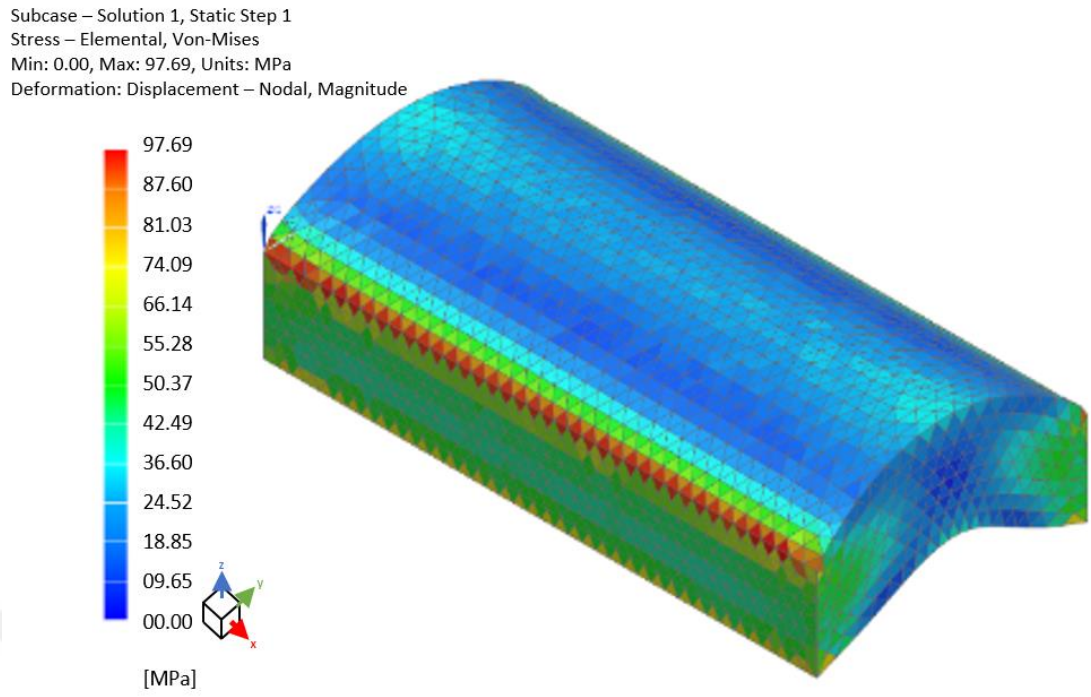

Figure 37C: Finite element analysis with 10 mm mesh size von Mises for AAC Blocks (Baz, 2023)

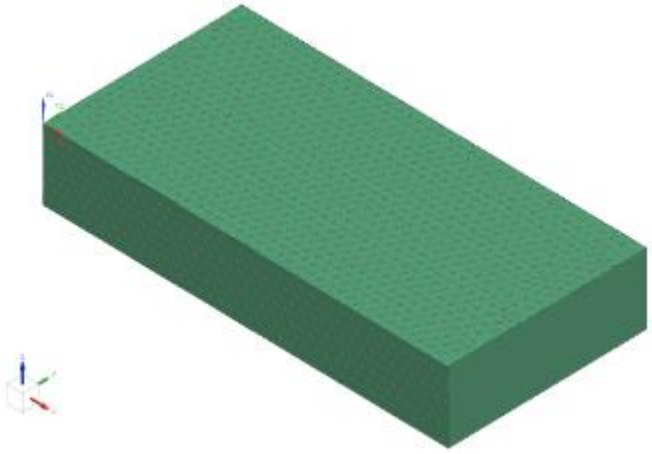

Figure 38A: Finite element analysis with 8 mm mesh size displacements and von Mises stresses (Baz, 2023)

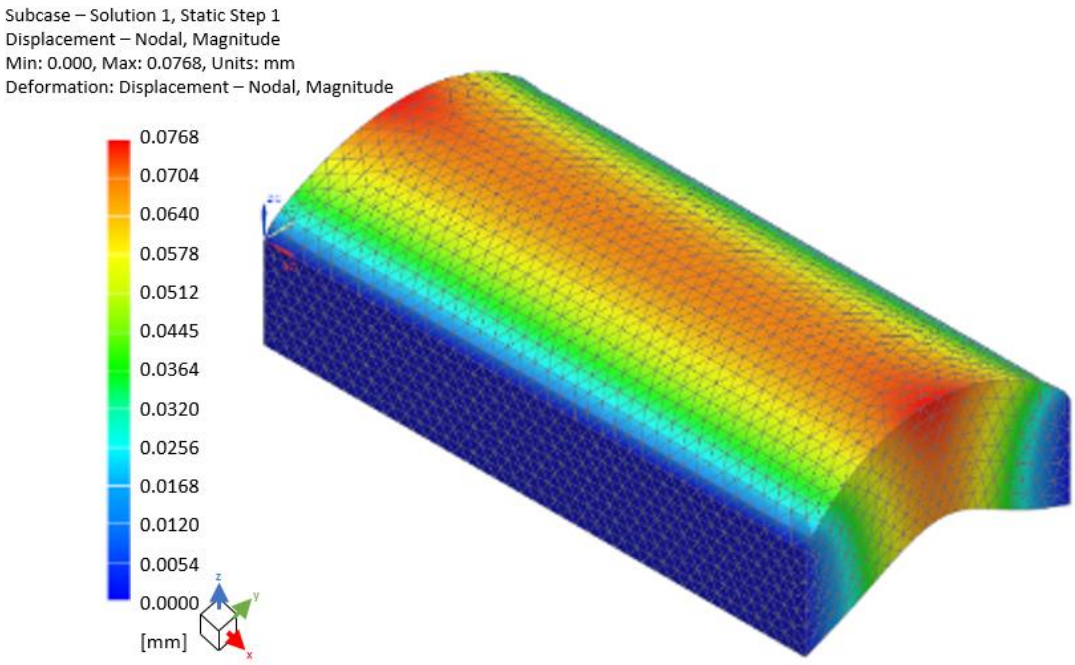

Figure 38B: Finite element analysis with 8 mm mesh size displacements for AAC Blocks (Baz, 2023)

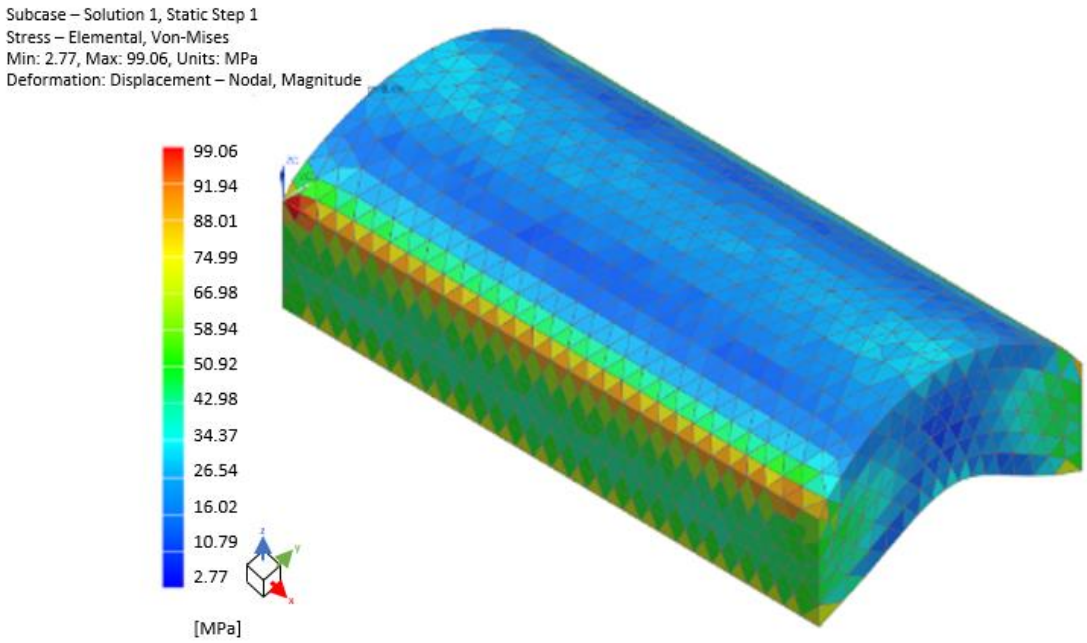

Figure 38C: Finite element analysis with 8 mm mesh size von Mises for AAC Blocks (Baz, 2023)

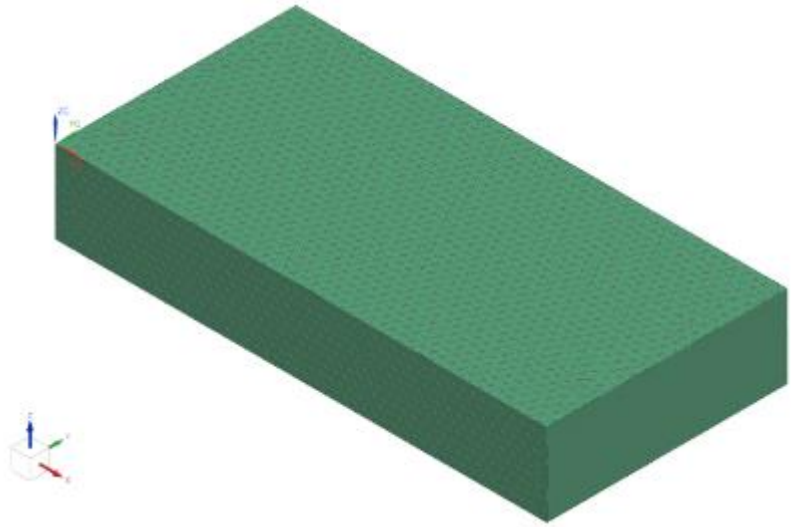

Figure 39A: Finite element analysis with 6 mm mesh size displacements and von Mises (Baz, 2023)

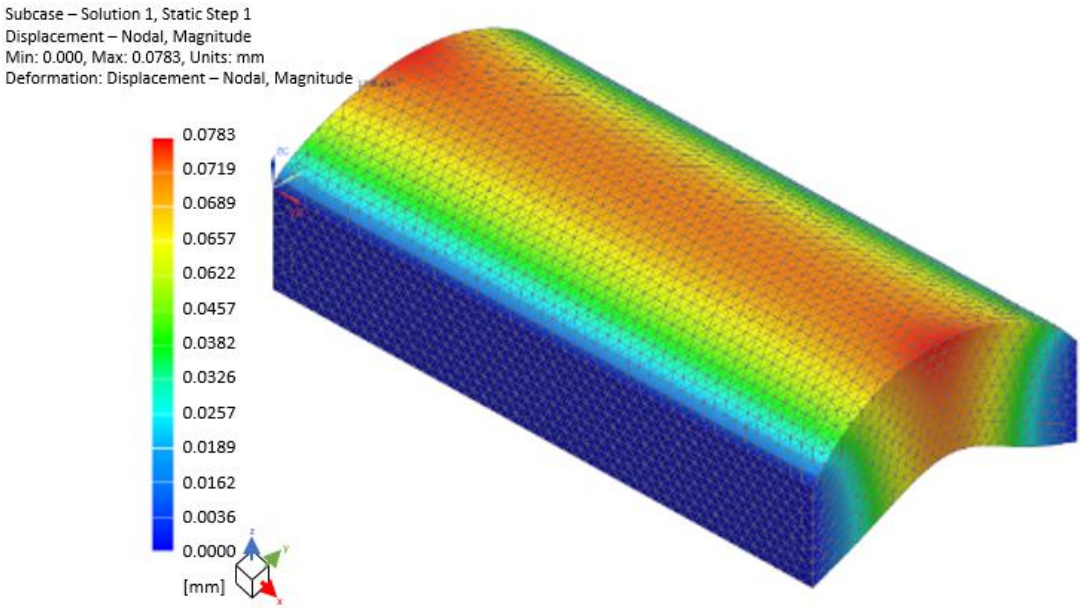

Figure 39B: Finite element analysis with 6 mm mesh size displacements for AAC Blocks (Baz, 2023)

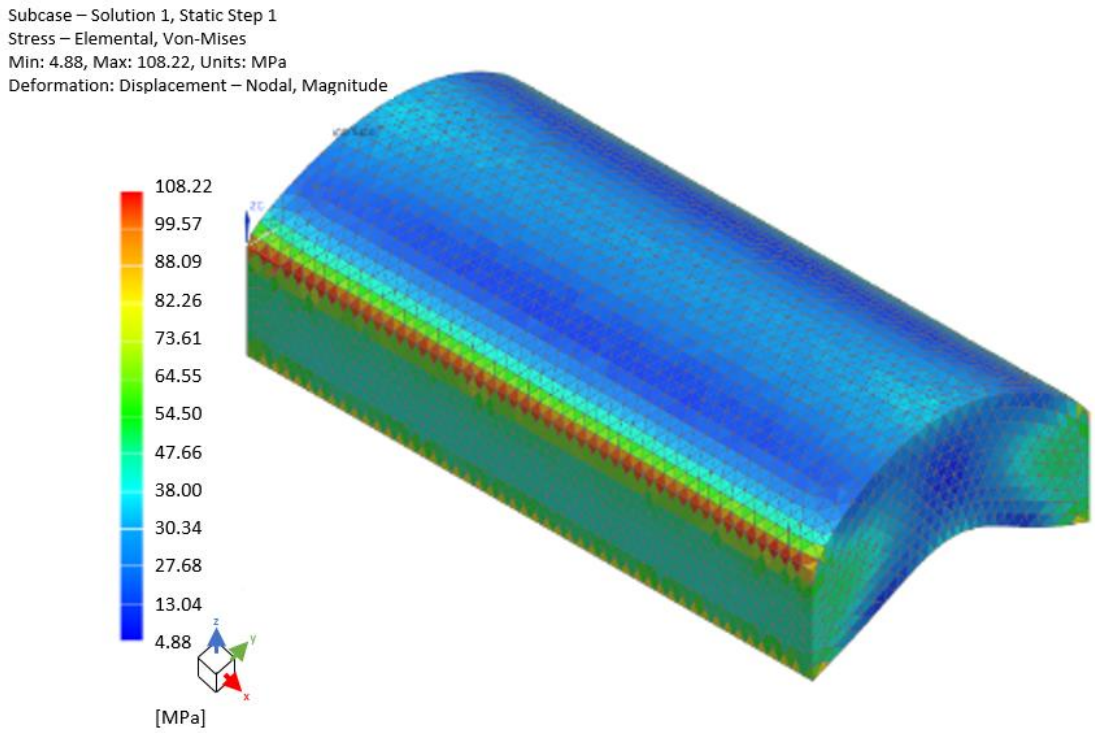

Figure 39C: Finite element analysis with 6 mm mesh size von Mises for AAC Blocks (Baz, 2023)

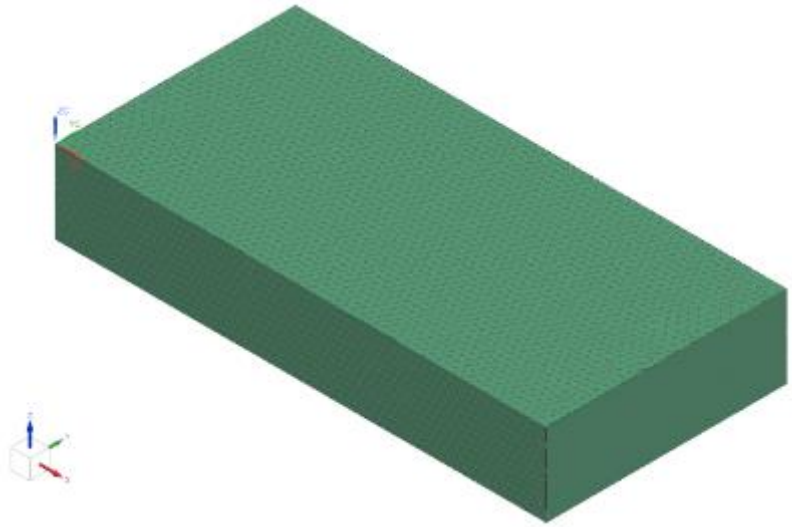

Figure 40A: Finite element analysis with 4 mm mesh size displacements and von Mises (Baz, 2023)

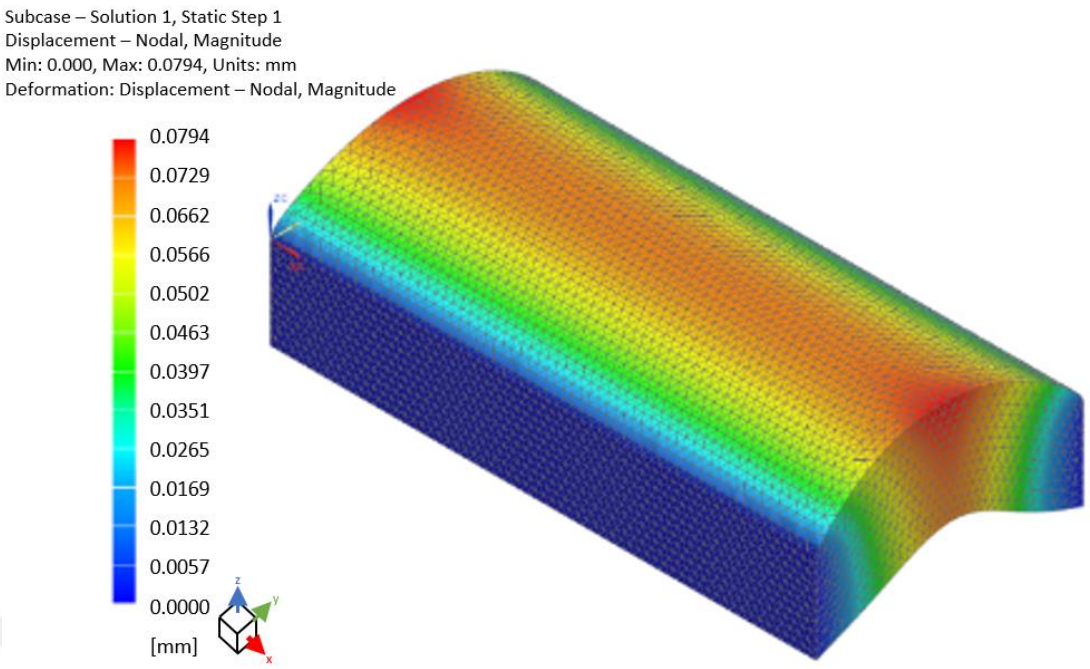

Figure 40B: Finite element analysis with 4 mm mesh size displacements for AAC Blocks (Baz, 2023)

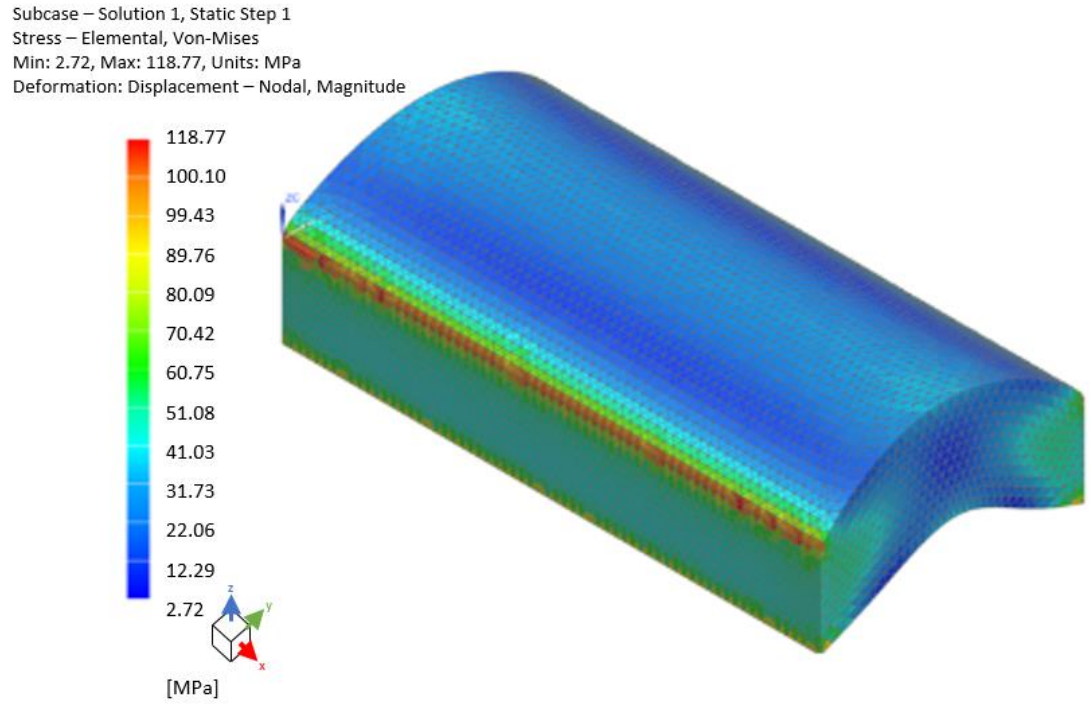

Figure 40C: Finite element analysis with 4 mm mesh size von Mises for AAC Blocks (Baz, 2023)

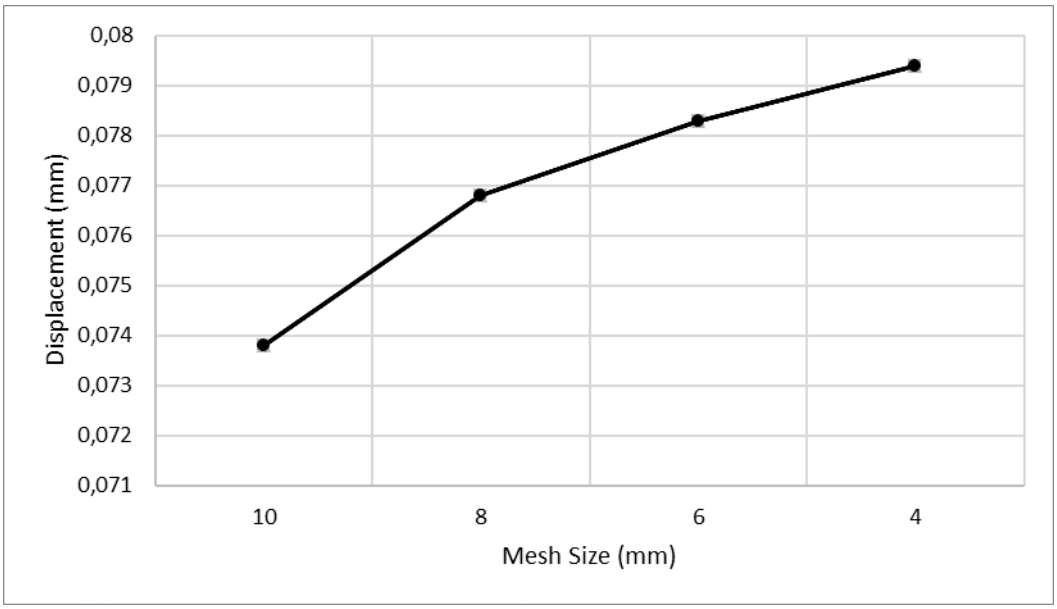

Figure 41: Graph of mesh size vs maximum displacement of AAC Block (Baz, 2023)

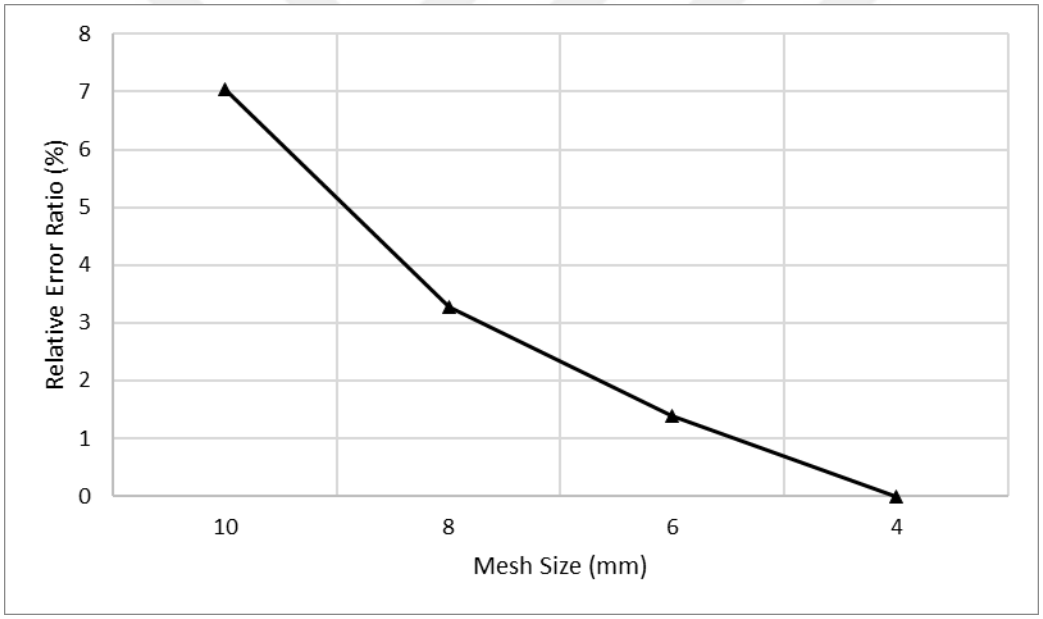

Figure 42: Graph of mesh size vs relative error ratio (%) for the displacement of AAC Block (Baz, 2023)

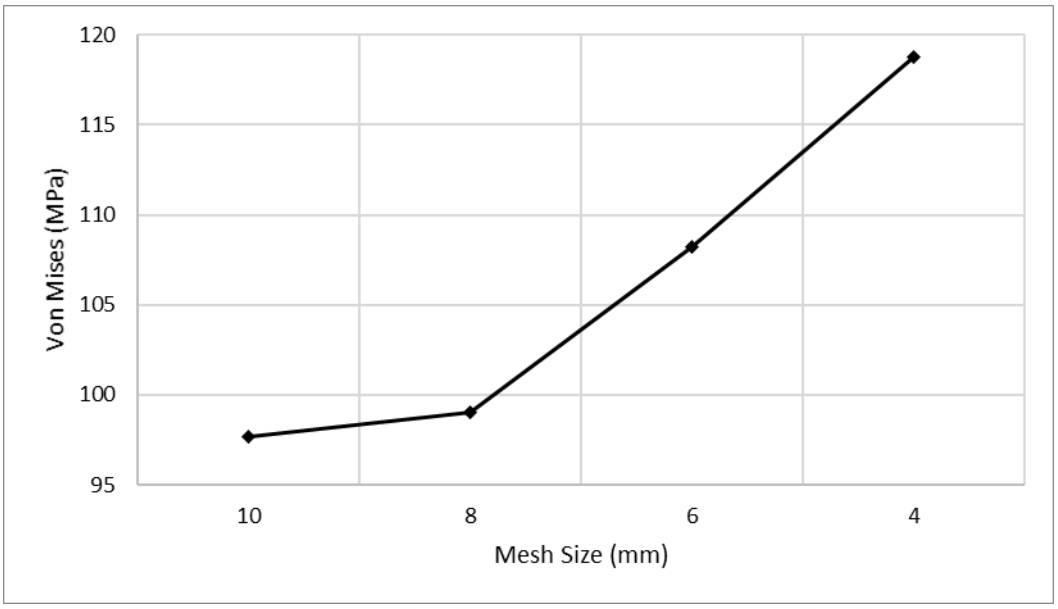

Figure 43: Graph of mesh size vs von Mises of AAC Block (Baz, 2023)

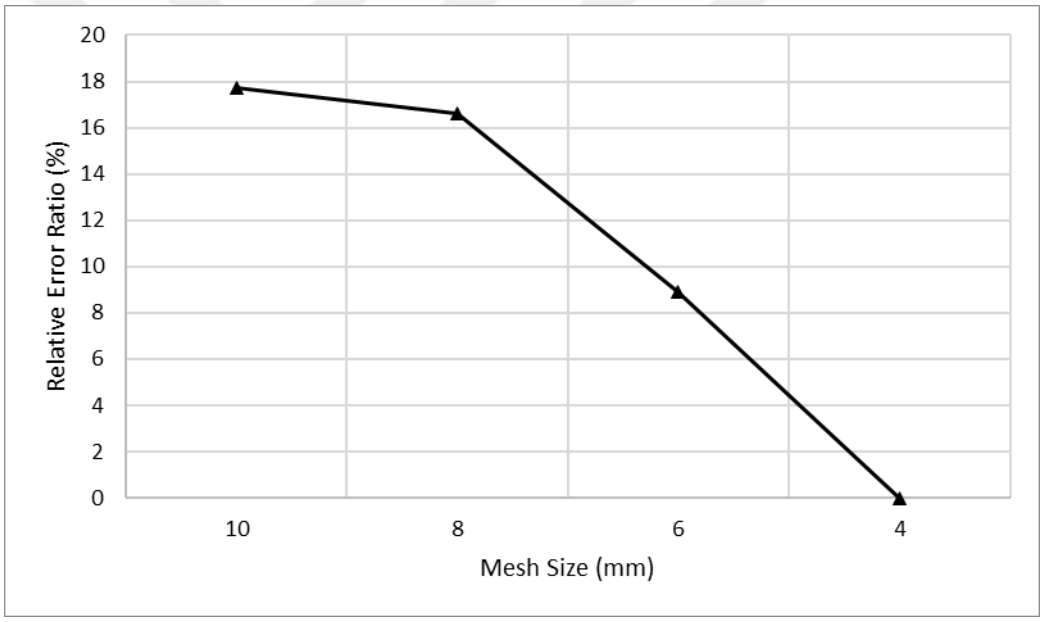

Figure 44: Graph of mesh size vs relative error ratio (%) for von Mises of AAC Block (Baz, 2023)

Figure 45 demonstrates the planar force application from below (it does not matter the direction of the force since the block is homogenous and can be located in both directions while applying), through the Z direction. That is why AAC is a rigid block, there are no holes in it, so the most important issue for AACs is bending. Carrying is not such an important problem for AACs. That is the reason why the simulations are made by considering the possible bending problems in both directions. Especially in

earthquakes, blocks are exposed to various forces from different directions. The strength and weaknesses of those blocks are those possible bending issues under high forces. Figure 45 shows the bending simulation when a distributed force is applied from below on the XZ plane, rectangular side surfaces are fixed, and Figure 46 shows a distributed force applied from below on the YZ plane to the block. For this analysis, the boundary condition is that the rectangular side surfaces are fixed.

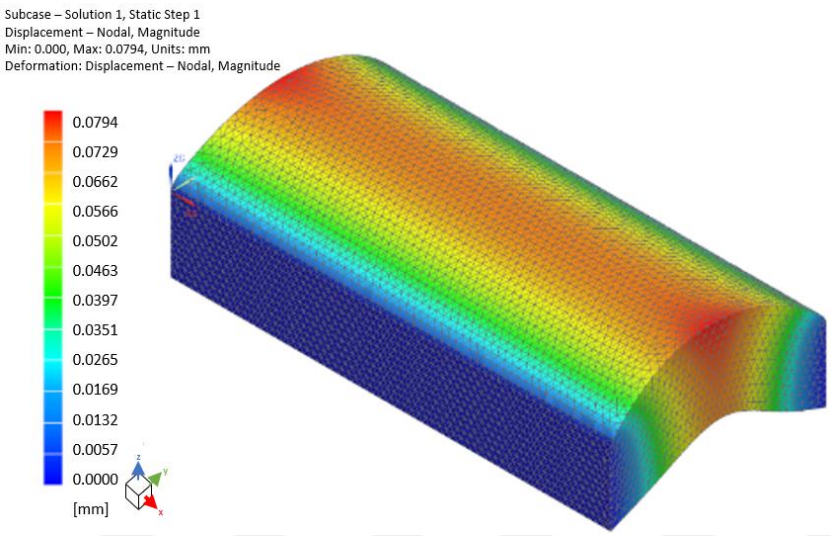

Figure 45: Simulation of Standard AAC Block's Under 300N Distributed Force from Below Middle Parallel to XZ Plane (Baz, 2023)

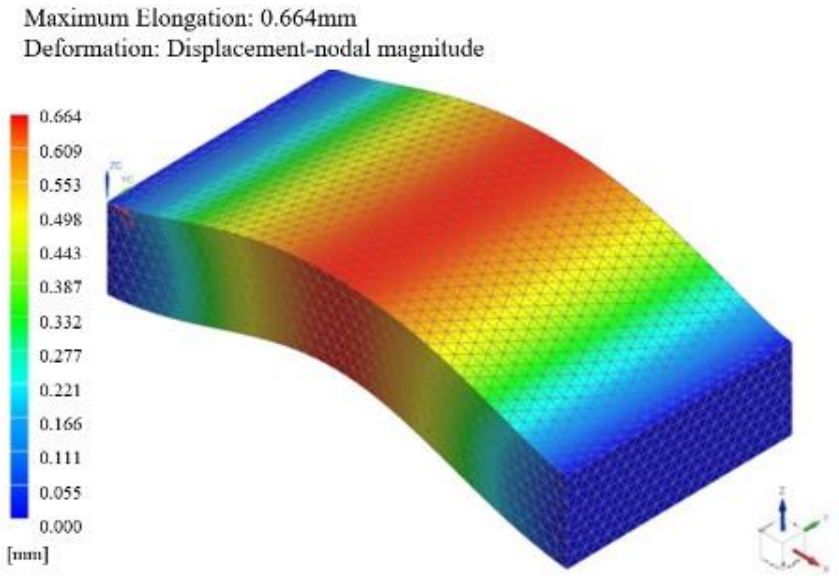

Figure 46: Simulation of Standard AAC Block's Under 300N Distributed Force from Below Middle Parallel to YZPlane (Baz, 2023)

When it is examined the results of the analysis of the pumice and AAC block, it can be implied that the AAC block is stronger, compared with the pumice block since the maximum displacement under the same force is lower than that of the pumice block. That is observed in von Mises stress analysis additionally.

3. ANALYSIS OF THE PROPOSED LIGHTWEIGHT MASONRY UNIT

The masonry unit which is studied provides some solutions to environmental and efficiency problems. In this context, three main aspects of the product will be examined. The first one is its design, the second is its raw material, and the third one is its additive material need. A comparison is made between the developed product and the other two common construction blocks.

3.1 Design

The developed construction block is composed of 6 pieces as shown in Figure 42. The logistics create a remarkable difference. These 6 pieces can be laid down on top of each other and can constitute a very small volume that can easily be shipped and stored in big amounts, with less consumption compared to the other widely used current construction blocks. In the aspects of both volume and mass, the new product brings remarkable advantages.

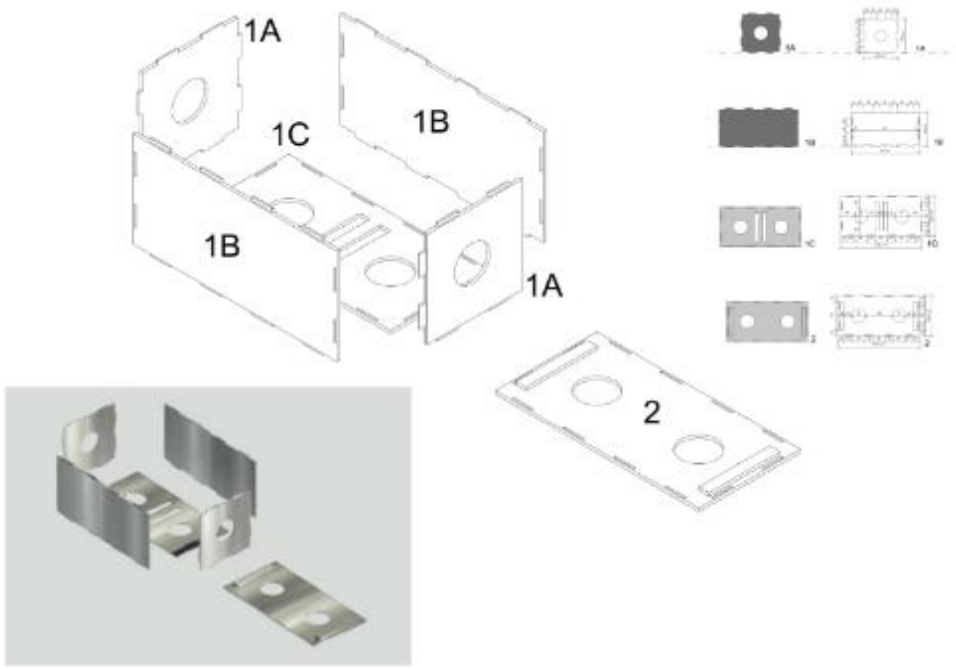

Figure 47: 3D and 2D visuals for the proposed construction block[1] (Baz&Mıhçıoğlu, 2021)

3.1.1 Interlocking Systems

The main cause why the interlocking system is a requirement for this design is the need for efficiency for the volume. The problem is the volume disadvantage of the common blocks since they have rigid bodies, and are not modular. There is an opportunity to store around 3-4 times more products in the same volume if the blocks are generated with interlocking systems. There are bulges and holes in them for interlocking systems. There are two bigger bulges on the top plane surface of the block and there are two other holes for these two on the bottom surface. As done standardly when building a wall with bricks or blocks, the joints are staggered, or are offset, between neighboring courses, the proposed bioplastic blocks are also assumed to be essentially woven together. Together with the interlocking system without any adhesive mortar, this bond will add strength to the construction as in the other cases. So, the blocks can be placed on top of each other, as well as sliding horizontally half-length on the long side.

[1]A national patent application is made and in process at the Turkish Patent Office, proposed by the Patent Evaluation Board of TOBB ETU with the number 2021/011994 since July 2021.

The first interlocking system provides stability between the plane surfaces which forms the bioplastic masonry unit. The second one provides stability between the blocks.

The special design of the proposed masonry unit provides space inside the blocks which can be used to pass all types of building installations, including wiring and plumbing pipes. As shown in Figure 47 there are 6 holes in the blocks. This design results in easy pipeline transfer in both vertical and horizontal directions. This is a clear advantage compared with the other standard systems because, in both of them, the worker has to cut the block or destroy the necessary parts of the wall material to be able to pass building installations.

This also results in a decrease in labor force need, another interlocking system which is within the unit itself forming it, is also very significant, as it provides a decrease in the labor force due to its advantages in logistics. Furthermore, the interlocking system between blocks also decreases the labor force from another point. In standard systems, a mixture is necessary to bind the blocks to each other to keep them together and standing. But, in the developed system, interlocking takes the place of this bonding adhesive. Those mixtures are generally cement-based materials. So, this system decreases the environmentally hazardous effects comparatively.

The last notable aspect is the strength of the product when compared with that of AACs and standard concrete masonry units.

Table 5 under section 4.1.1 shows the compressive stress of the autoclaved aerated concrete (AAC) blocks. Also, when related literature is checked, it is observed that it is around 20 MPa.

For the pumice block under standard conditions, it is seen that it is about 3 MPa when the same dimensioned AAC masonry units are compared with concrete masonry units, it is seen that AAC is about four times stronger than concrete masonry units.

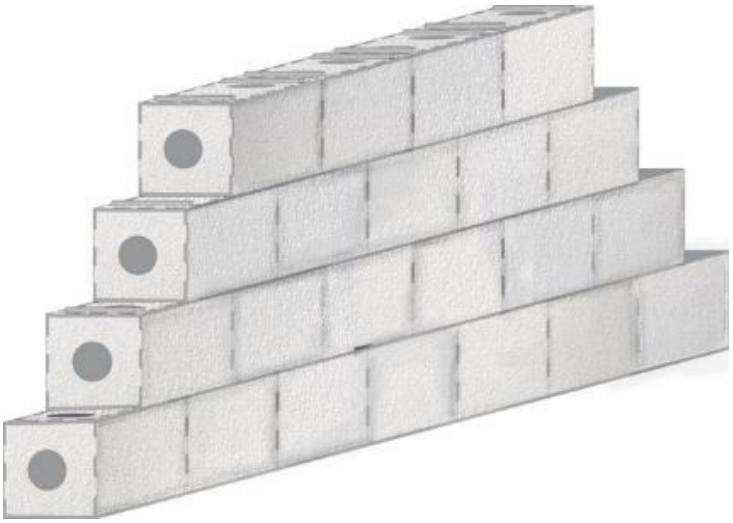

Figure 48**:** 3D visual of the wall built with the proposed construction blocks (Baz & Mıhçıoğlu, 2021)

3.1.2 Alternatives with Similarities

The proposed lightweight masonry unit has been examined for a patent application by TOBB ETU's Technology Transfer Office and its contracted patent office. After a thorough examination, it has been decided to apply first for a national, then for an international patent (2021/011994,29/07/2021). After two years of investigation on similar patents from all over the world, the investigation report dated 24/02/2023 was received. According to this report, there is only one patent with high similarity and two patents with low similarities. These will be examined as follows.

The first patented product is the only one with some similar properties. The patent number is US5664387A and the drawings are in Figure 49.

From the aspect of the design, it can be said that the interlocking systems can have some similarities. In this design, there are also two interlocking systems within the unit. One is for the interlocking of the unit itself and when it is examined, the parts which are coming together for assembling the unit are different from each other and it is necessary to select the appropriate one for bringing together. As an advantage, it does not require any materials like iron sticks or aggregate to obtain durability.

For practical use for the applier, it can be difficult to select and combine, and for the manufacturing process, there can also be some difficulties and problems. The main difference can occur in the manufacturing process, as there are many holes and small joints to provide durability. Such a bioplastic or sustainable material manufacturing

process will not be appropriate for this kind of design because the molding process brings some difficulties when it has been considered the raw material. This design is decided to be more appropriate for CNC laser cutting machines and more rigid bodies. Moreover, this unit does not allow the pipelines for any direction. It can provide storage and logistic advantages. The unit is also modular in itself, as a unit. There are storage and logistic advantages, but raw material is not mentioned specifically as bioplastics, or made of sustainable or eco-friendly materials.

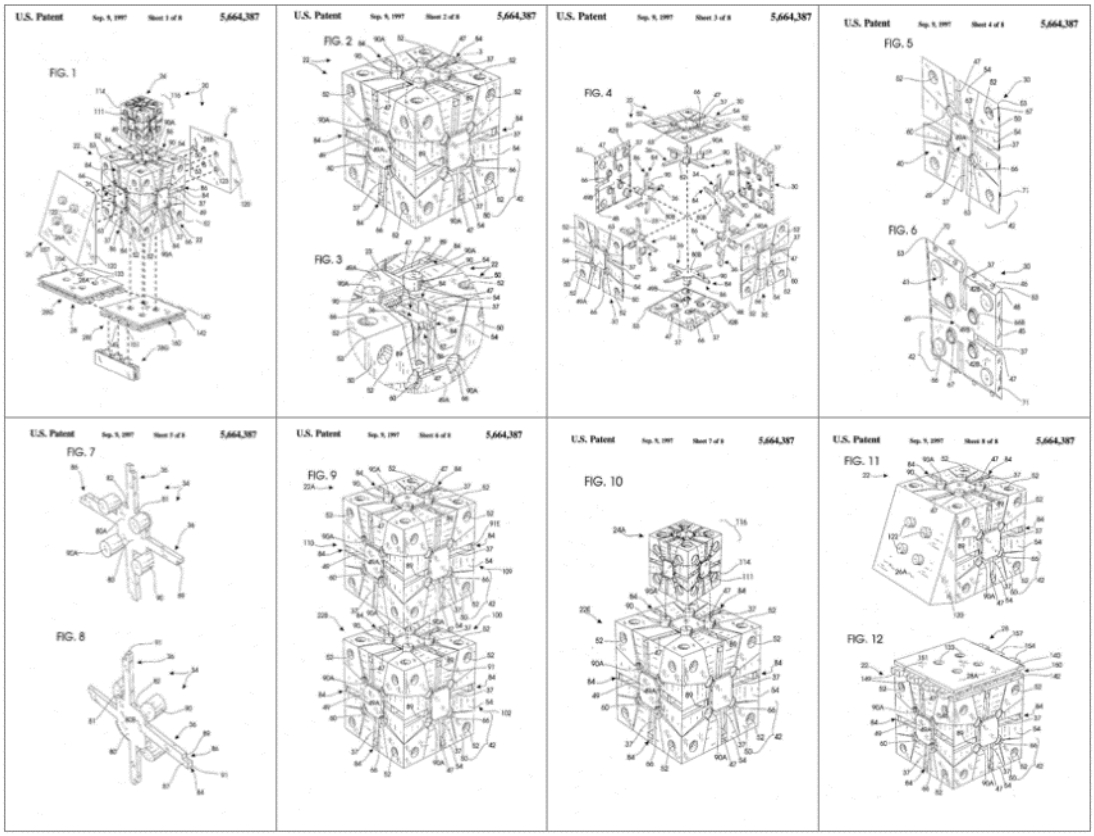

Figure 49**:** Drawings of patent US5664387A (Bhatti, 1997)

The second is the product with the patent number US2016281357A1 shown in Figures 50A-50B and 50C. This patent includes some extra material to obtain durability. As it is shown on the drawings, holes on the unit are for a rope. The unit provides durability with the help of the rope. The product allows the installation of the pipelines inside the wall in just one direction. Parts assembling the unit require different manufacturing processes since the design is not uniform. The unit is modular in itself and provides storage and logistic advantages. The raw material is not mentioned at all, including bioplastics or any sustainable or eco-friendly materials.

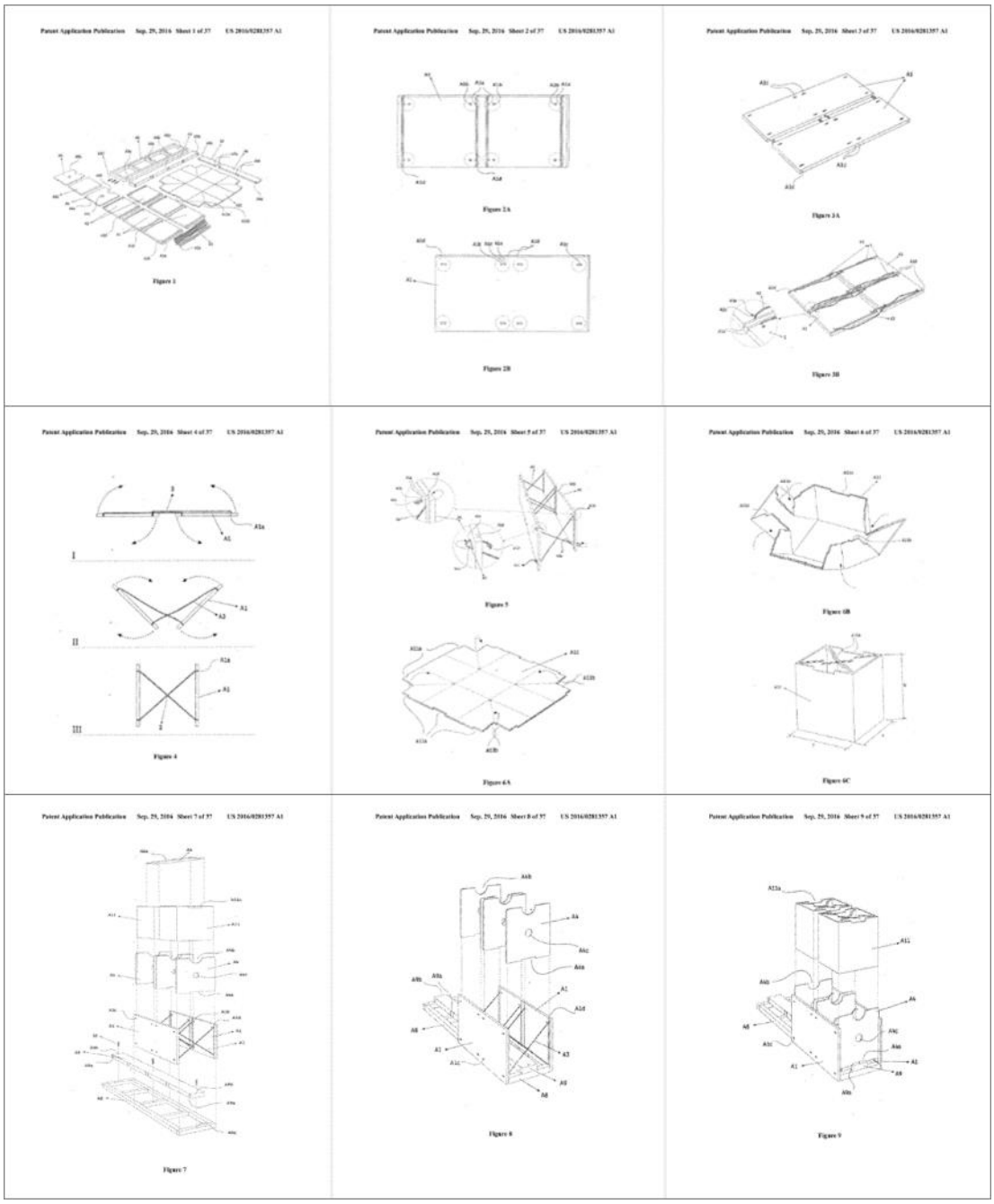

Figure 50A**:** Drawings of Patent US2016281357A1 (Arıbaş & Özler, 2016)

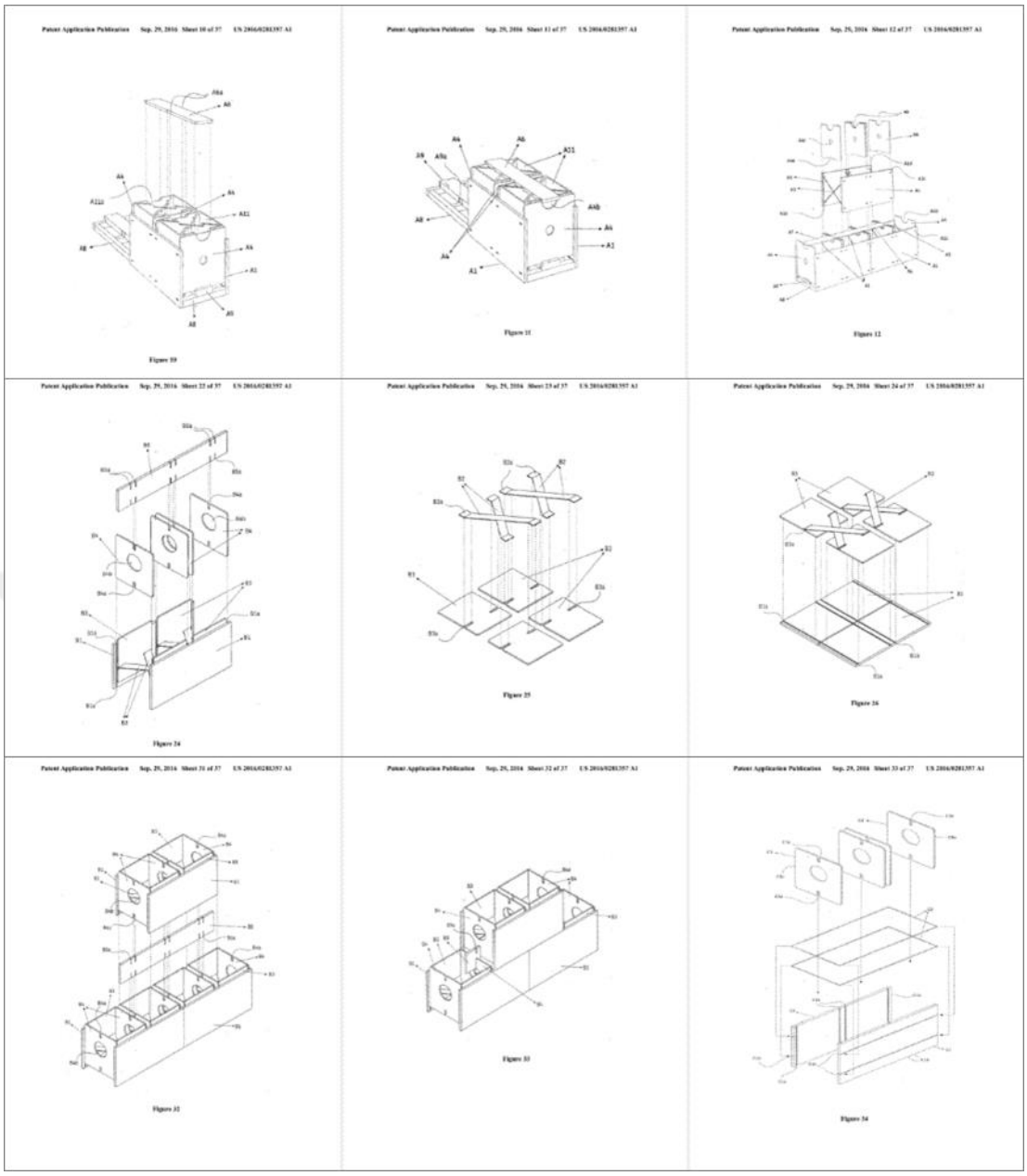

Figure 50B**:** Drawings of Patent US2016281357A1 (Arıbaş & Özler, 2016)

The third product is the one with the patent number CZ35145U1 in Figure 51. This patent includes a uniform unit which is not modular itself, but modular when the units come together. The unit is a rigid body and does not allow or support the installation of the pipelines through the wall. The parts constituting the unit require different manufacturing processes since their forms are not the same. The unit is not modular in itself and requires differently shaped parts while interlocking. It is understood that there are no storage or logistic advantages. The raw material is not mentioned as bioplastics or such a sustainable or eco-friendly material.

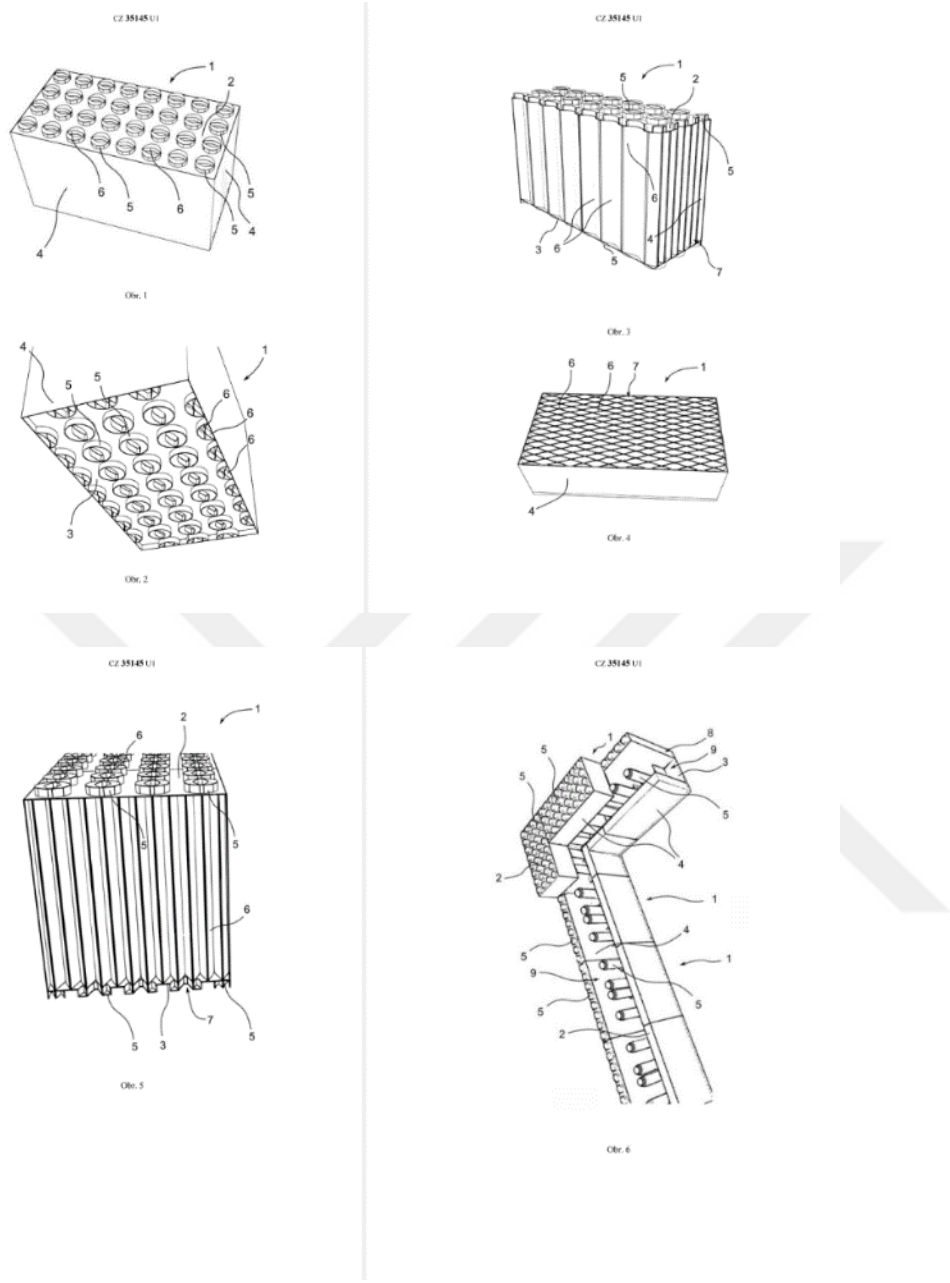

Figure 51**:** Drawings of patent CZ35145U1 (Hajek & Sitar, 2021)

In addition to four patents that the Turkish Patent Institute found and mentioned in its investigation report, four other patents were found before the report during the literature research.

The fourth patent is the one with the patent number US6088987. This patent includes some iron parts to obtain durability. As it is shown in the drawings in Figure 52, the three holes on the unit are for sticks for strengthening. It uses iron sticks in both

directions, Furthermore, there are also some iron joints for durability. The patented product does not allow the installation of pipelines inside the wall. Parts generating the unit require different manufacturing processes since their designs are not uniform. The unit is not modular in itself. There are no storage or logistic advantages. The raw material is mentioned and understood to be not bioplastic or such a sustainable, eco-friendly material.

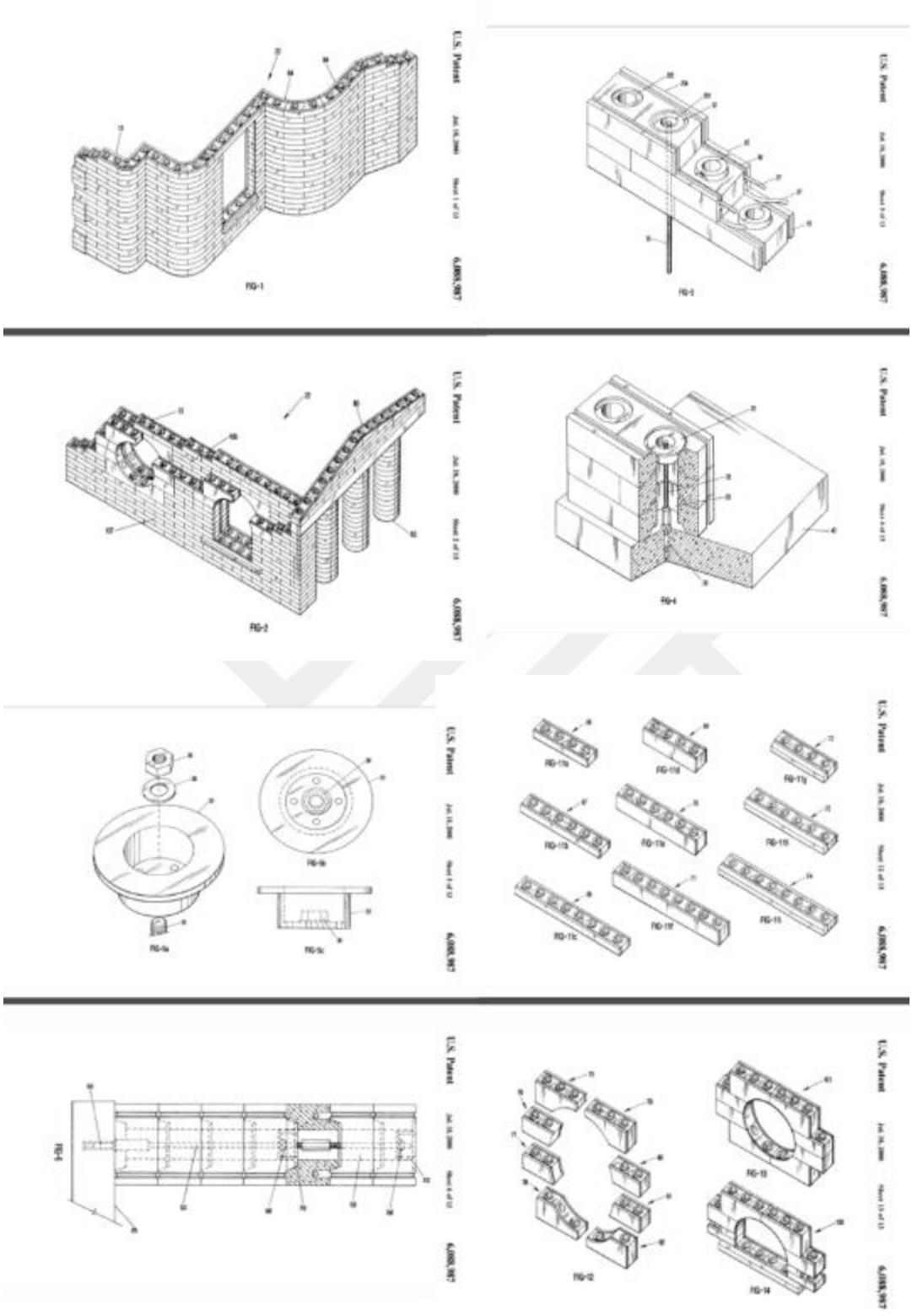

Figure 52: Drawings of patent US6088987 (Simmons & Simmons,2000)

The fifth patent is the one with the patent number US5024035 as shown in Figure 53. This patent includes some extra aggregate-like material to obtain durability. As it is shown on the drawings, holes on the unit are for that aggregate. After the placement that aggregate will be fulfilled inside the units. The product does not allow or support pipelines to be installed through the walls. The components of the product require different manufacturing processes since the design is not uniform. The product unit is not modular in itself. There are no storage or logistic advantages. The raw material is not mentioned at all, including bioplastics or any sustainable or eco-friendly materials.

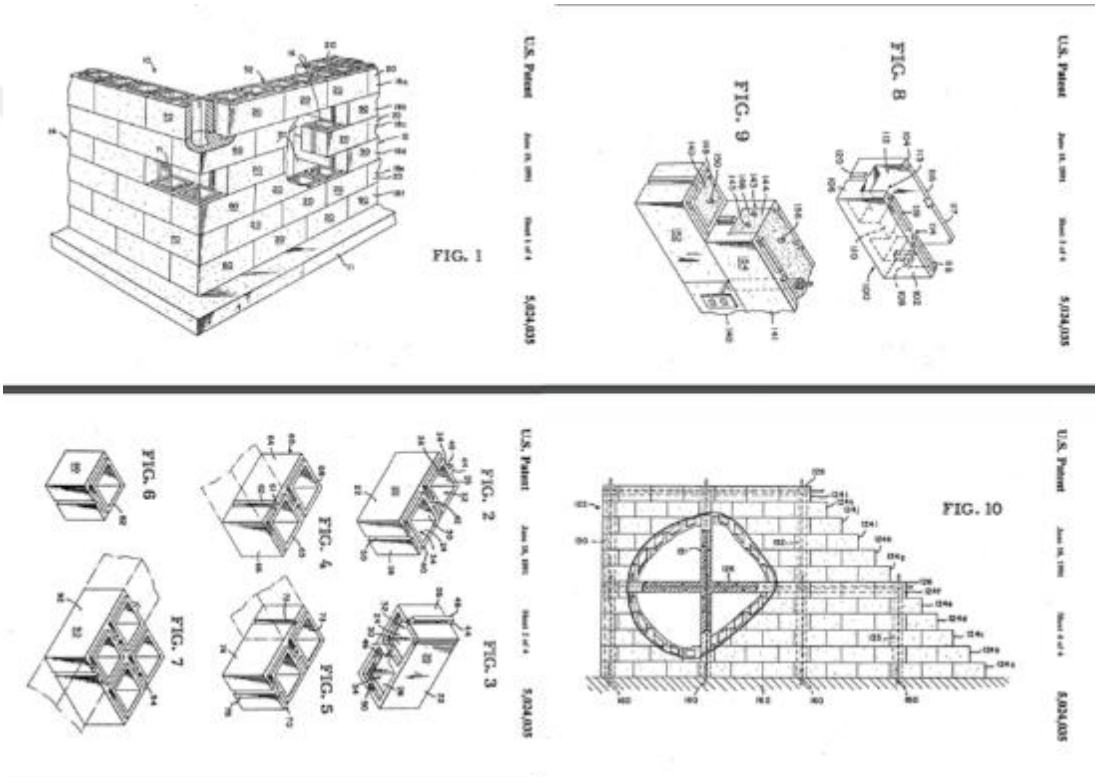

Figure 53: Drawings of patent US5024035 (Hanson &Inness, 1991)

The sixth patent is the one with the patent number CN2532140Y in Figure 54. This patent includes some iron sticks to obtain durability. As shown in the drawings, the three holes on the unit are for sticks to strengthen the wall's durability, which is generated by those bricks. The patented product does not allow or support the installation of the pipelines inside the wall. Parts assembling the unit require different manufacturing processes since designs are not uniform. The unit is not modular in itself. There are no storage or logistic advantages. The raw material is not mentioned, including bioplastics or any type of sustainable, or eco-friendly materials.

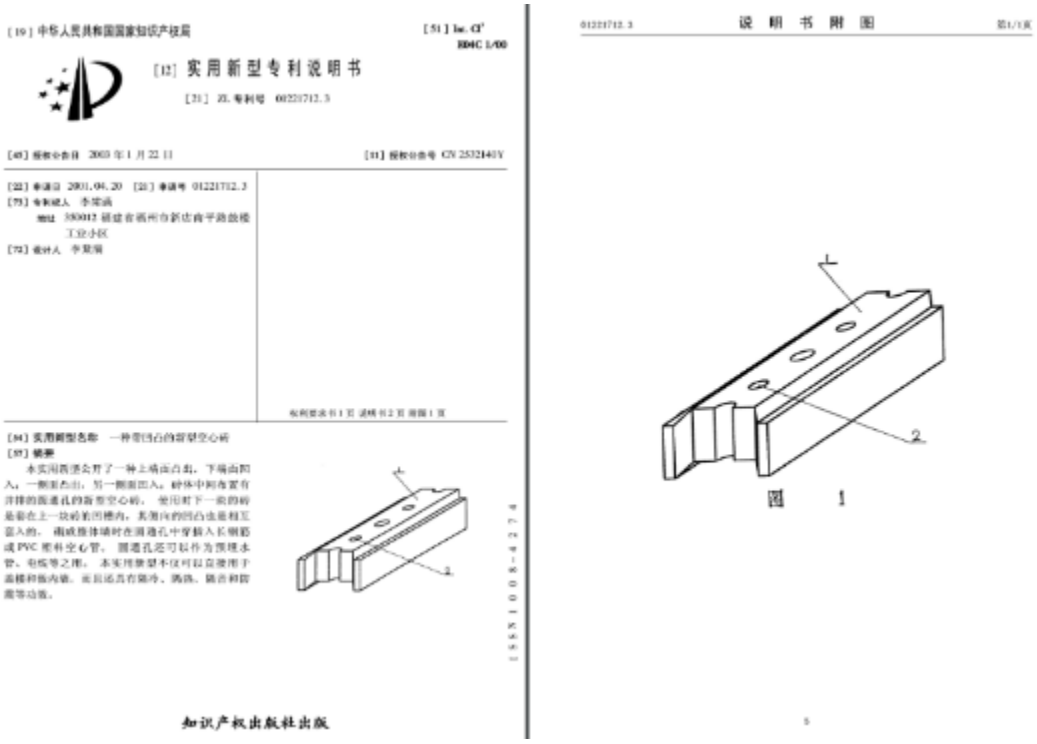
[19] 中华人民共和国国家知识产权局

[12] 实用新型专利说明书

[11] 授权公告号 CN 2532140Y

[22] 申请日 2001.09.20 [21] 申请号 01221712.3

[73] 专利权人 李双福

[72] 设计人 李双福

[54] 实用新型名称 一种带凹台的容腔空心砖

[57] 摘要

知识产权出版社出版

01221712.3 说 明 书 附 图 第1/1页

图 1

Figure 54**:** Drawings of patent CN2532140Y

The last patent is the one with the patent number KR101429894B1 as shown in Figure 55. This patented product includes some iron sticks to obtain durability. It does not allow or support the installation of pipelines inside the walls. The parts assembling the unit requires different manufacturing processes since designs are not uniform. The unit is not modular inside itself. There are no storage or logistic advantage. The raw material is not bioplastic or such a sustainable, eco-friendly material.

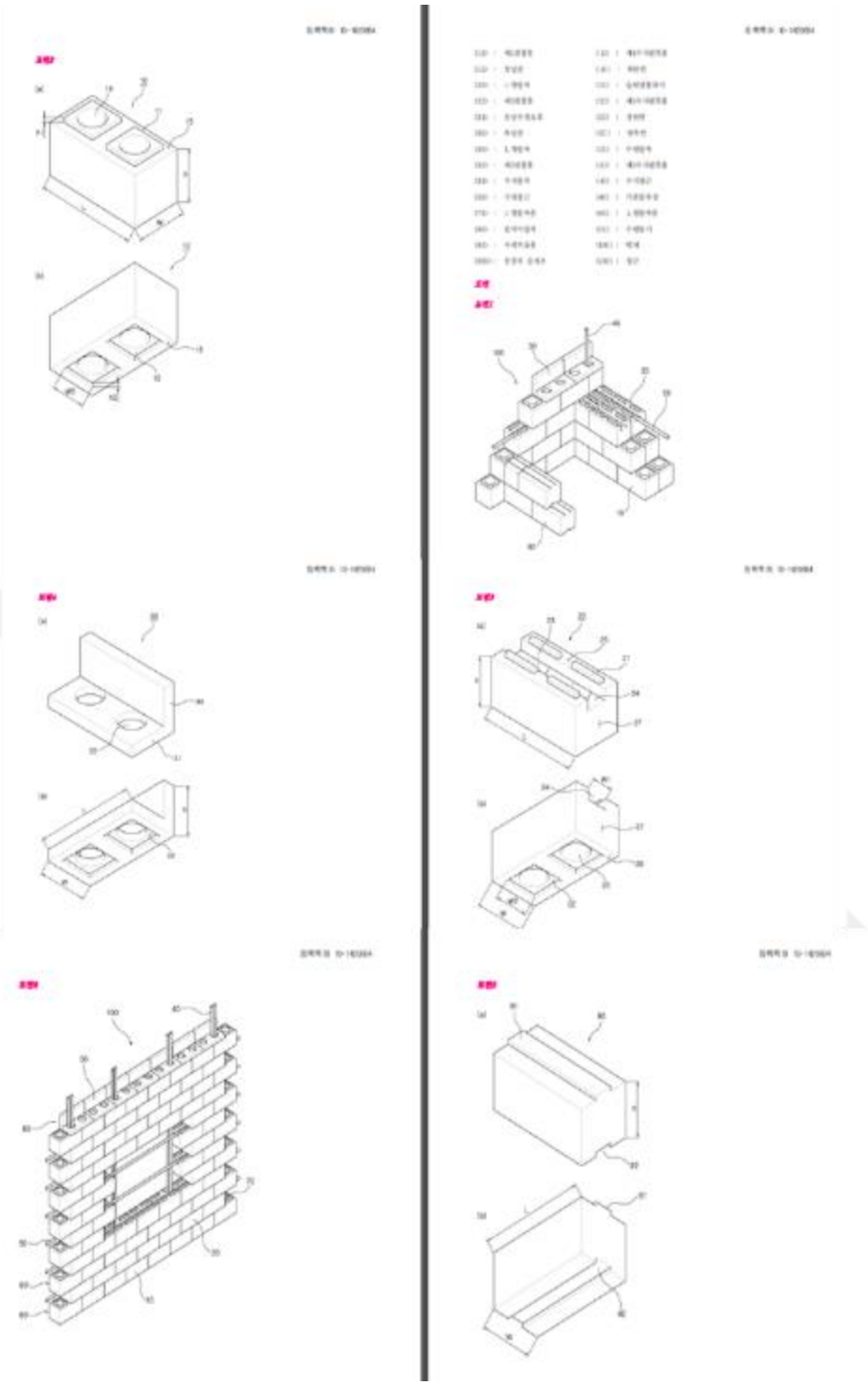

Figure 55: Drawings of Patent KR101429894B

3.2 Finite Element Analysis of the Proposed Modular Masonry Block

The strength of the proposed block under a certain static load is another issue. To address this issue, static finite element analysis of the proposed block was performed in this study using the Siemens NX software. A linear isotropic material was used with a modulus of elasticity of 2.24 GPa and Poisson's ratio of 0.38 ul that of ABS plastic material. These material properties are listed in Table 4 (Url-11).

Table 4: Physical and Mechanical Properties of ABS Plastics used in the finite element analysis of the proposed masonry block (Url-11)

Strength at Break (Tensile)	29.8 – 43 Mpa
Strength at Yield (Tensile)	29.8 – 48 Mpa
Toughness (Notched Izod Impact at Room Temperature)	200 - 215 J/m
Toughness at Room Temperature (Notched Izod Impact at Room Temperature)	20 – 180 J/m
Young Modulus	1.79 – 9.2 GPA

ABS plastic was used in this study as a representative material in the finite element analysis because its material properties have similarities with standard bioplastics without any remarkable additive support like lignocelluloses or a consistently durable amount of graphene oxide.

3.2.1 Boundary Conditions and Force

A distributed force of 300 N has been applied on the upper surface, and all nodes on the lower face are constrained. This way, the maximum load must be handled by the unit at the bottom, as mentioned in the finite element analysis of the pumice block in Section 2.3.

3.2.2 Mesh Refinement

A mesh refinement study was done to identify the most appropriate mesh size for the finite element analysis. The boundary condition is the bottom surface is fixed to the ground. Different mesh sizes of 8mm, 6 mm, 4.5 mm, 4 mm, and 3.7 mm were analyzed for obtaining the optimum one. Figures of analysis are listed below in Figure

56 to 60 with different mesh sizes respectively. In Figure 61 maximum displacement values are examined and in Figure 63 von Mises stress values are examined. Because of the convergence of the values the 4 mm mesh size has been chosen.

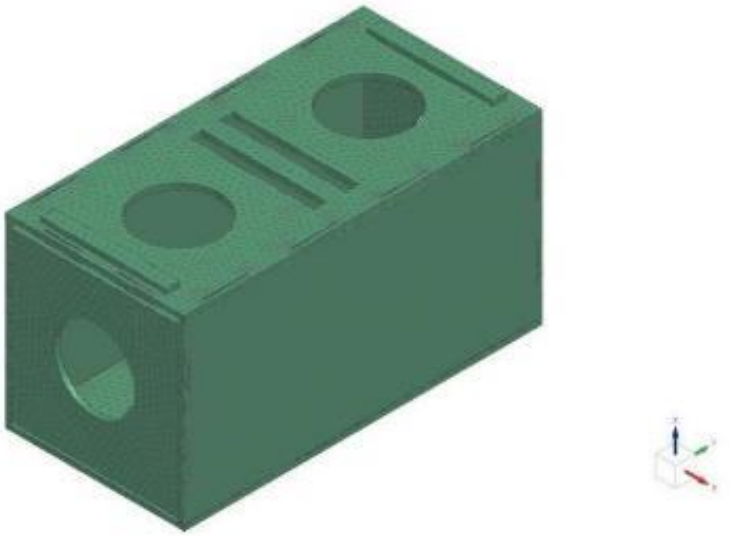

Figure 56A: Analysis under 8 mm mesh size (Baz, 2023)

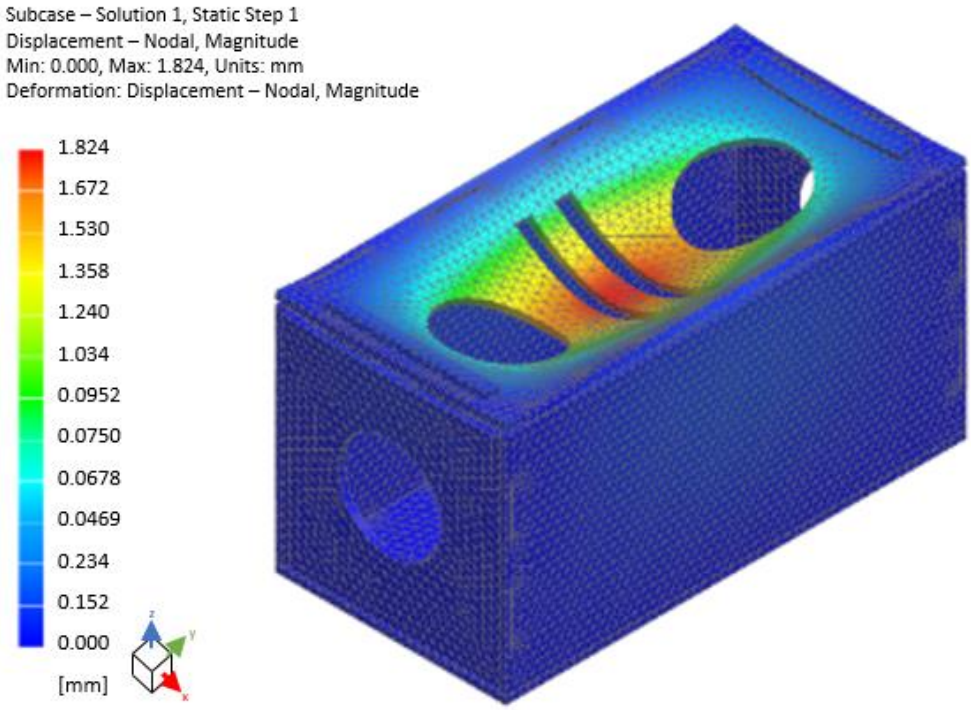

Figure 56B: Analysis under 8 mm mesh size displacement (Baz, 2023)

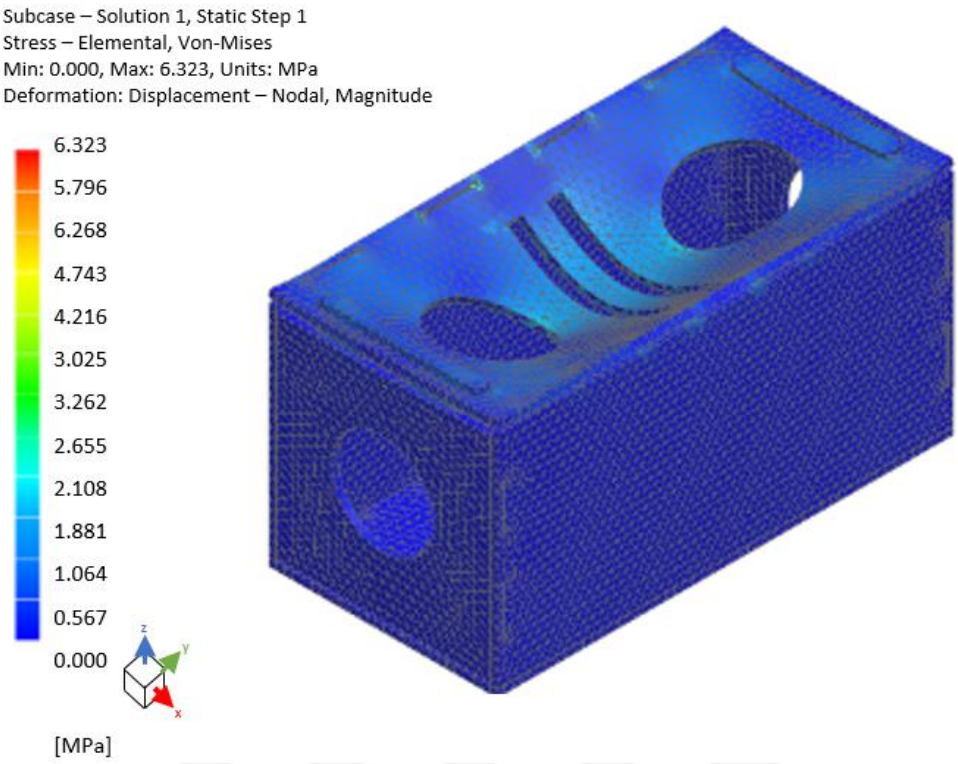

Figure 56C: Analysis under 8 mm mesh size von Mises (Baz, 2023)

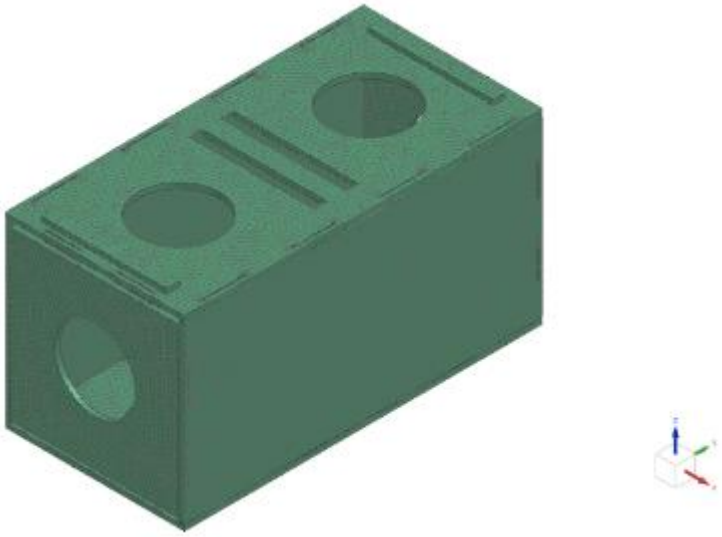

Figure 57A: Analysis under 6 mm mesh size (Baz, 2023)

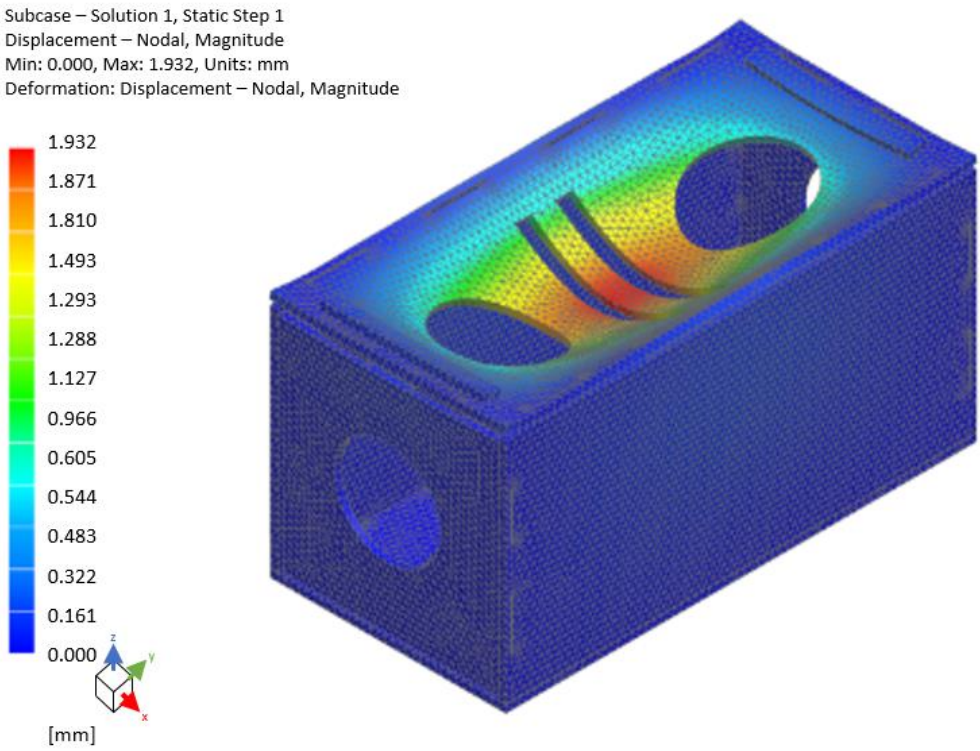

Figure 57B: Analysis under 6 mm mesh size displacement (Baz, 2023)

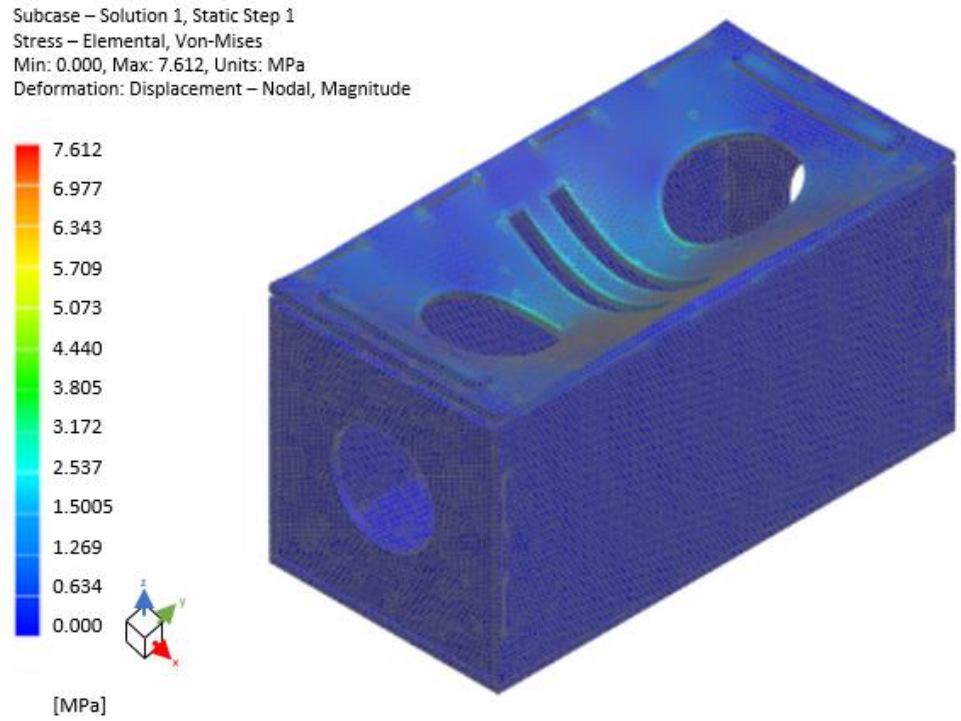

Figure 57C: Analysis under 6 mm mesh size von Mises (Baz, 2023)

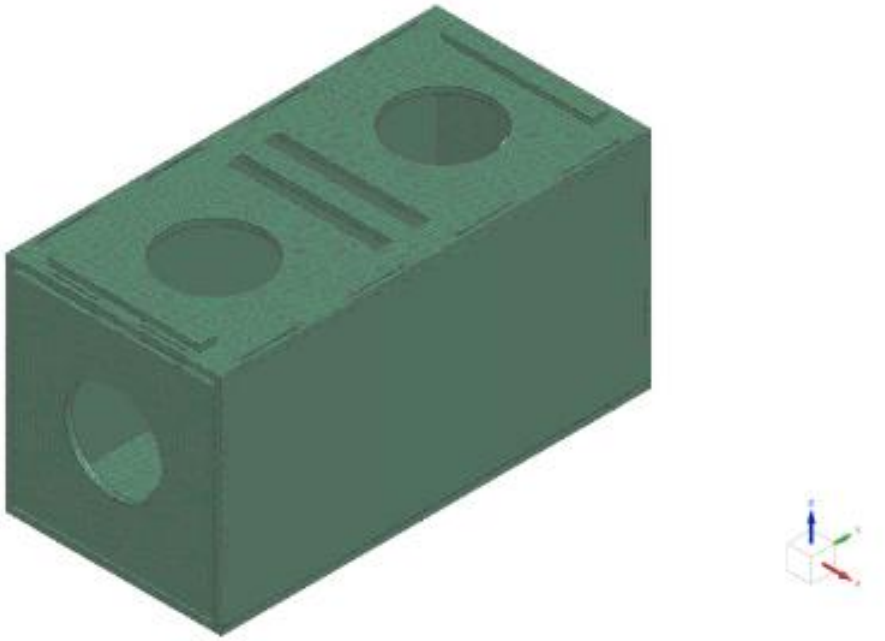

Figure 58A: Analysis under 4,5 mm mesh size (Baz, 2023)

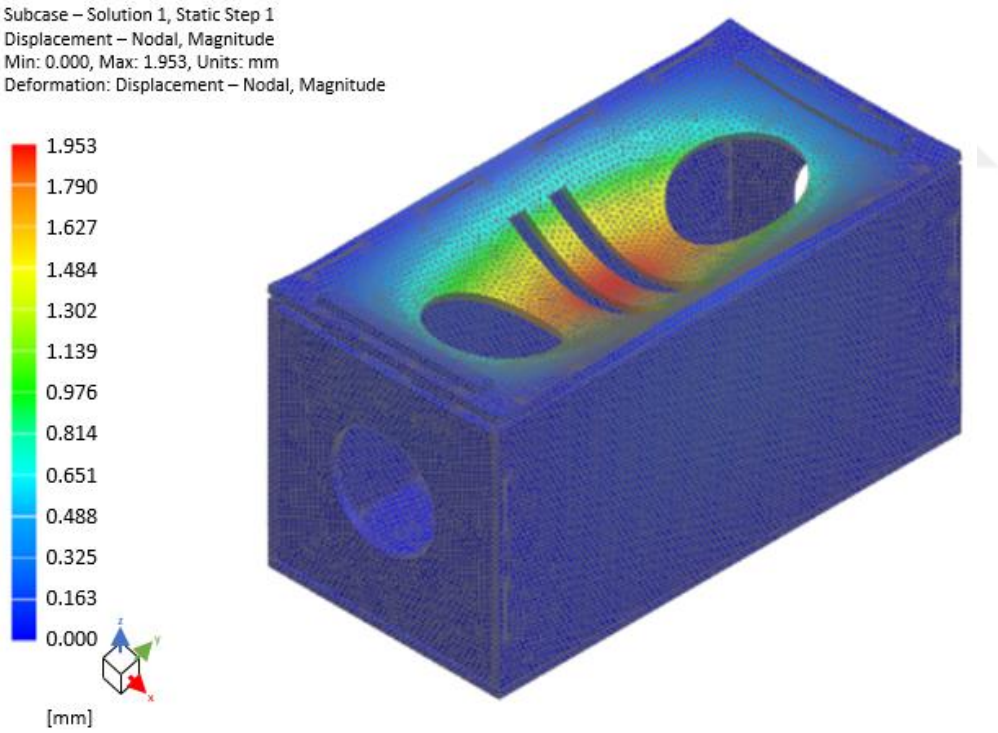

Figure 58B: Analysis under 4,5 mm mesh size displacement (Baz, 2023)

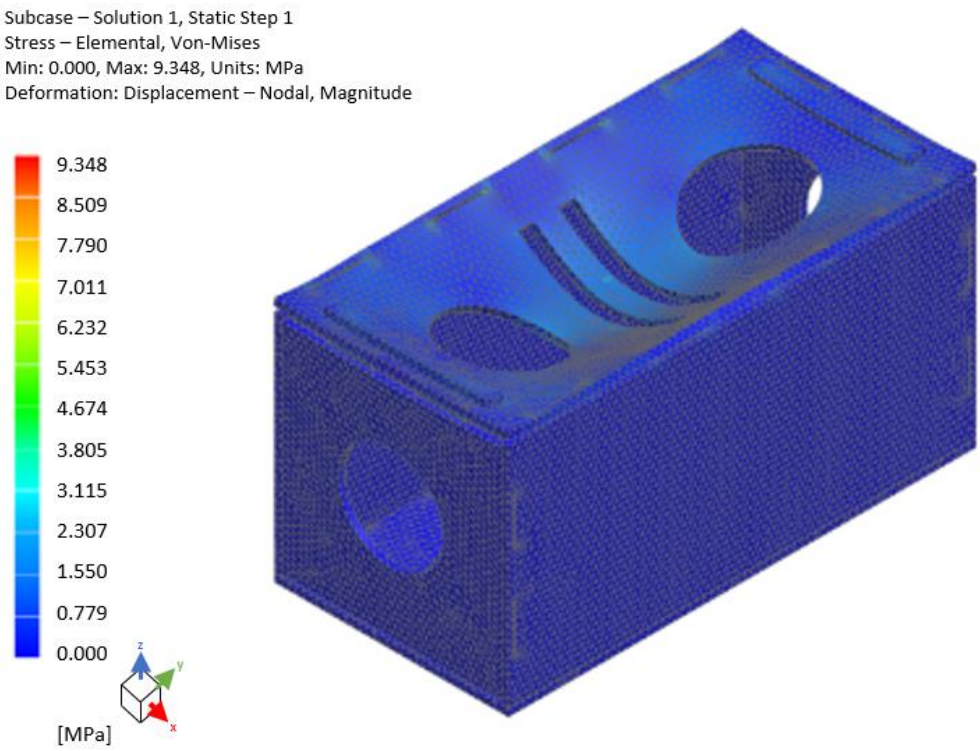

Figure 58C: Analysis under 4,5 mm mesh size von Mises (Baz, 2023)

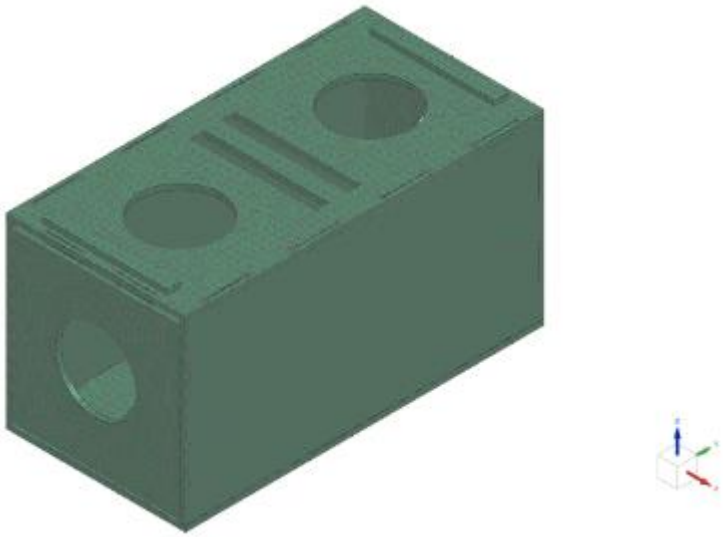

Figure 59A: Analysis under 4 mm mesh size (Baz, 2023)

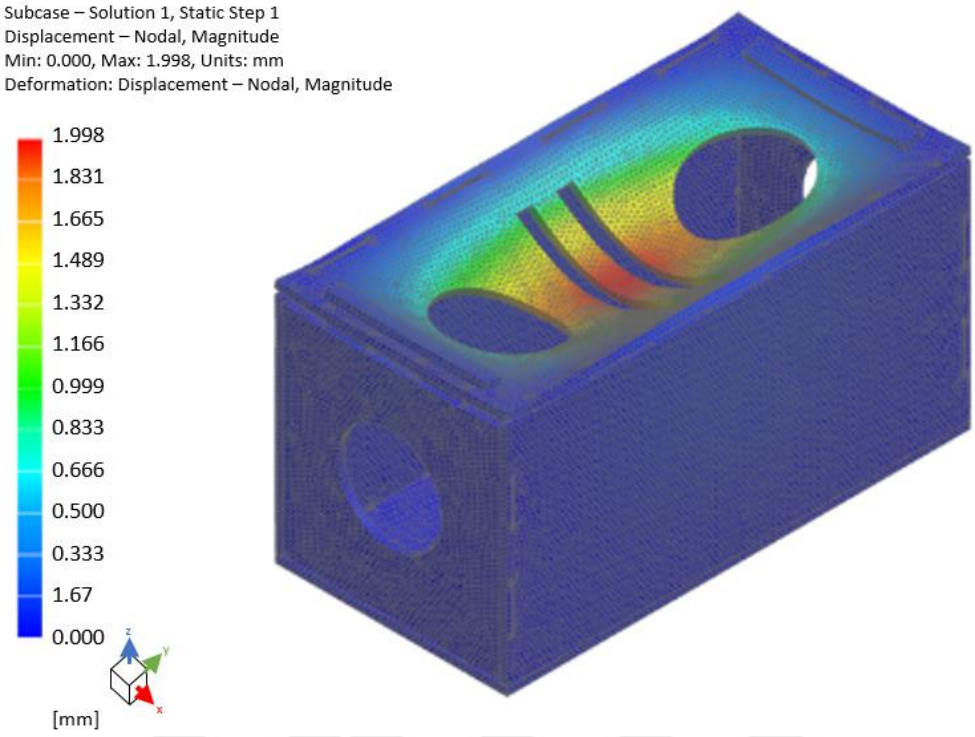

Figure 59B: Analysis under 4 mm mesh size displacement (Baz, 2023)

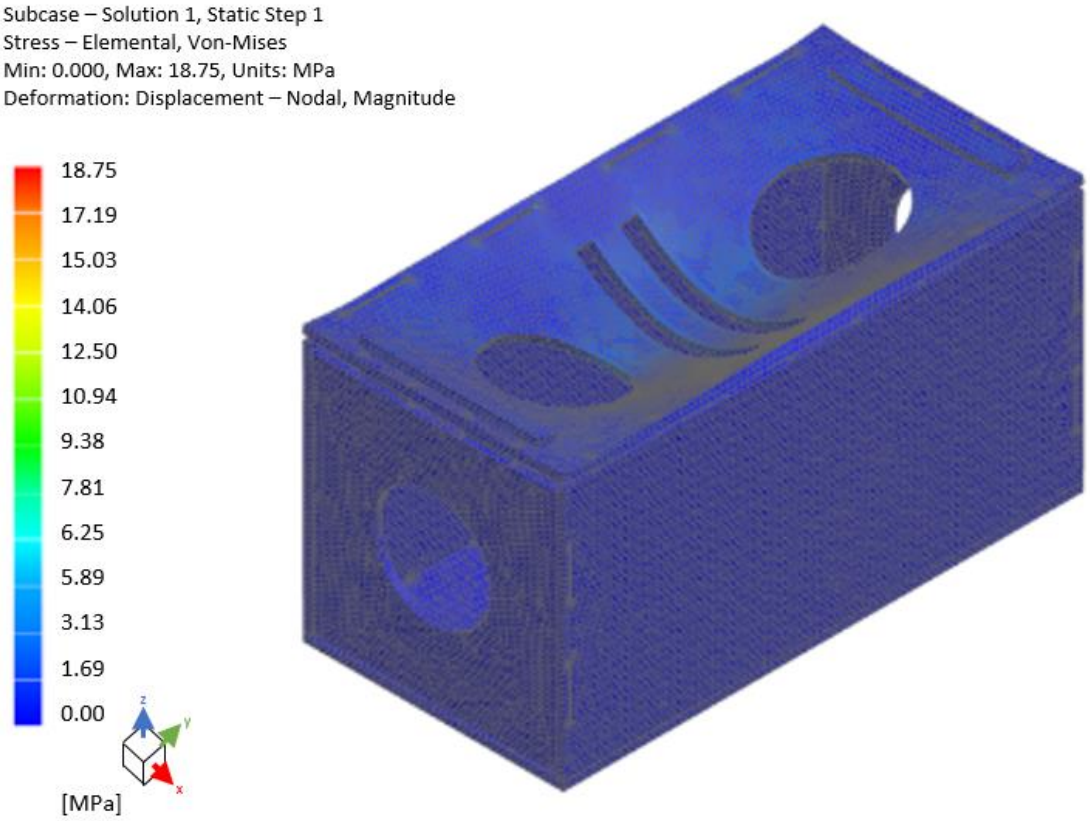

Figure 59C: Analysis under 4 mm mesh size von Mises (Baz, 2023)

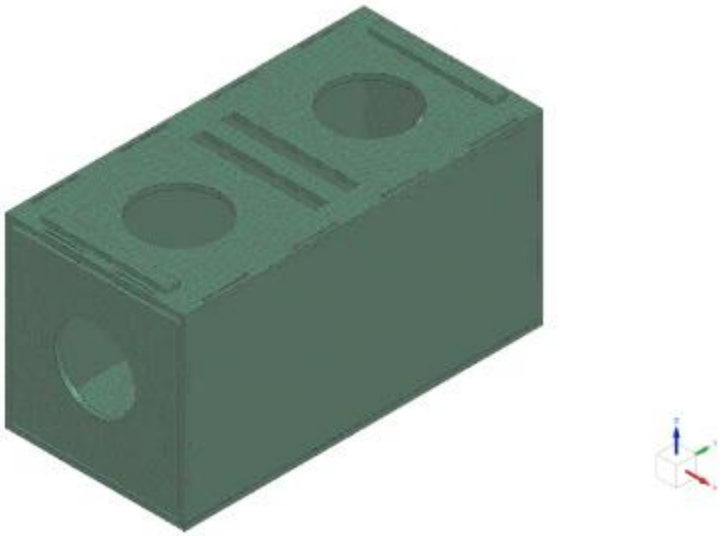

Figure 60A: Analysis under 3,7 mm mesh size (Baz, 2023)

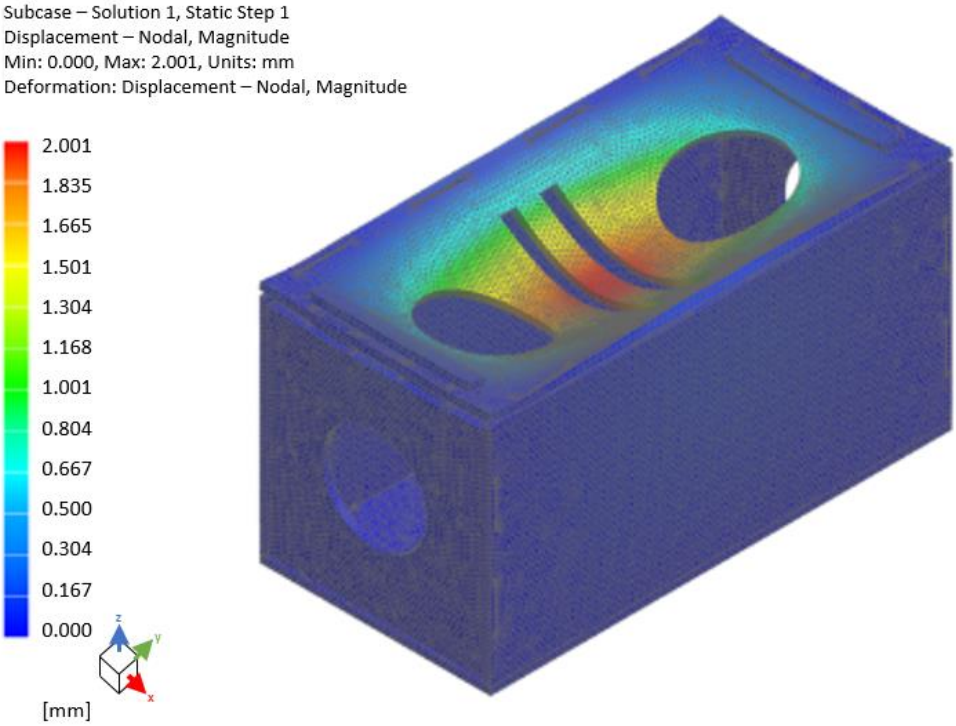

Figure 60B: Analysis under 3,7 mm mesh size displacement (Baz, 2023)

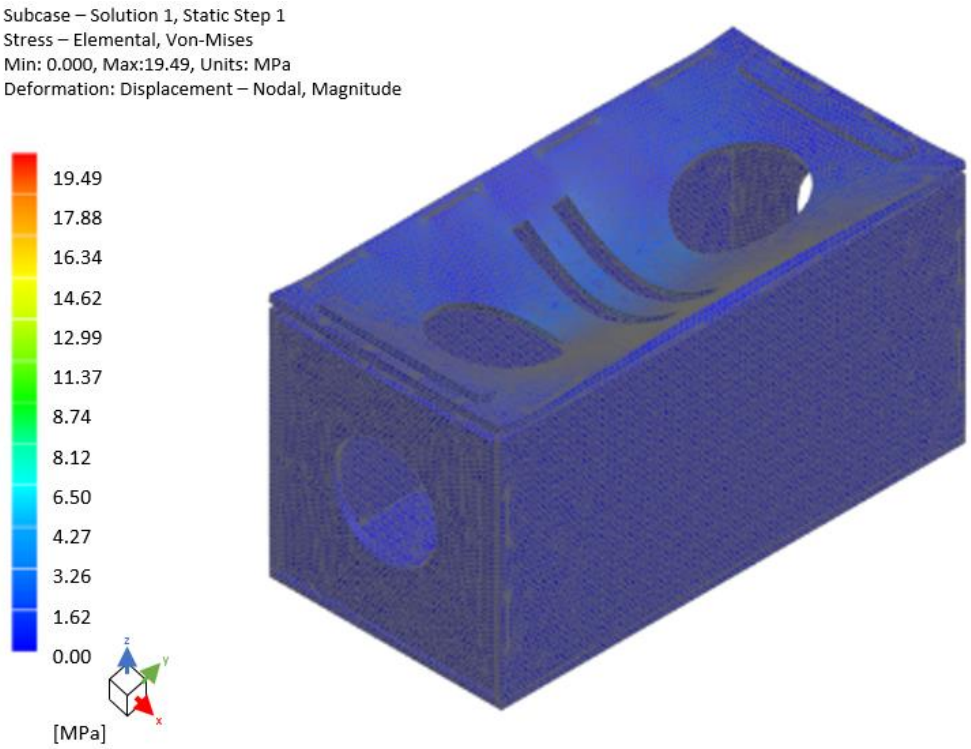

Figure 60C: Analysis under 3,7 mm mesh size von Mises (Baz, 2023)

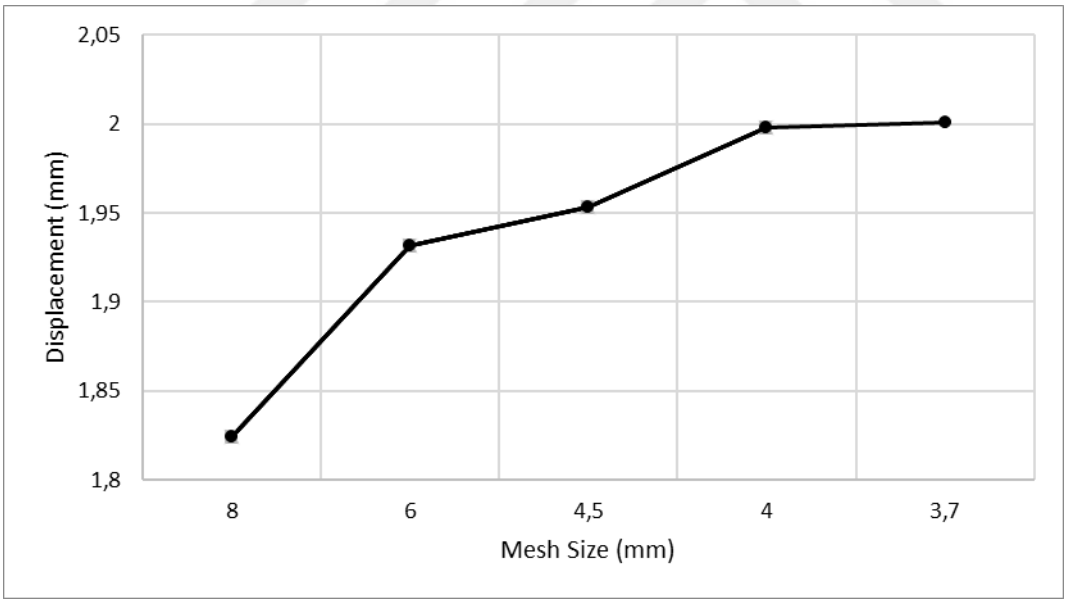

Figure 61: Graph of mesh size vs maximum displacement for the proposed modular design (Baz, 2023)

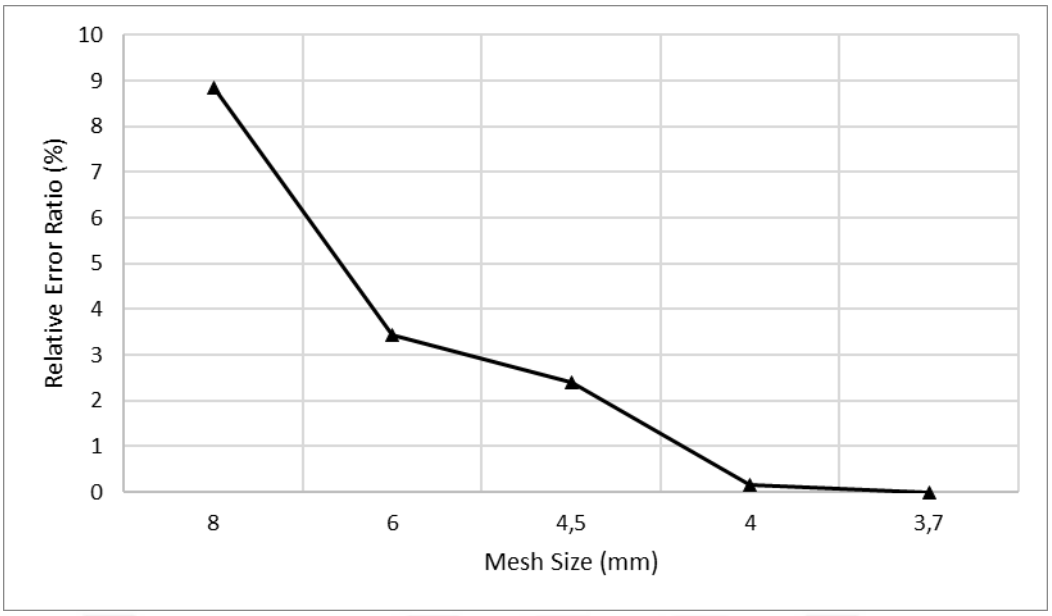

Figure 62: Graph of mesh size vs relative error ratio (%) for displacement for the proposed modular design (Baz, 2023)

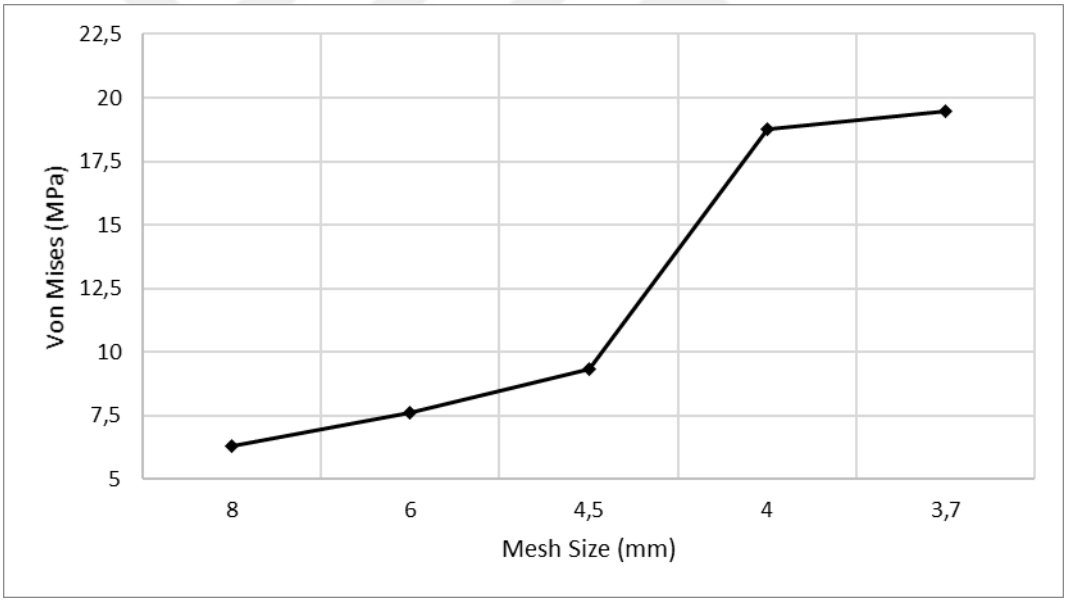

Figure 63: Graph of mesh size vs von Mises for the proposed modular design (Baz, 2023)

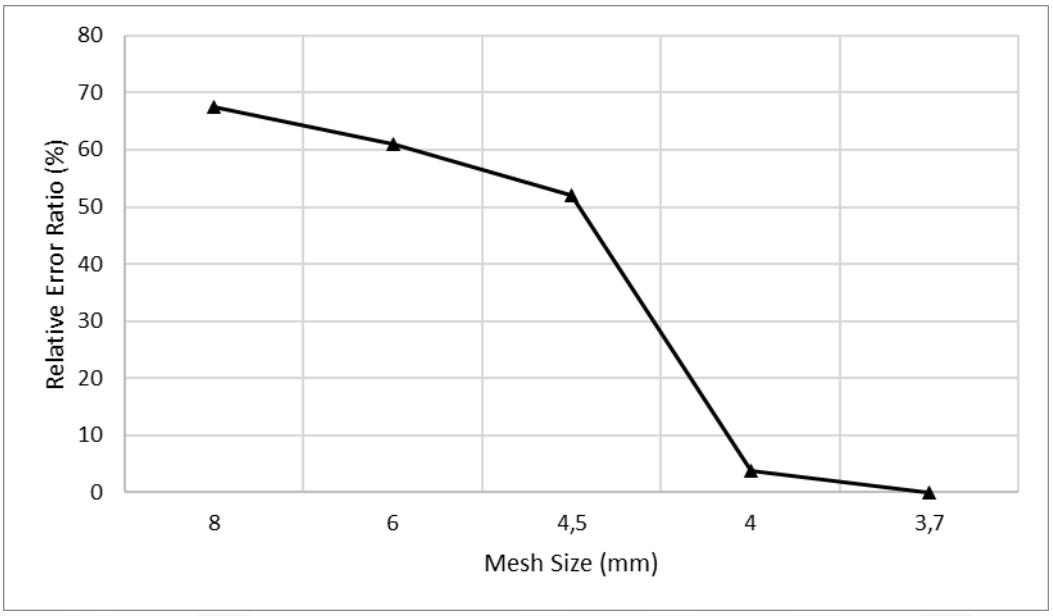

Figure 64: Graph of mesh size vs relative error ratio (%) for von Mises for the proposed modular design (Baz, 2023)

The mesh size of 4 mm has been chosen as the optimum one because, after the 4 mm mesh size analysis, the relative error values are seen to be very small (less than 1%) according to Figure 64.

3.2.3 Static Finite Element Analysis with 4 mm Mesh Size

Static finite element analysis was performed for the proposed modular design. 4 mm mesh size determined in the mesh refinement study in Section 3.2.3 was used in the analysis. All degrees of freedom were fixed for the bottom surface nodes while a 300 N distributed force was applied in negative X, Y, and Z directions separately in three different analyses. Figure 65 shows the displacement results when the load is applied in a negative Z-direction. It is seen that the maximum displacement is about 2 mm at the center of the top surface. Since 2 mm is a small displacement, it is concluded that the proposed design can be used in constructions.

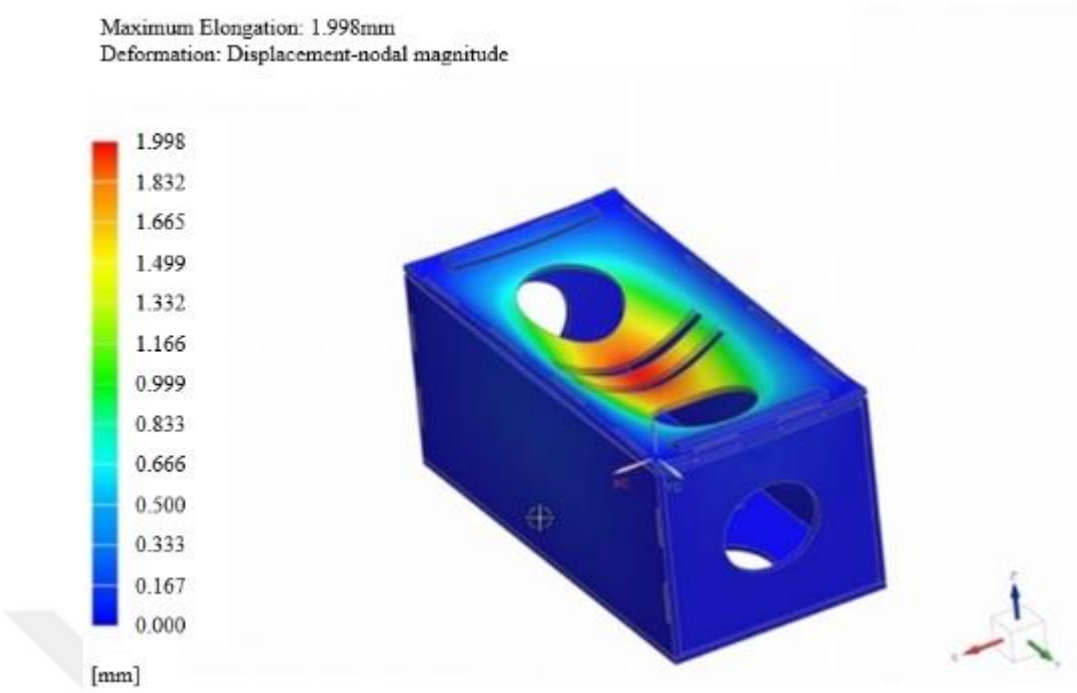

Figure 65: Displacement results of the static finite element analysis of the Proposed Lightweight Masonry Unit Under 300 N Distributed Force from the Top Middle (Baz, 2022)

It is also important to observe the separation of the modular parts from each other at the connected edges. To observe the separation, a close-up image of the deformation behavior is shown in Figure 66. It should be noted that the deformation magnitude in the image is 100 times greater than the actual value. Hence, the deformations are seen clearly in the figure. However, the edges have blue regions, which means the displacement is in the range of 0 and 0.2 mm according to the legend in Figure 66. Hence, there are very small displacements at the edges indicating that the separation is negligible. As seen in Figure 67 and Figure 68, displacements are negligible like the previous situation when the different directional force is applied. Thus, it is concluded that the modular design is suitable for carrying the load considered in this study according to the static finite element analysis results.

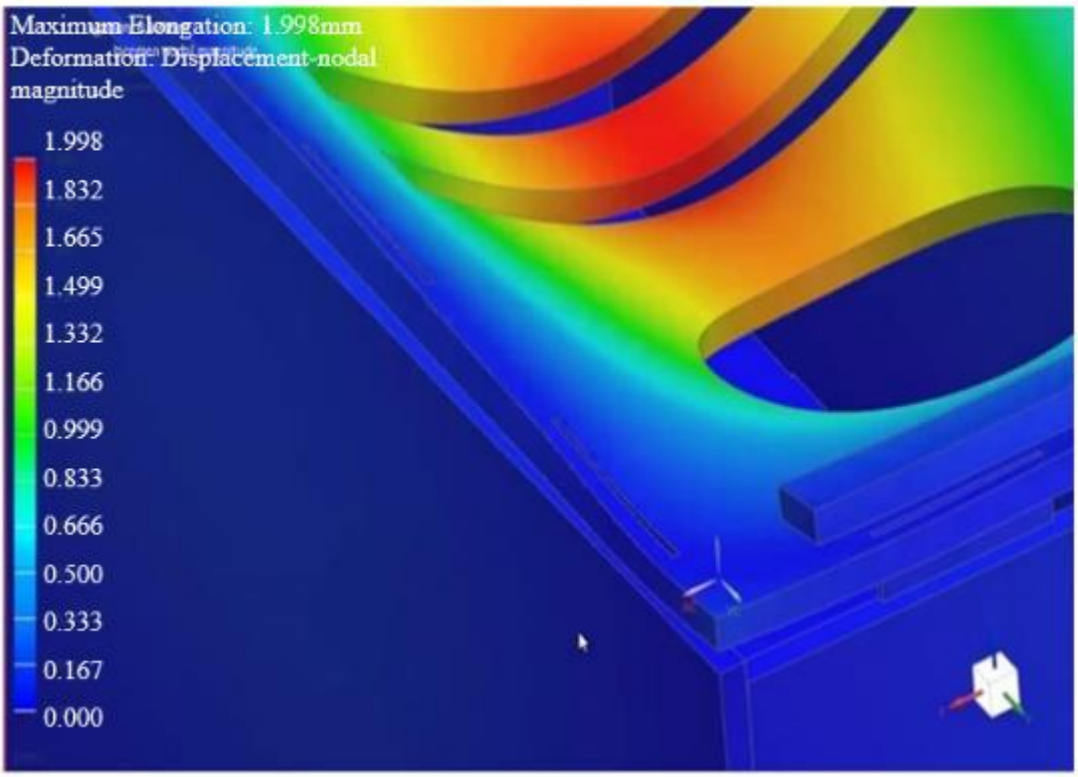

Figure 66: A close-up image of the displacement results of the static finite element analysis of the Proposed Lightweight Masonry Unit Under 300 N Distributed Force from the Top Middle, (Baz, 2022)

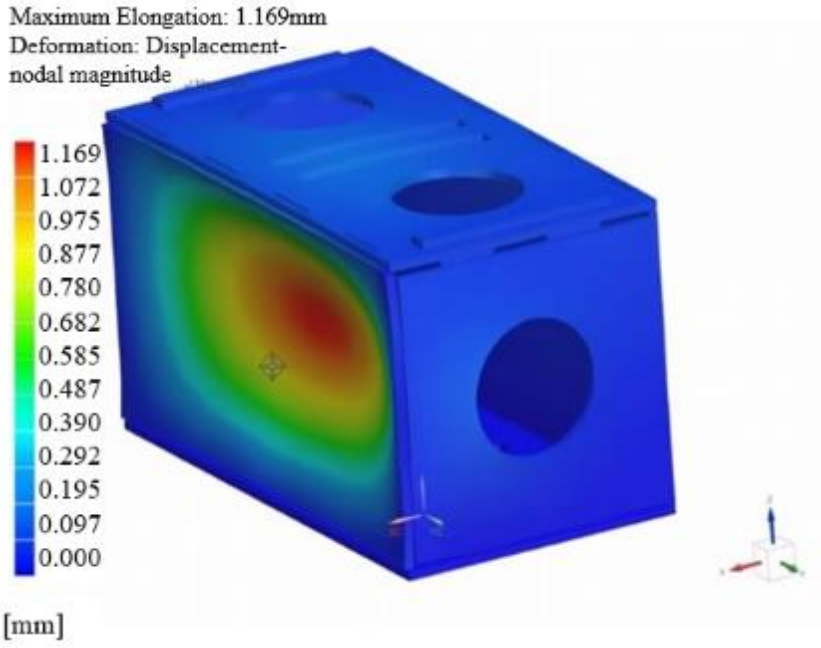

Figure 67: Simulation of Proposed Lightweight Masonry Unit Under 300 N Distributed Force from -X Direction to The Middle of Left Surface (Baz, 2022)

For further examination, alternative force directions are considered in the finite element analysis. When earthquakes are considered, it is observed that the lateral

forces are remarkably high. Lateral displacements or lateral deformations cause direct and hazardous effects due to disasters. Consequently, many injuries and casualties will be caused by the falling off bricks which must not be neglected. For this reason, a distributed load of 300 N was applied from the surface on the side and the other side is fixed. The displacement results are shown in Figure 68. Although the loads are not statically applied during earthquakes, this analysis can still give some initial insights about the displacements observed on the structure when the static load is assumed to be applied. It is seen that the maximum displacement is 1.169 mm according to this analysis, which is small enough to conclude that the proposed geometry is suitable for the static construction load used in this study. Furthermore, a more durable material will be determined in the following section, which means that the maximum displacement will be much smaller.

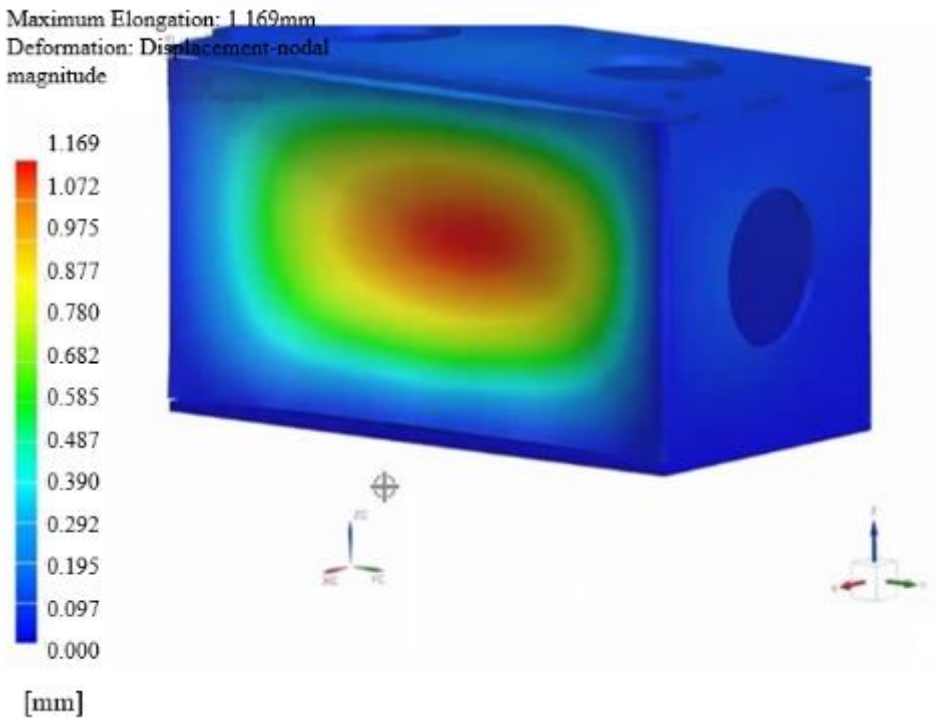

Figure 68: Displacement results of the static finite element analysis of the Proposed Lightweight Masonry Unit Under 300 N Distributed Force from -X Direction to The Middle of Left Surface from Another Perspective (Baz, 2022)

Furthermore, a close-up picture is given in Figure 69 where it is seen that there are no discernable separations of the modular parts from each other according to this analysis results. Thus, it can be concluded that the proposed modular design is suitable to be

used in constructions according to the static finite element analysis results obtained in this study.

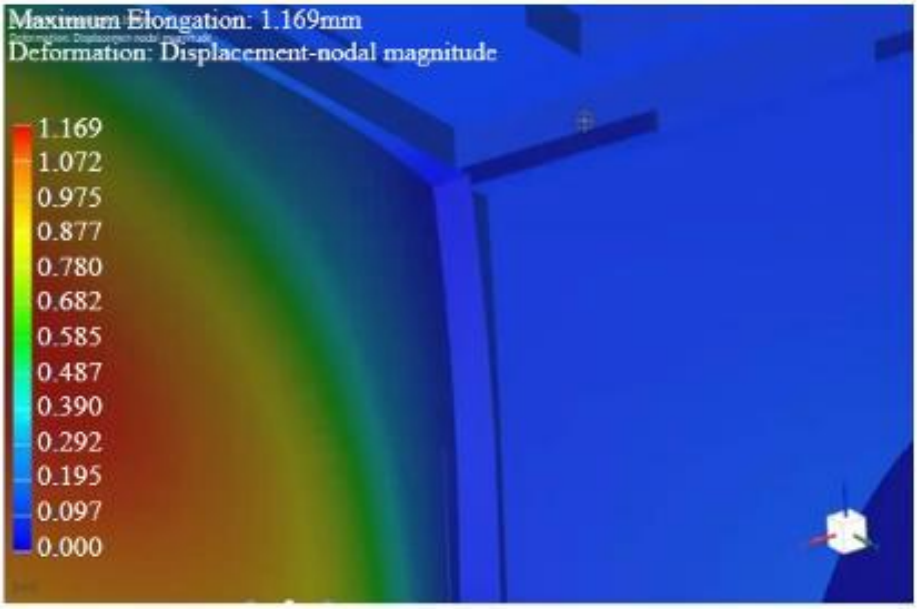

Figure 69: Close-up image of the displacement results of the static finite elements analysis of the Proposed Lightweight Masonry Unit Under 300 N Distributed Force from -X Direction to the Middle of the Left Surface, Zoomed towards the Edges (Baz, 2022)

As another alternative loading application, the force is applied on the surface of the front side while the rear surface is fixed. The displacement results are shown in Figure 70. The maximum displacement was observed to be 1.044 mm which is again small enough to conclude that the design is successful in each of three directions under 300 N distrusted load applied in a static finite element analysis.

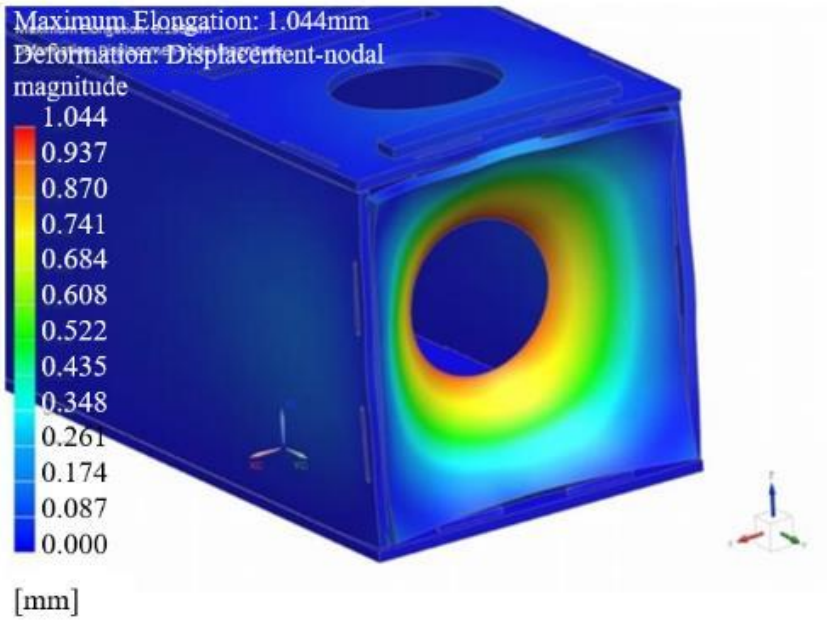

Figure 70: Close-up image of the displacement results of the finite element analysis of the Proposed Lightweight Masonry Unit Under 300 N Distributed Force from -Y Direction to the Middle of the Front Surface (Baz, 2022)

Figure 71 shows the von Mises stresses from different directions forces in the same arrangement 300N. From X direction a 300 N force is exceeding the limits because the tensile strength of the ABS material changes between 29.8-43 Mpa (Url-11).

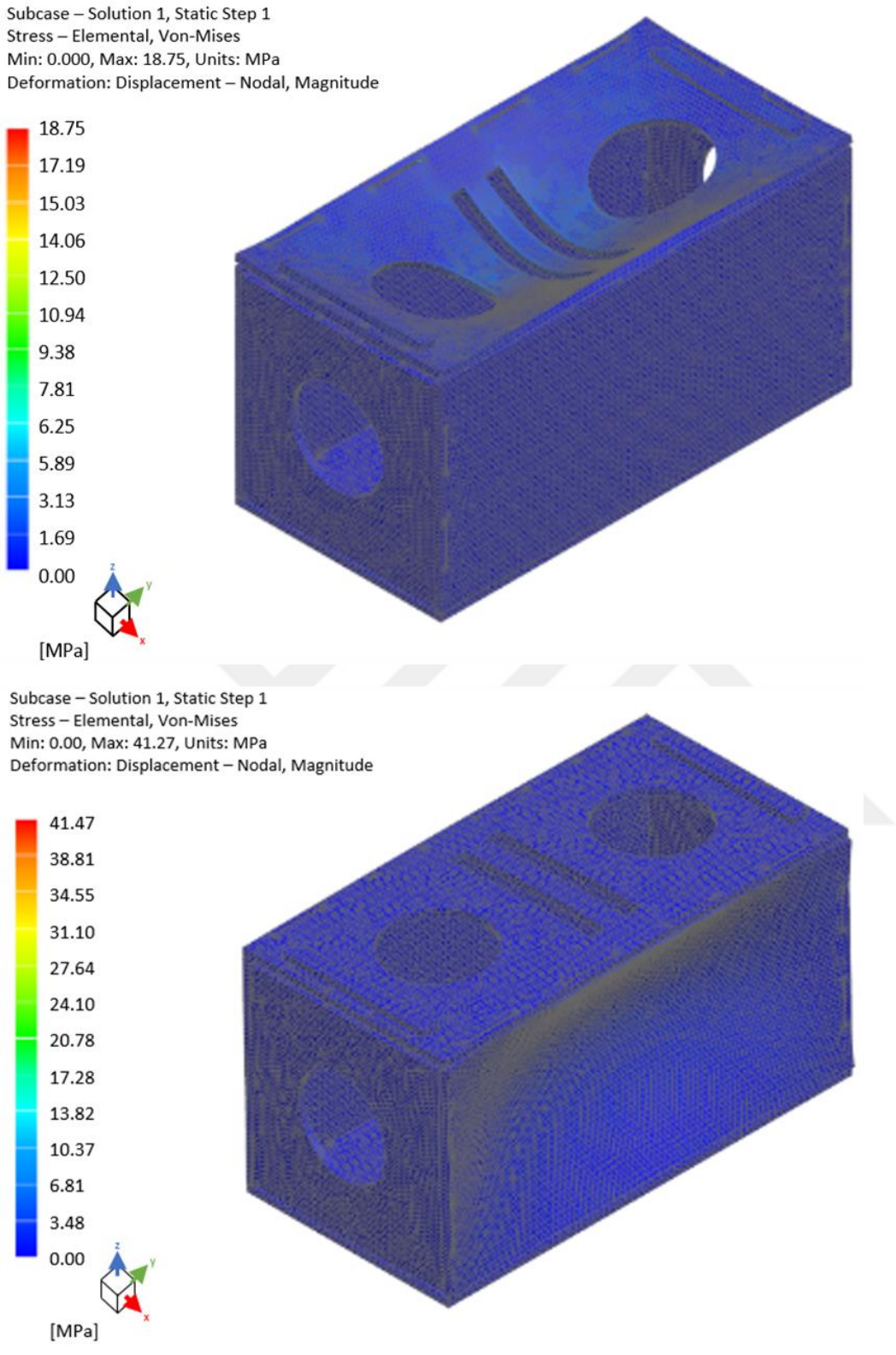

Figure 71A: Finite element analysis von Mises results with 300 N Force applied from different directions to ABS (Baz, 2022)

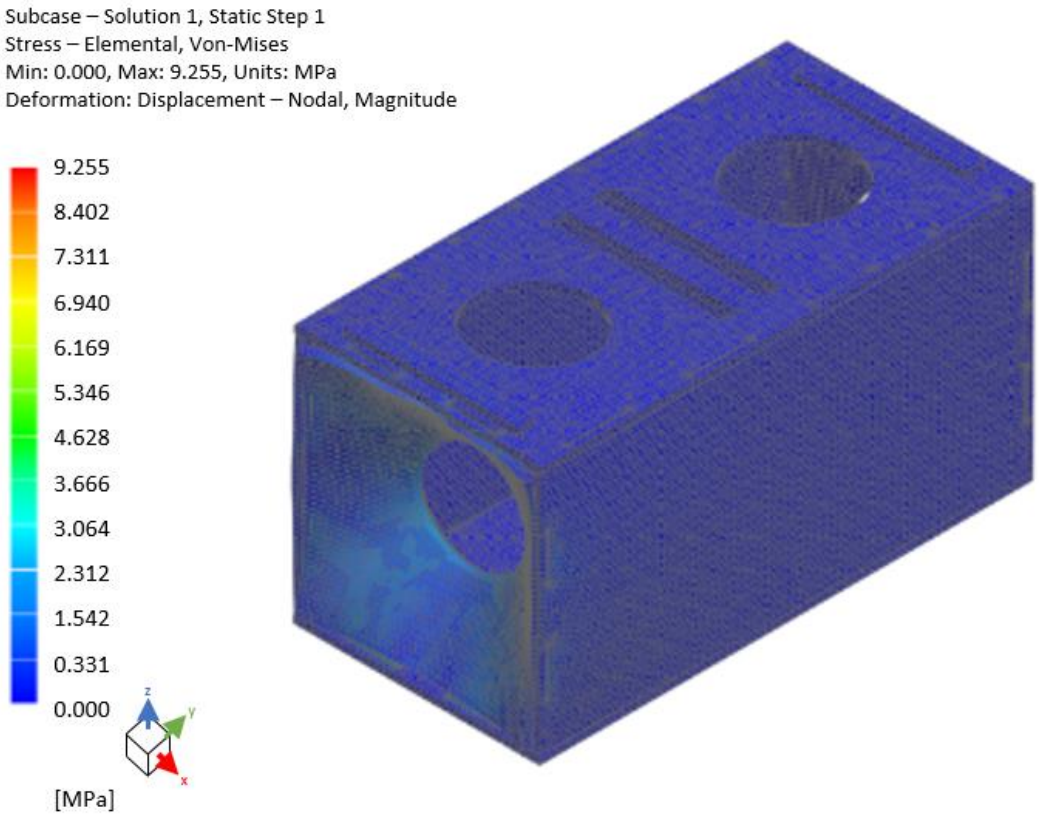

Figure 71B: Finite element analysis von Mises results with 300 N Force applied from different directions to ABS (Baz, 2022)

It should be noted that ABS material is used for demonstrative purposes. When more durable bioplastics with additives are used, the strength of these materials will be much higher as discussed in Section 3.3. Hence, although for the ABS material, the stress results are not in the safe region, for more durable bioplastics, the design should be safe enough to use in construction.

Furthermore, 300 N was considered for the pumice blocks which are heavier than the proposed modular design. In other words, when the proposed design is used instead of a pumice block, a lower static load than 300 N will be applied on a one-unit block. As an example, a static load of 200 N was applied in another finite element analysis. The von Mises results are shown in Figure 72. As seen in Figure 72 von Mises's results are below 11 Mpa so it can be implied that it does not exceed 29 Mpa the tensile stress of the ABS so the designed block is even safe for the bioplastics which have similar material qualities with the ABS material.

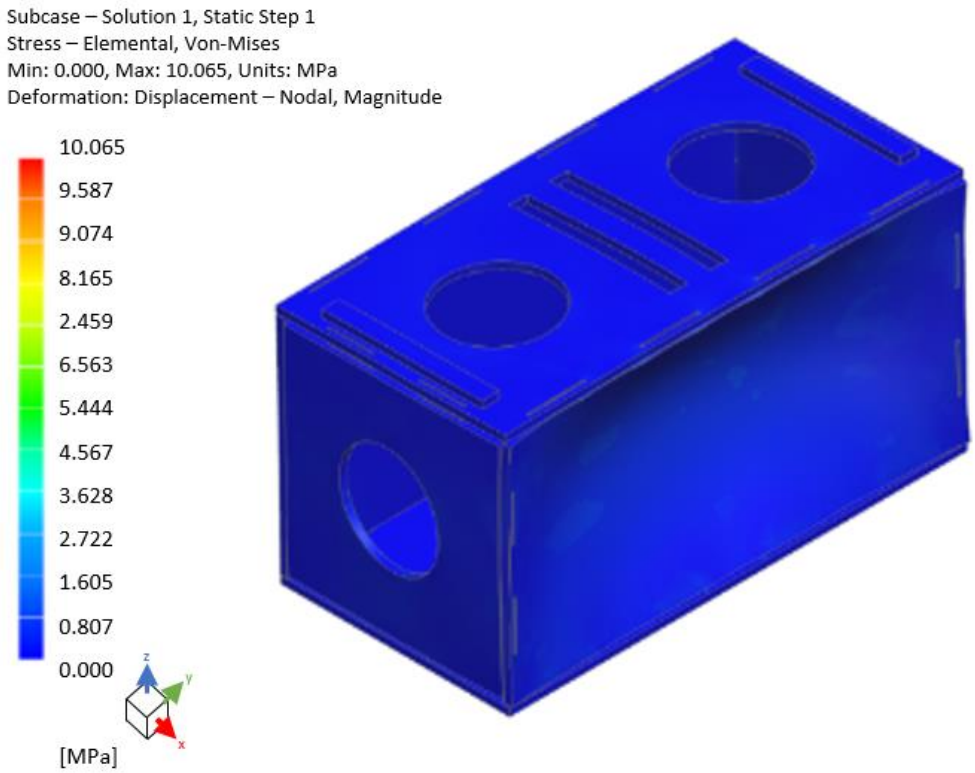

Figure 72: Finite element analysis von Mises results with 200 N Force applied from different directions to ABS (Baz, 2022)

3.2.4 Critical Buckling Analysis

Linear buckling is the behavior of the thin structure under pressure and force. Buckling is defined as a strain in which the lattice structure exhibits a visibly large transverse strain. Buckling failure can occur prematurely at yield points in elastic regions, particularly for thin ones. Therefore, the twist should be considered in the optimization of thin structures.

The critical load at which the lattice buckles the structure can be determined by a linear Eigenvalue buckling analysis method. Eigenvalues found in the analysis are predictions of buckling loads. The linear Eigenvalue is given by;

$$(K_0^{NM} + \lambda_i K_\Delta^{NM})\, v_i^M = 0$$

where K_0^{NM} is the ground state stiffness matrix. Prestress (PN), including the effect of $K^{NM,}$ is by differential initial stress and load stiffness matrix QN, λi is the Eigenvalue, v_i^M is the buckling mode shape, and M and N are the degrees of freedom of the entire model. Then the critical buckling load becomes

$$\mathbf{Fb = PN + \lambda iQN}$$

Buckling loads are calculated relative to the ground state structure. For classical Eigenvalue problems, the preload PN is often zero. When loading a structure by unit pressure, the first resulting Eigenvalue, λ1, represents the critical buckling load Fb for buckling-based optimization of lattice structures, the goal is pursued in the proposed method.

Maximize the critical load obtained from the modal buckling analysis to the volume of the structure (Vtotal). Must be less than or equal to the specified allowable amount (Vallow) (Görgülüarslan et al., 2015).

The proposed unit has six surfaces, and those surfaces are thin, so this leads to another analysis requirement. This is a critical buckling analysis. In this analysis method, the buckling issue is elaborately examined under different direction forces. The unit is exposed to different direction forces from many different points from all the surfaces while the bottom surface of the unit is fixed to the ground and the 1 N force is applied from all X, Y, and Z directions.

Figure 73 shows the critical buckling analysis under 1 N force applied from above to different locations of the top surface with an isometric view. In Figure 74 the opposite isometric view is shown for the same analysis and the Figure 75 shows the von Mises stresses for the same arrangement.

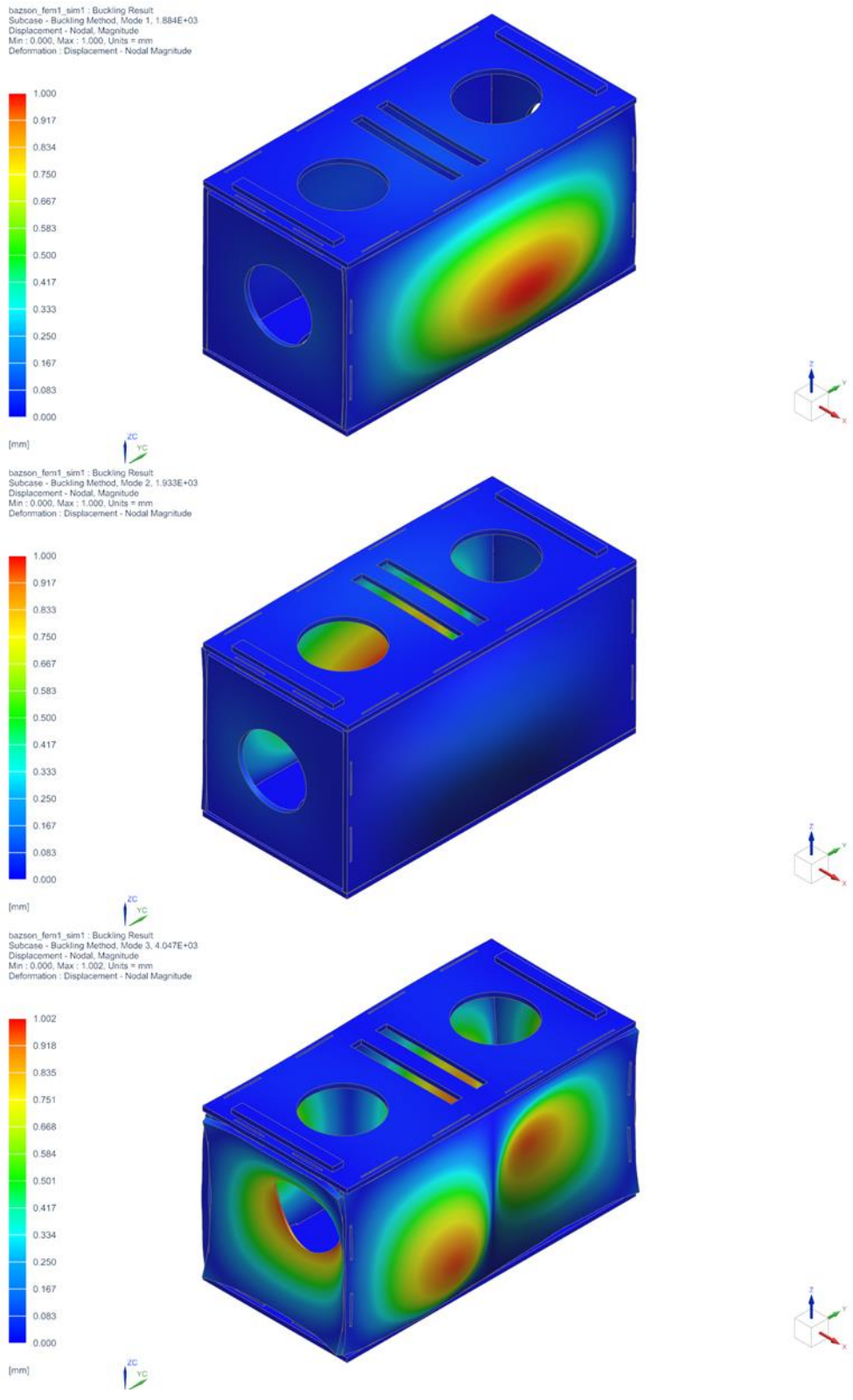

Figure 73A: Critical buckling displacement analysis under 1 N Force applied from -Z direction isometric view (Baz, 2023)

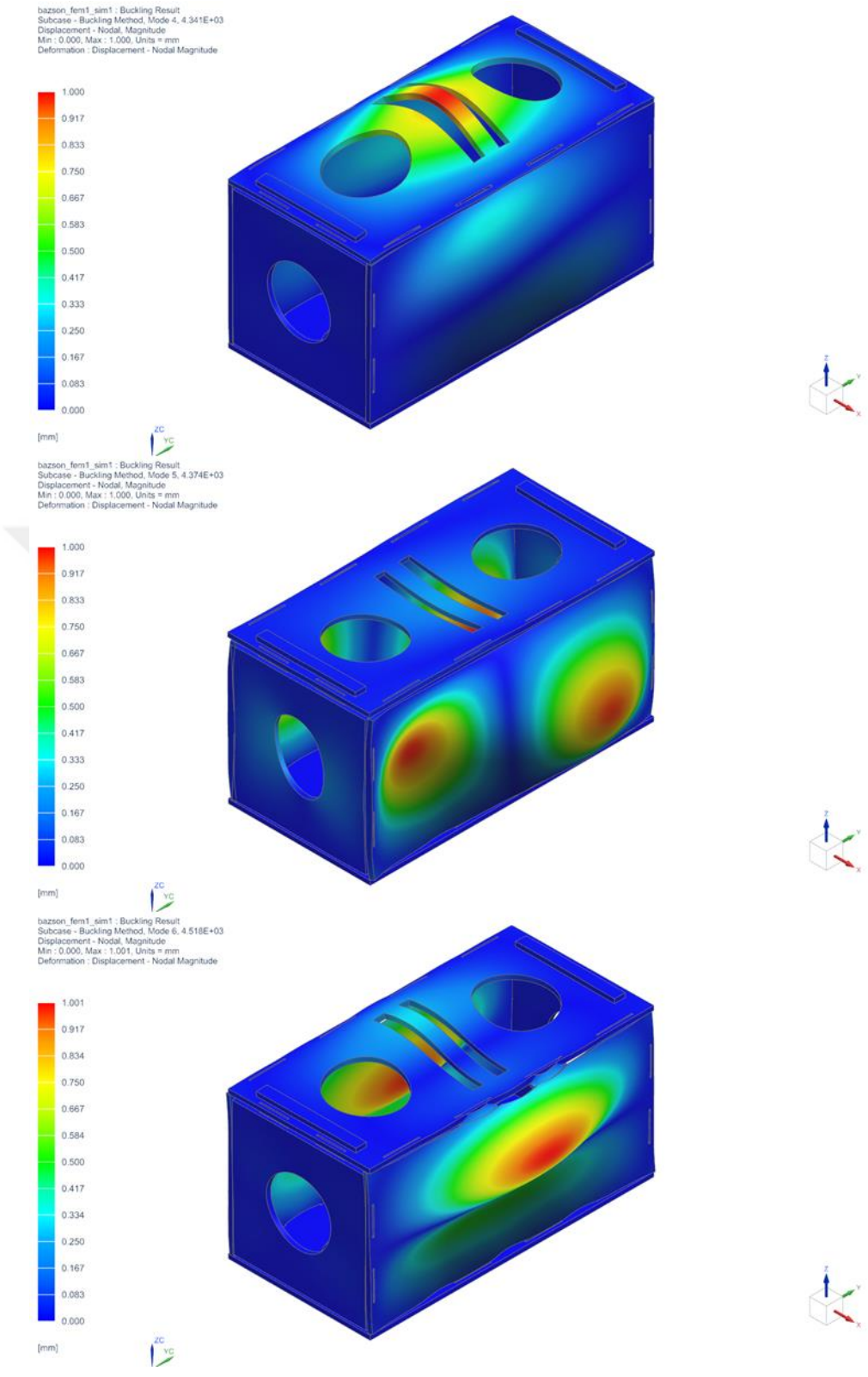

Figure 73B: Critical buckling displacement analysis under 1 N Force applied from -Z direction isometric view (Baz, 2023)

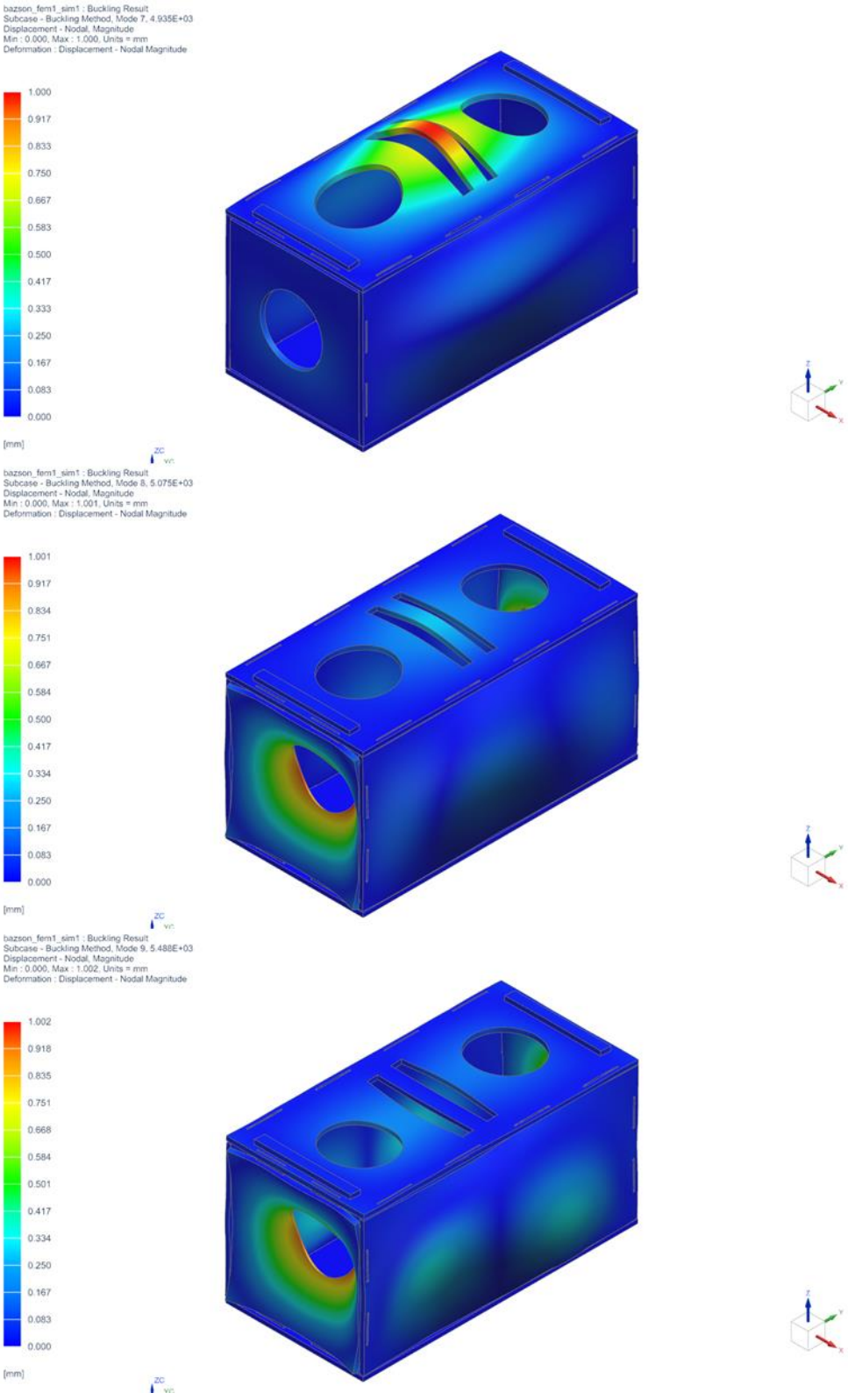

Figure 73C: Critical buckling displacement analysis under 1 N Force applied from -Z direction isometric view (Baz, 2023)

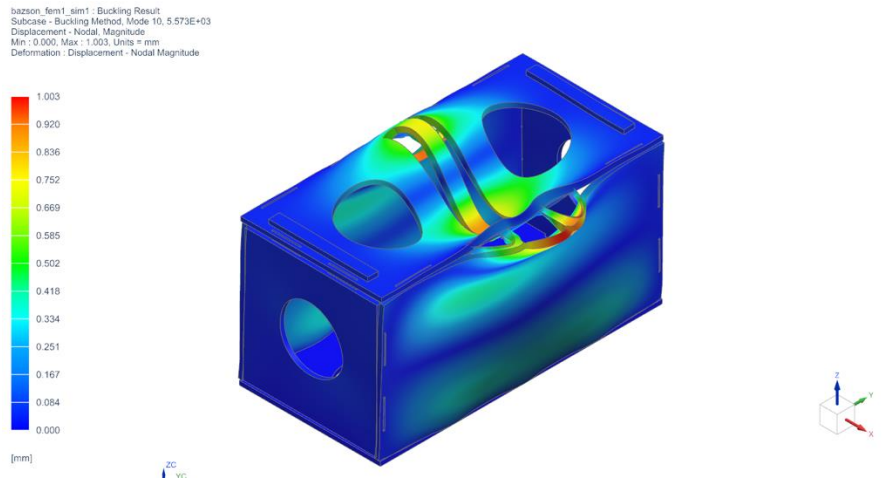

Figure 73D: Critical buckling displacement analysis under 1 N Force applied from -Z direction isometric view (Baz, 2023)

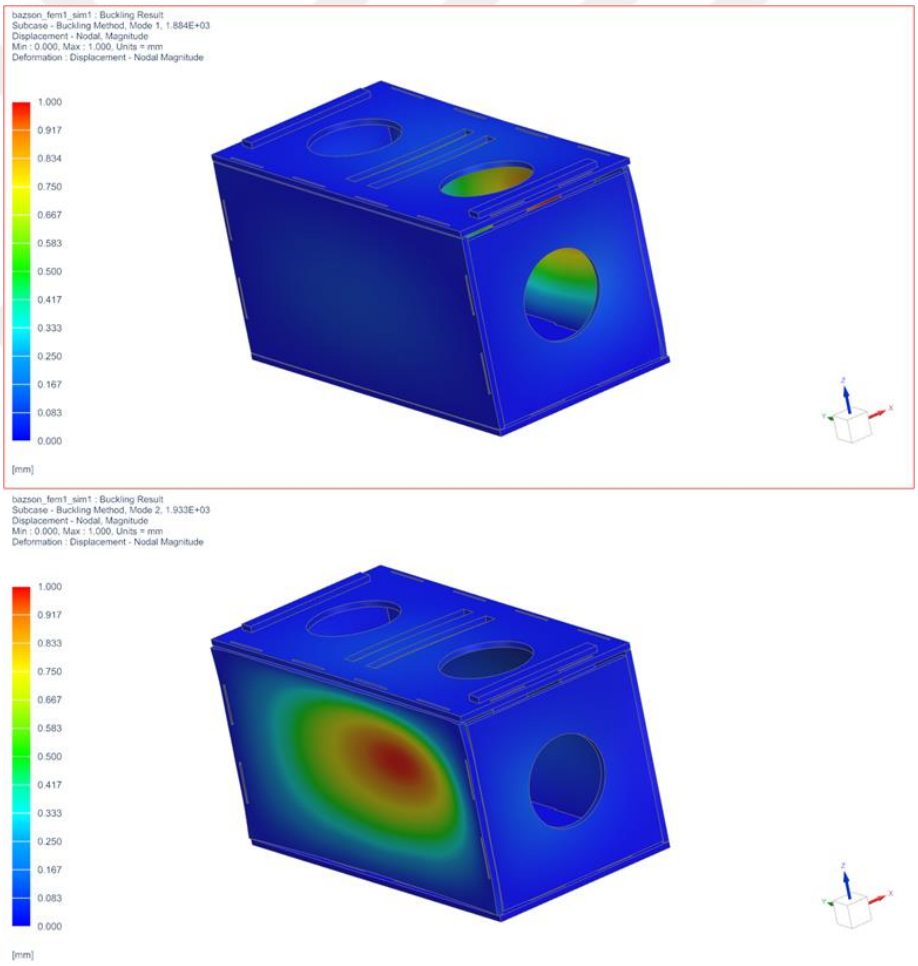

Figure 74A: Critical buckling displacement analysis under 1 N Force applied from -Z direction inverse isometric view (Baz, 2023)

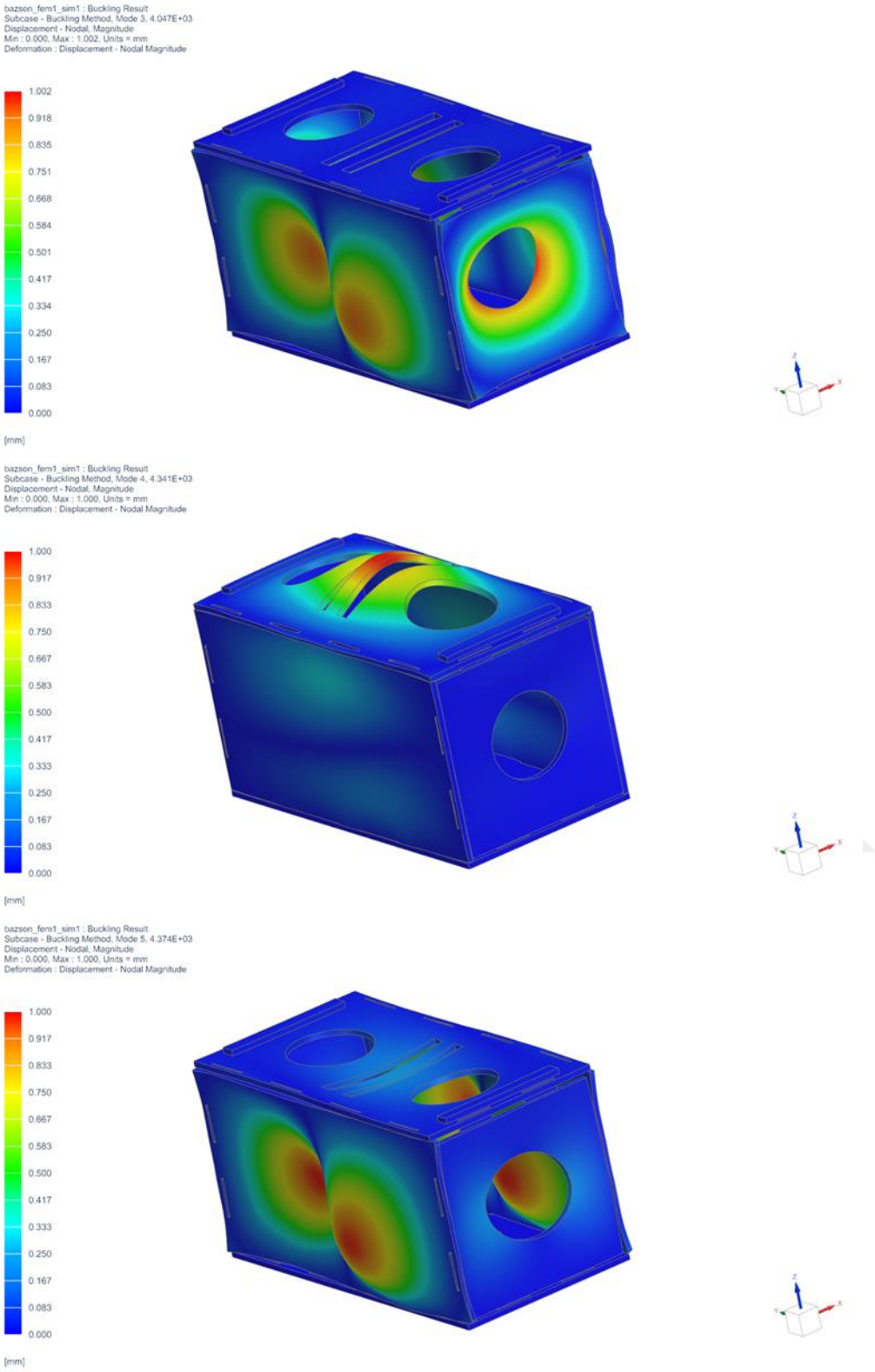

Figure 74B: Critical buckling displacement analysis under 1 N Force applied from -Z direction inverse isometric view (Baz, 2023)

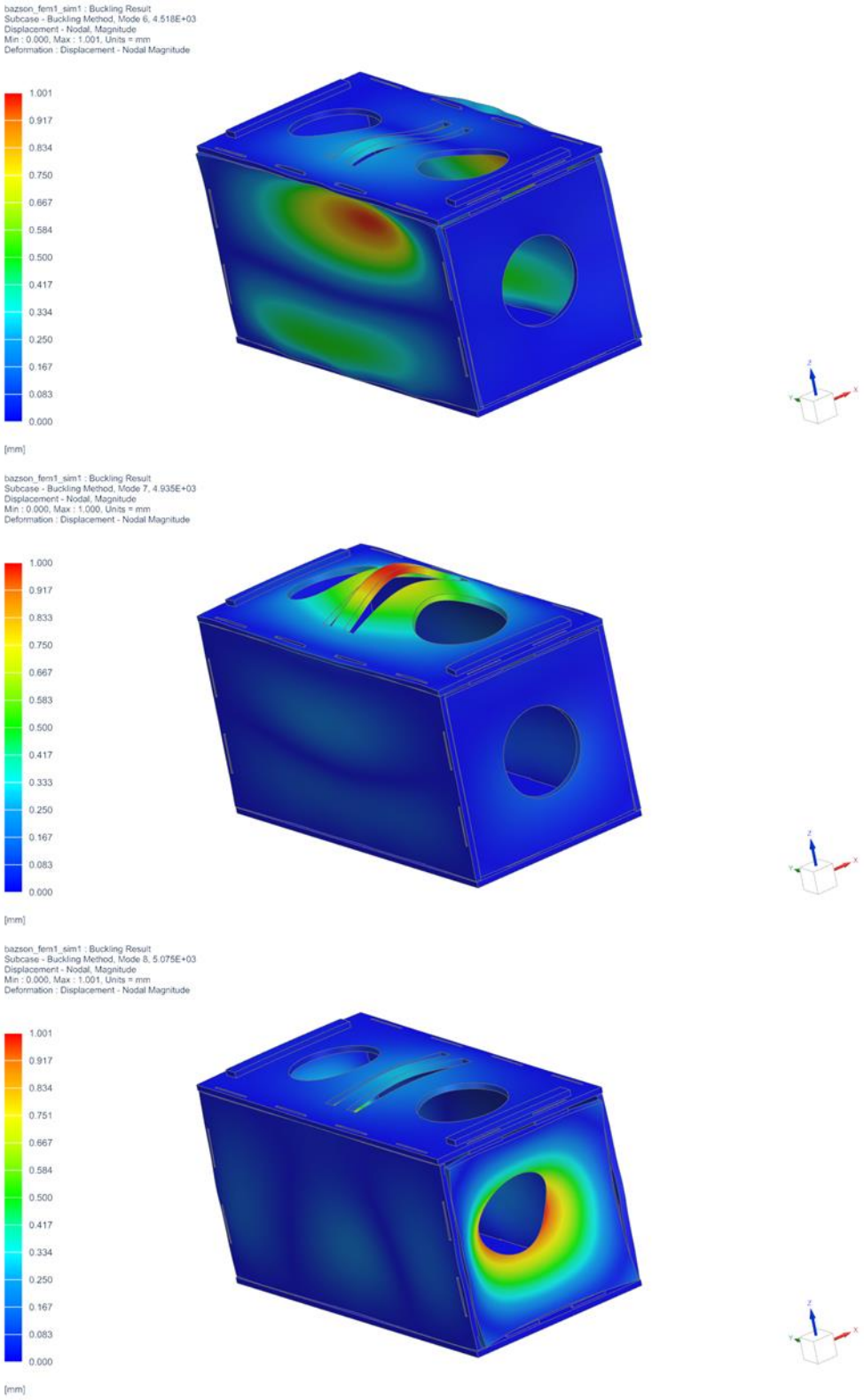

Figure 74C: Critical buckling displacement analysis under 1 N Force applied from -Z direction inverse isometric view (Baz, 2023)

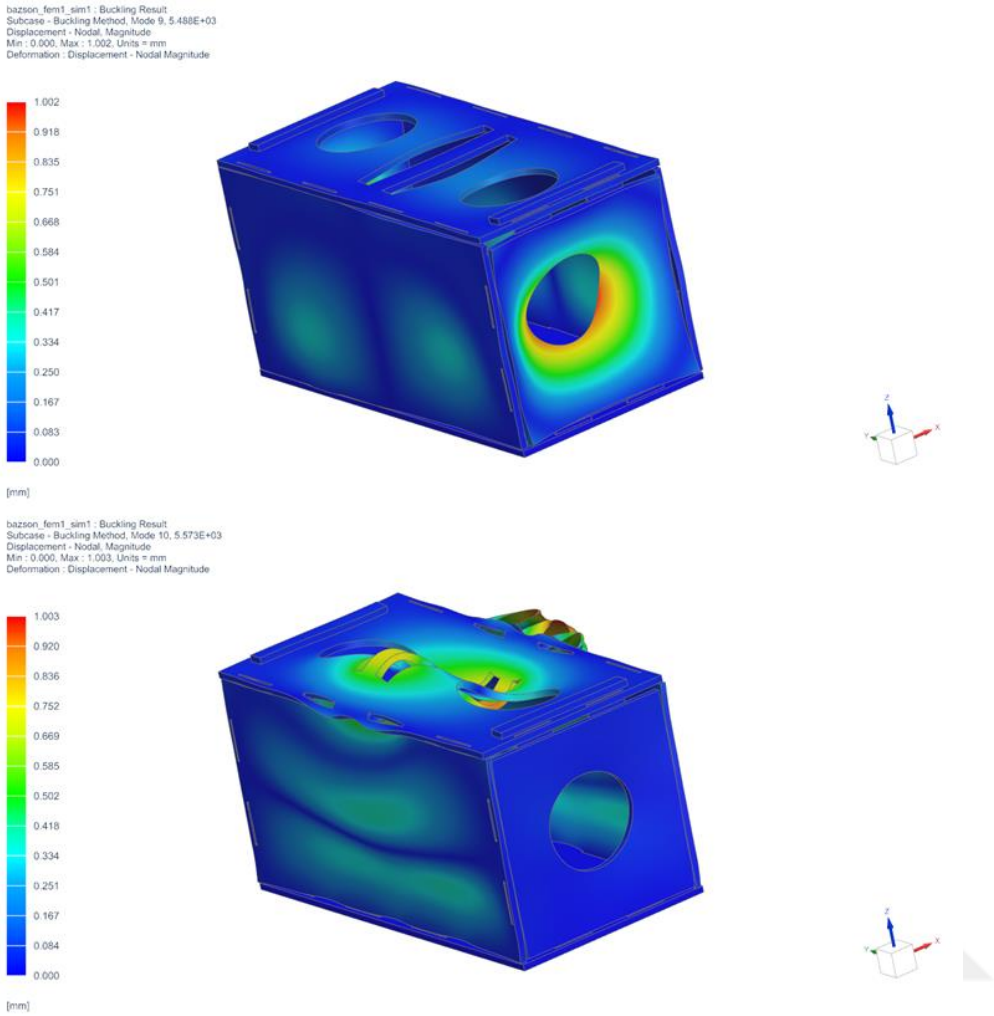

Figure 74D: Critical buckling displacement analysis under 1 N Force applied from -Z direction inverse isometric view (Baz, 2023)

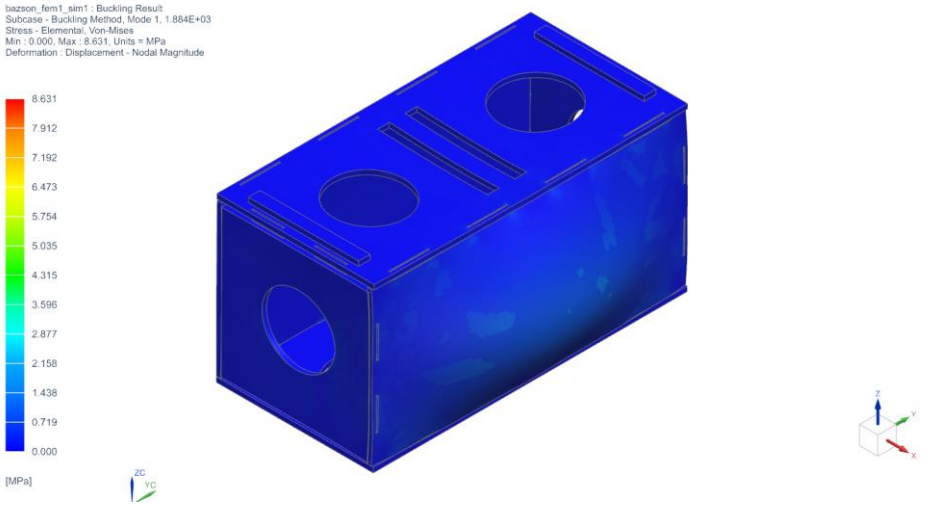

Figure 75A: Critical buckling von Mises analysis under 1 N Force applied from -Z direction isometric view (Baz,2023)

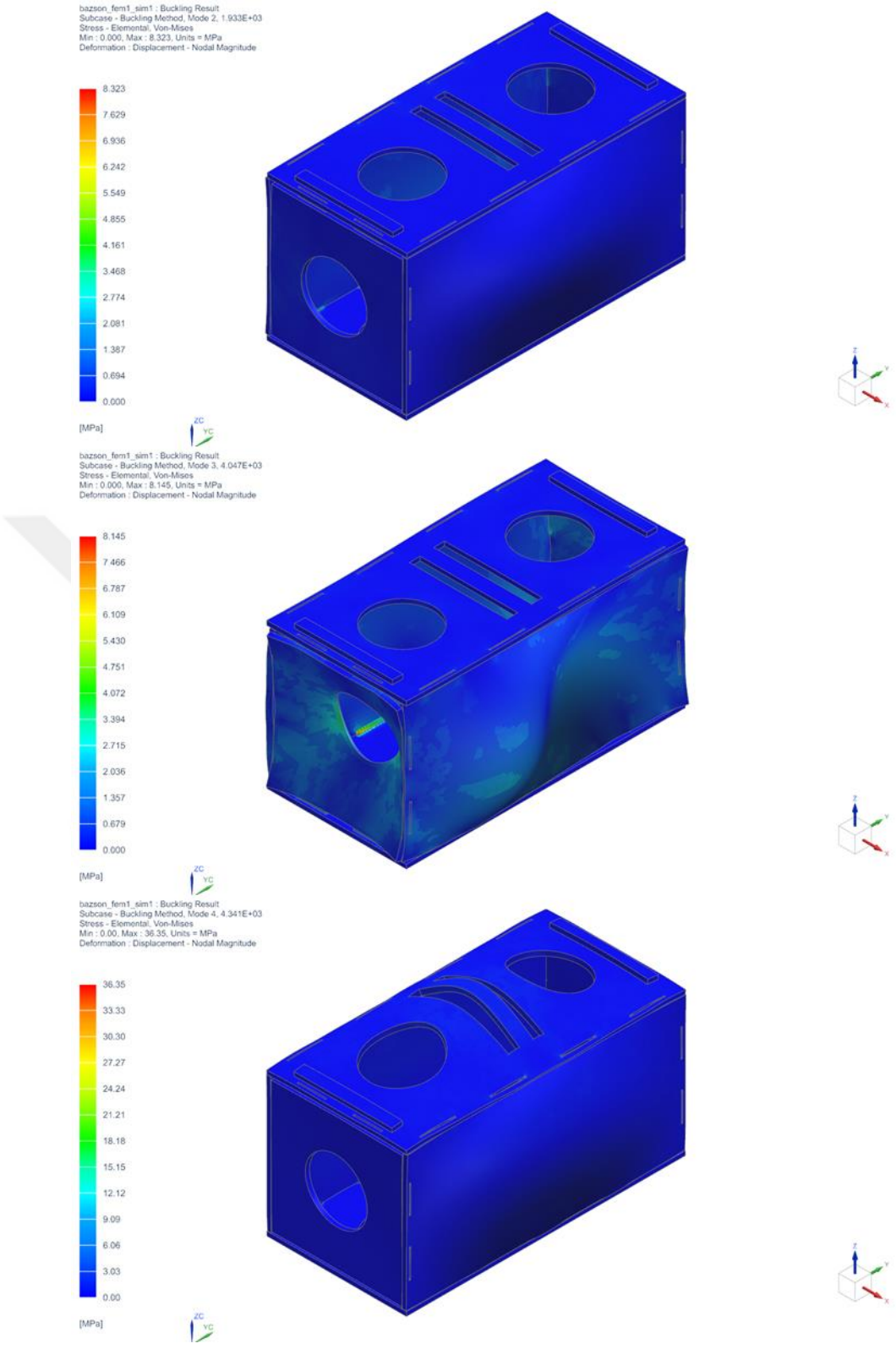

Figure 75B: Critical buckling von Mises analysis under 1 N Force applied from -Z direction isometric view (Baz, 2023)

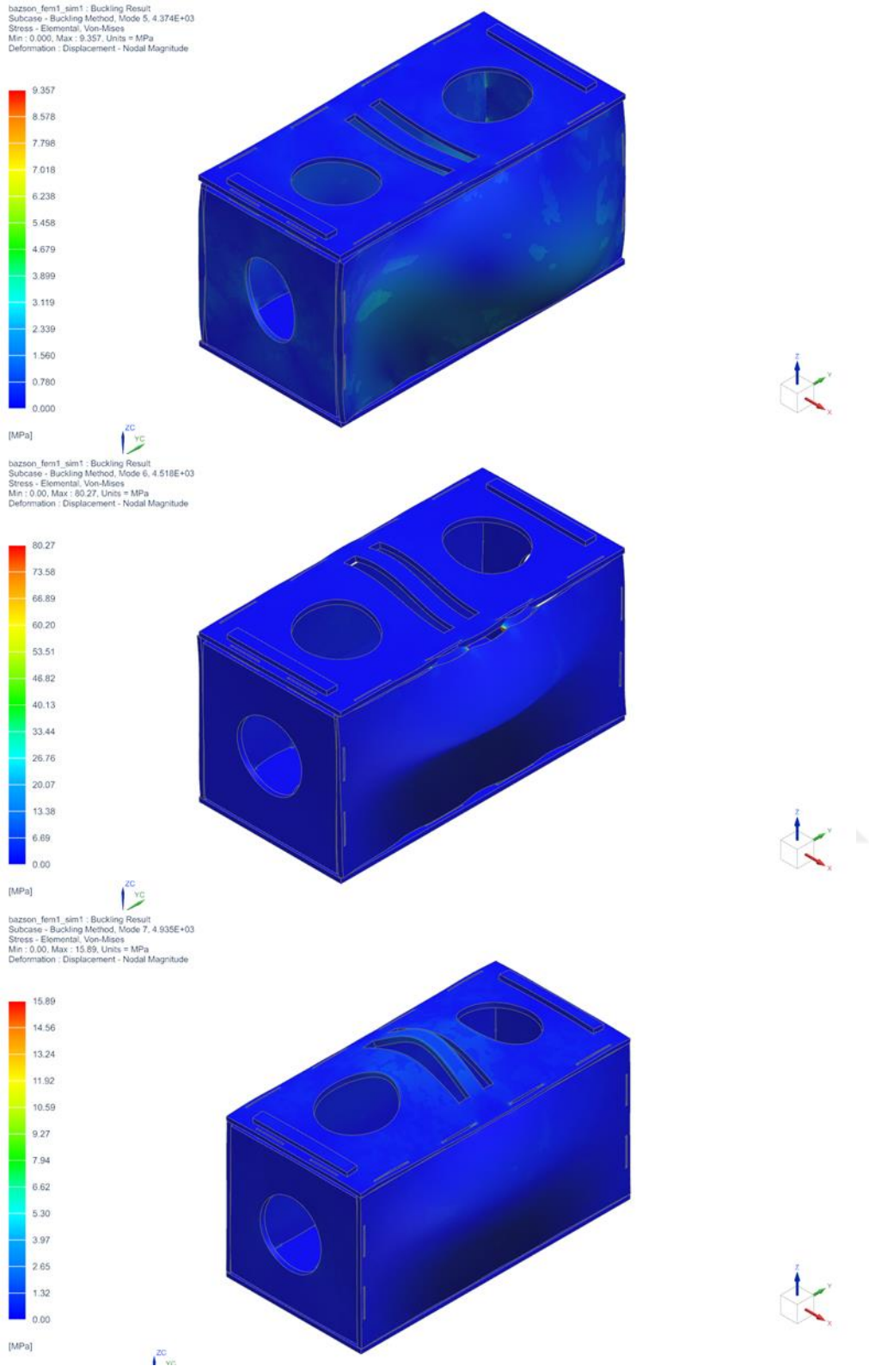

Figure 75C: Critical buckling von Mises analysis under 1 N Force applied from -Z direction isometric view (Baz, 2023)

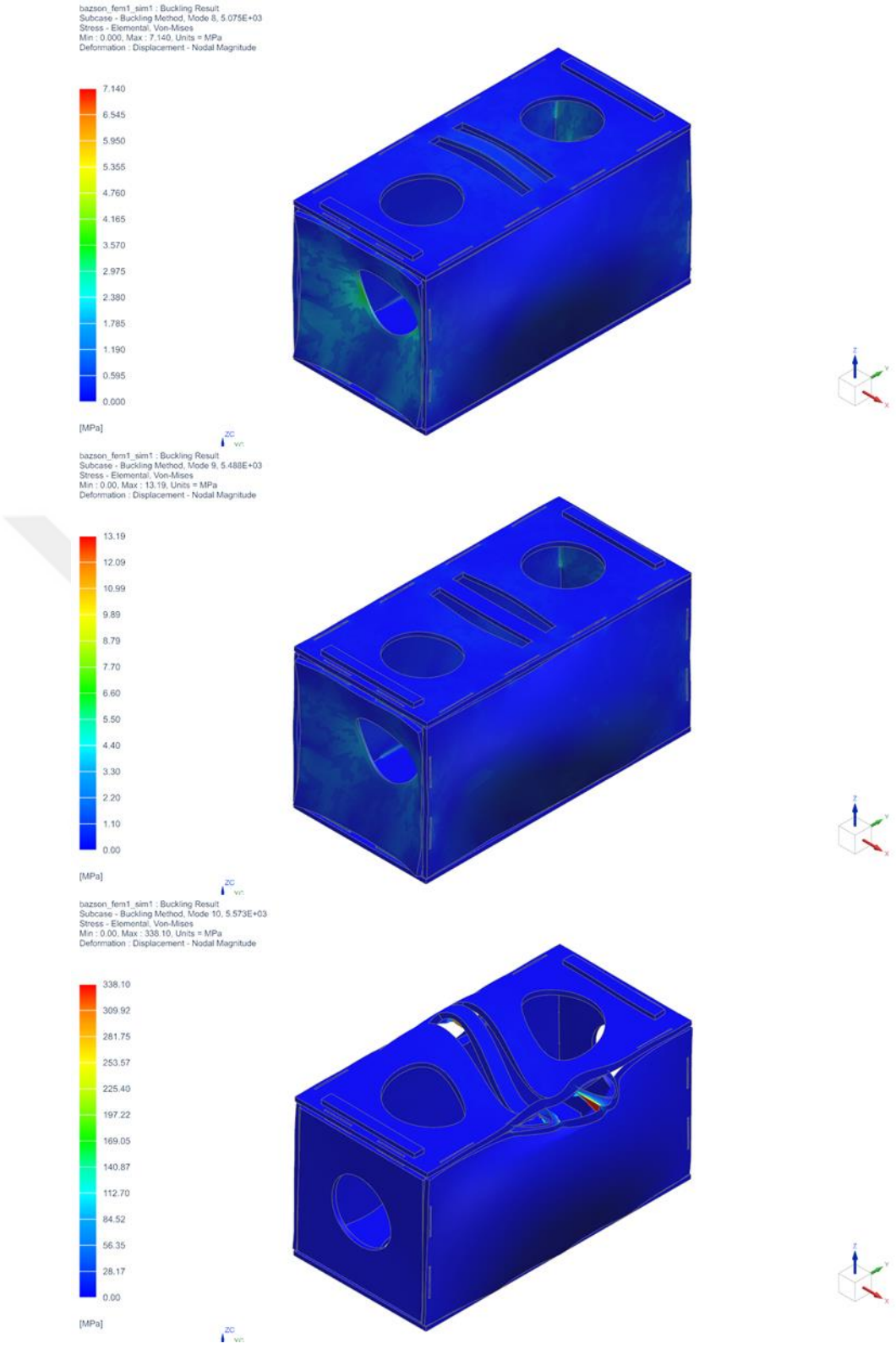

Figure 75D: Critical buckling von Mises analysis under 1 N Force applied from -Z direction isometric view (Baz, 2023)

In Figure 76 the force is applied from the X direction to the side surfaces and the displacement results are shown from an isometric view. In Figure 77 the displacements

are shown with an opposite isometric view and in Figures 78A-78B-78C the von Mises stress values are shown.

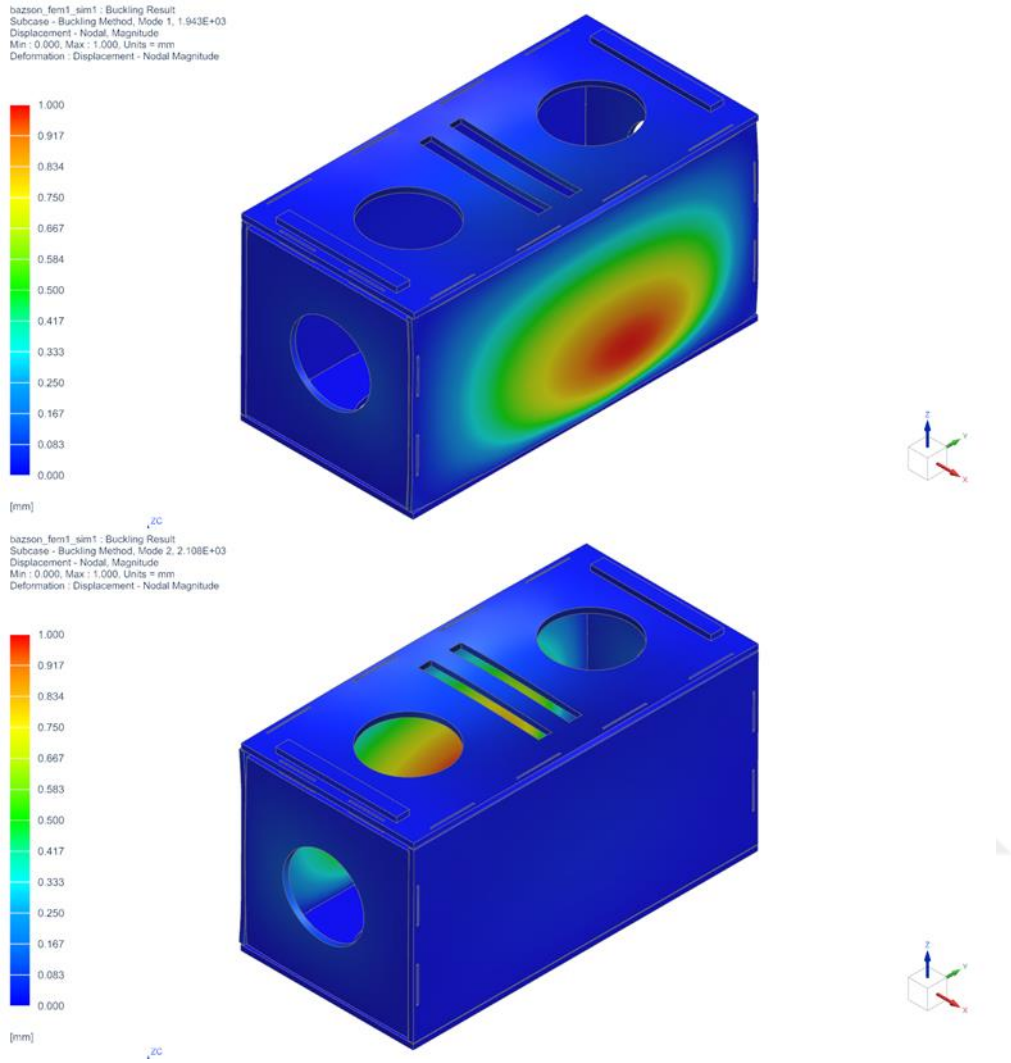

Figure 76A: Critical buckling displacement analysis under 1 N Force applied from -X direction isometric view (Baz, 2023)

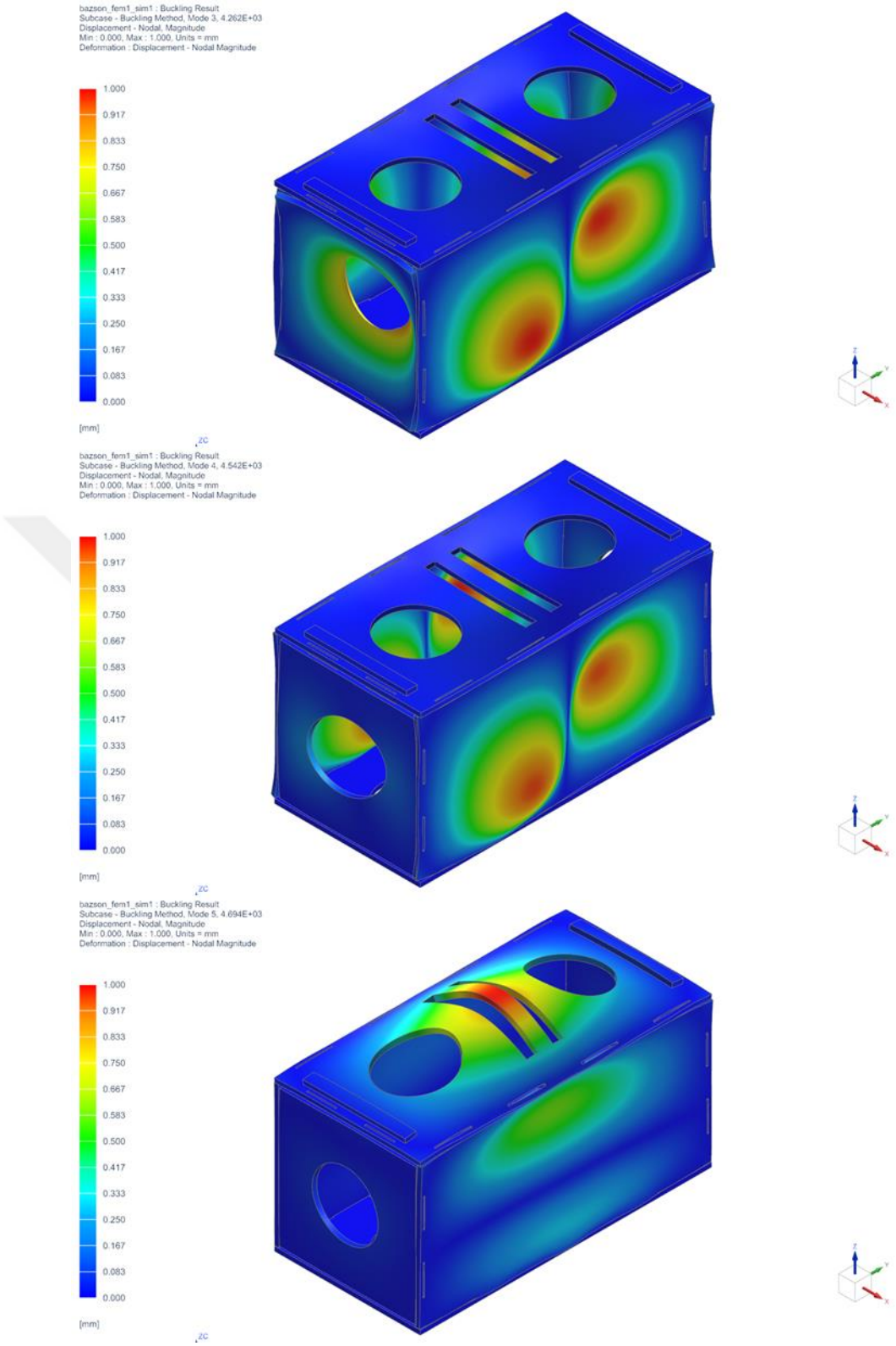

Figure 76B: Critical buckling displacement analysis under 1 N Force applied from -X direction isometric view (Baz, 2023)

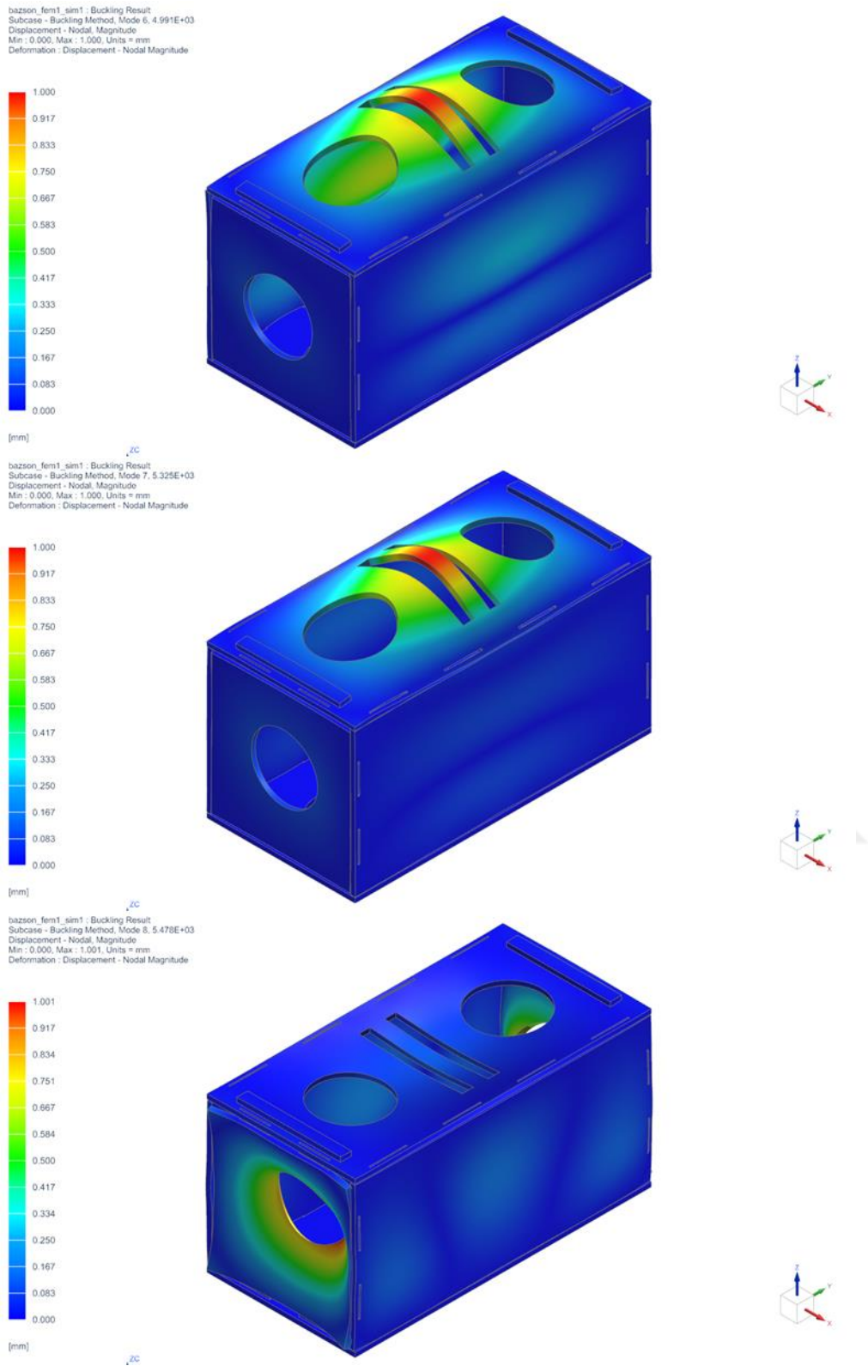

Figure 76C: Critical buckling displacement analysis under 1 N Force applied from -X direction isometric view (Baz, 2023)

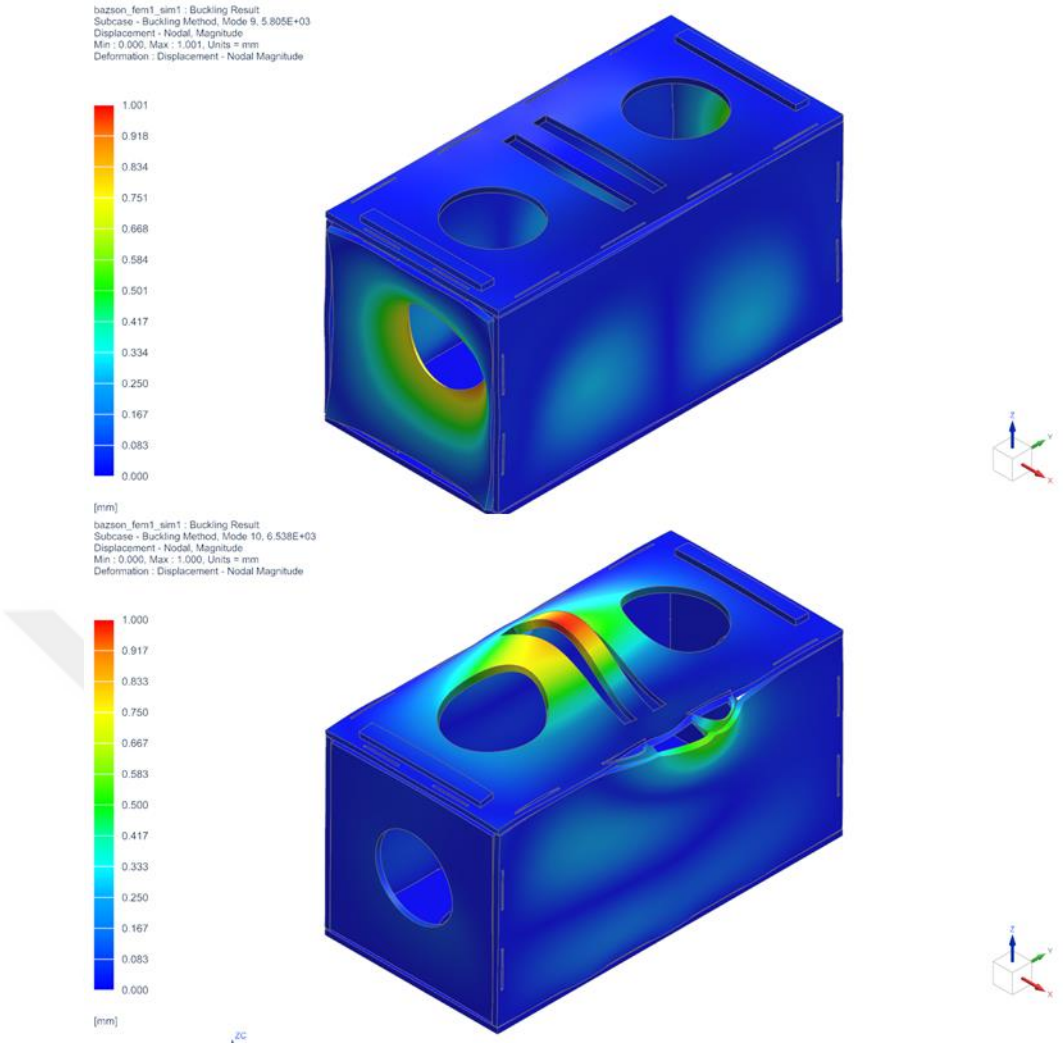

Figure 76D: Critical buckling displacement analysis under 1 N Force applied from -X direction isometric view (Baz, 2023)

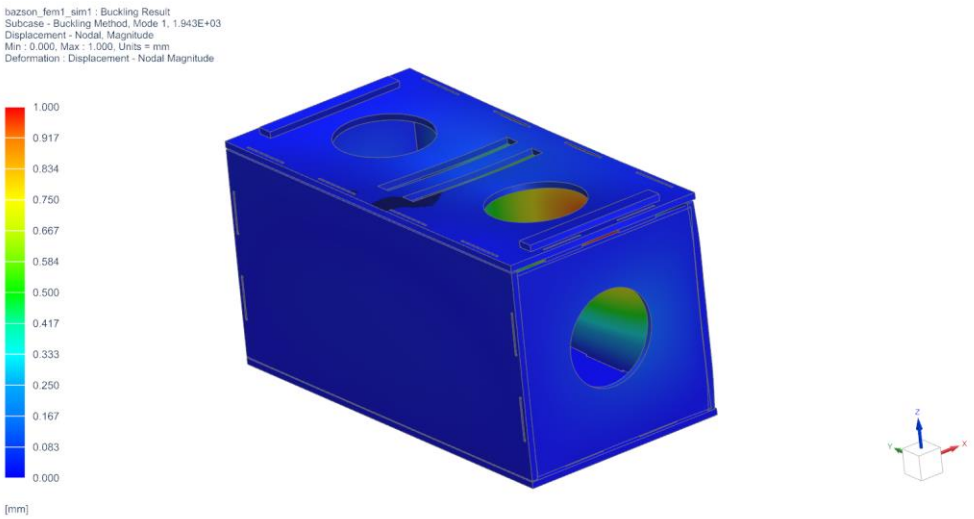

Figure 77A: Critical buckling displacement analysis under 1 N Force applied from -X direction inverse isometric view (Baz, 2023)

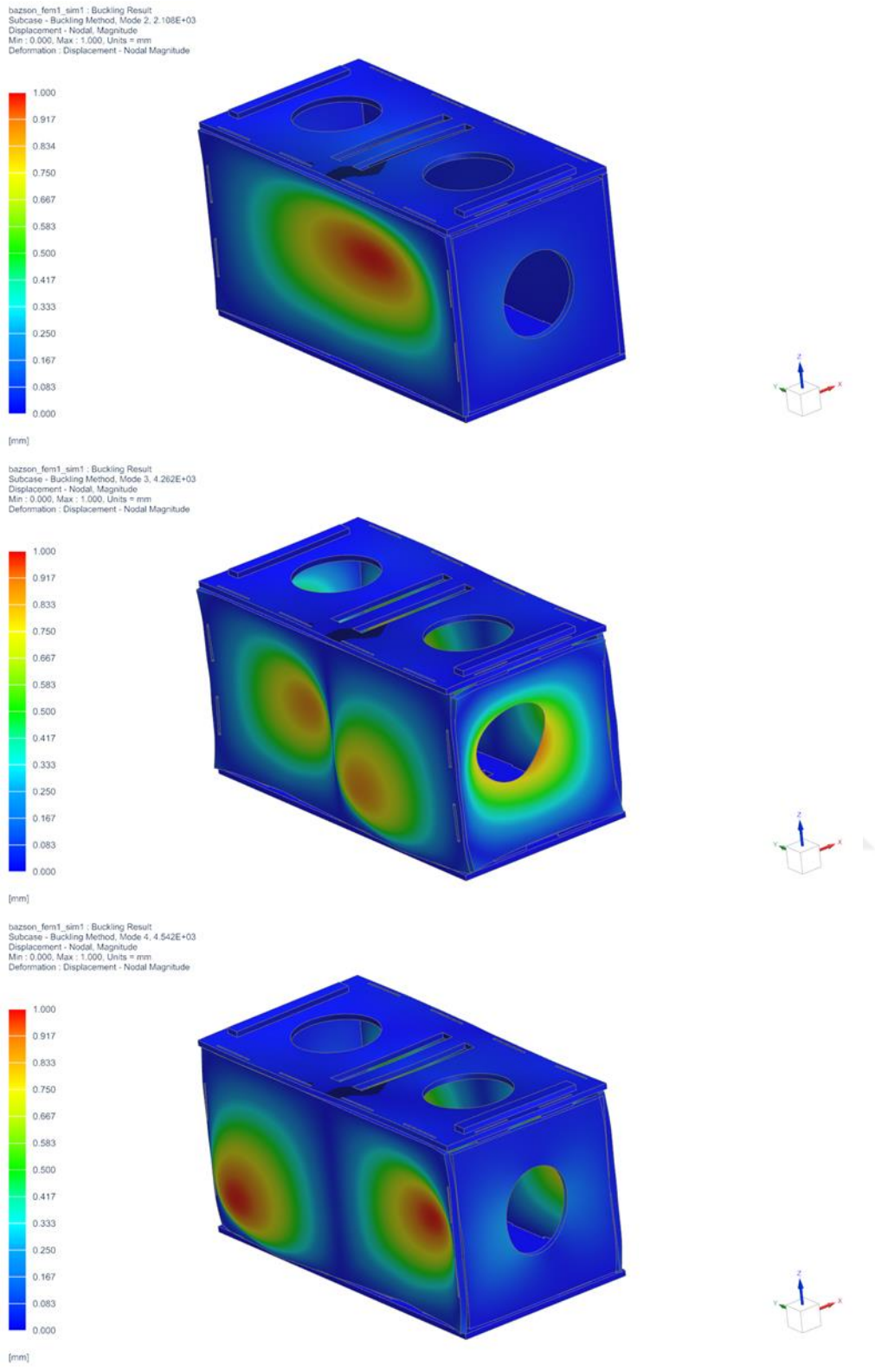

Figure 77B: Critical buckling displacement analysis under 1 N Force applied from -X direction inverse isometric view (Baz, 2023)

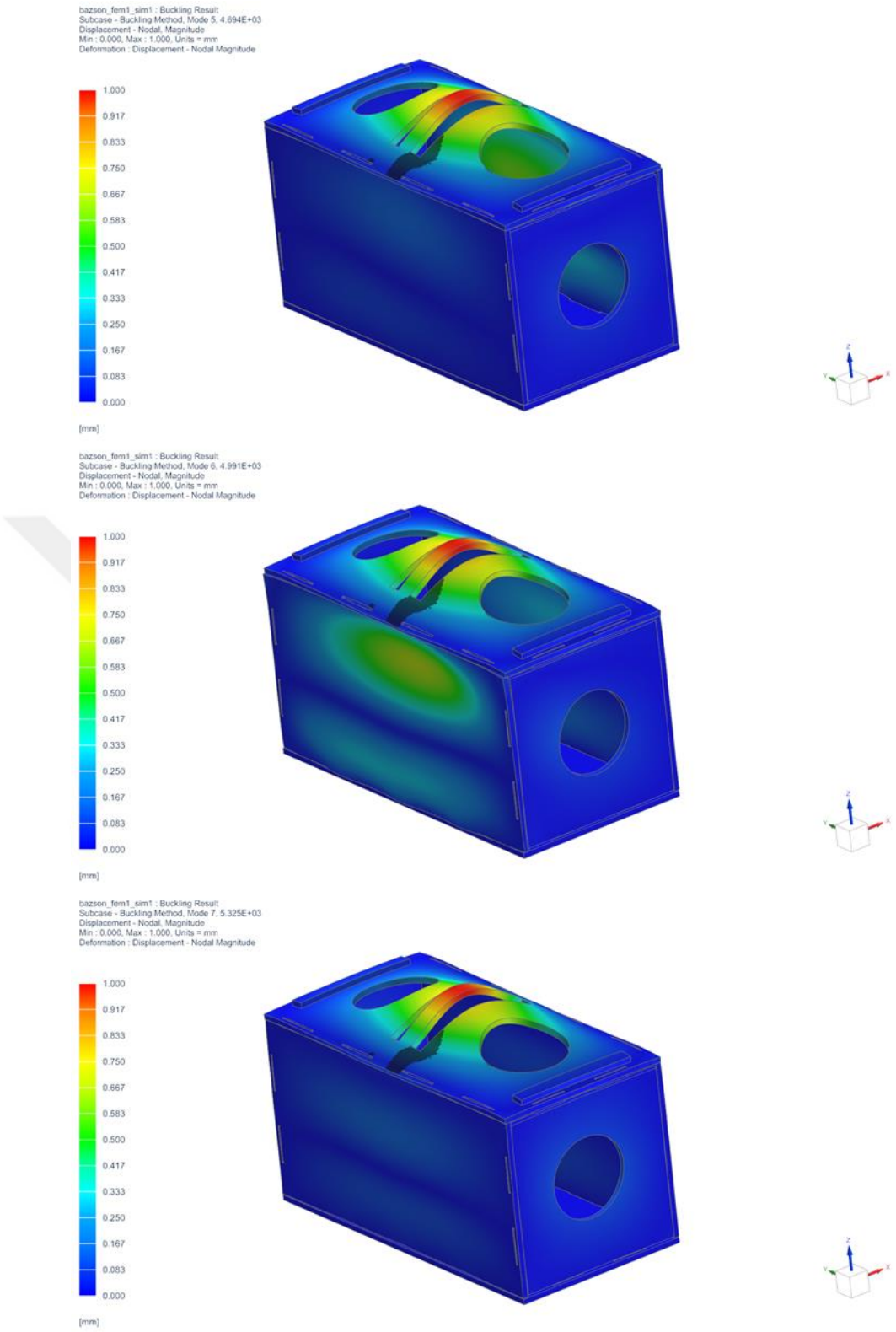

Figure 77C: Critical buckling displacement analysis under 1 N Force applied from -X direction inverse isometric view (Baz, 2023)

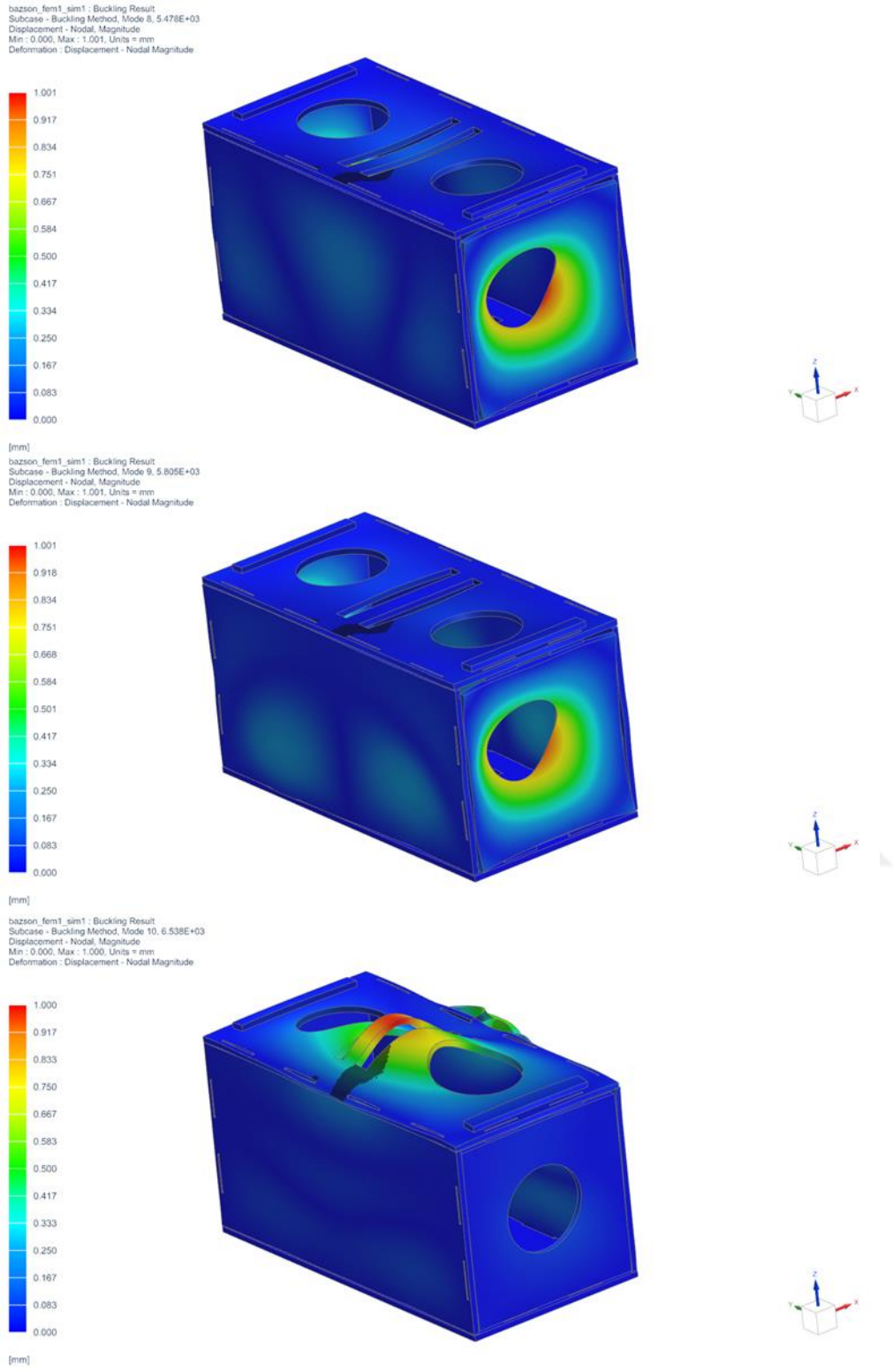

Figure 77D: Critical buckling displacement analysis under 1 N Force applied from -X direction inverse isometric view (Baz, 2023)

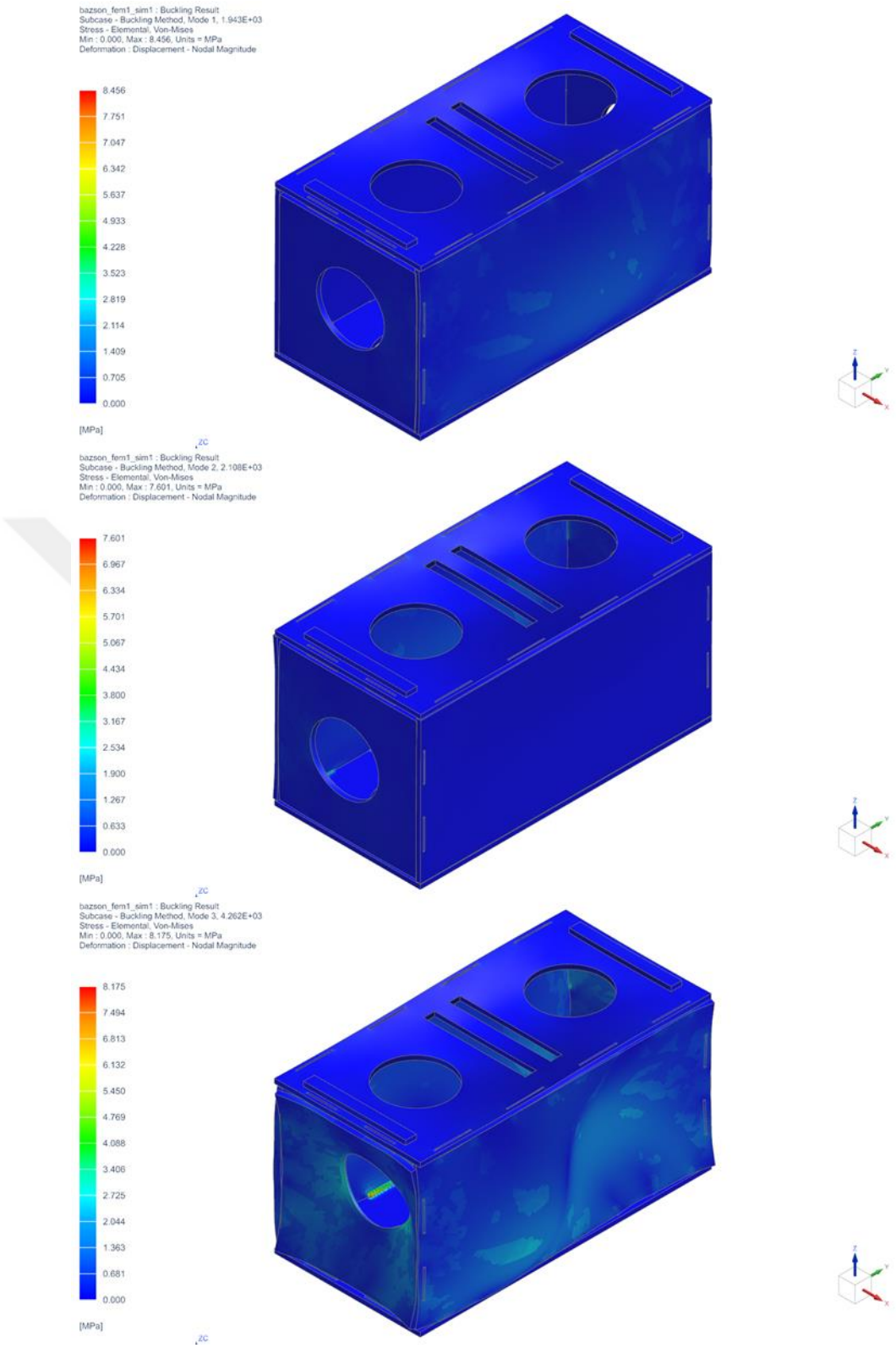

Figure 78A: Critical buckling von Mises analysis under 1 N Force applied from -X direction isometric view (Baz, 2023)

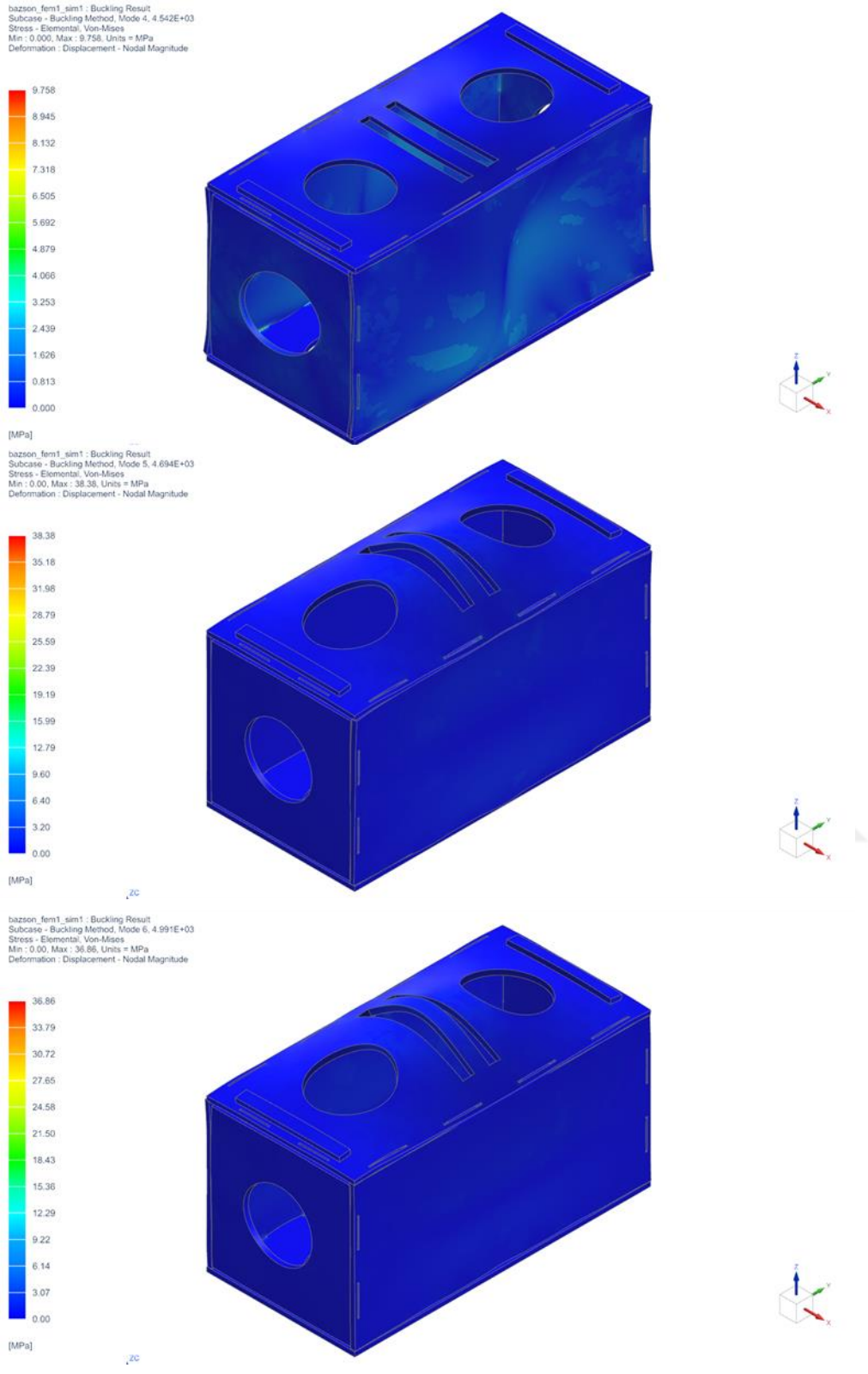

Figure 78B: Critical buckling von Mises analysis under 1 N Force applied from -X direction isometric view (Baz, 2023)

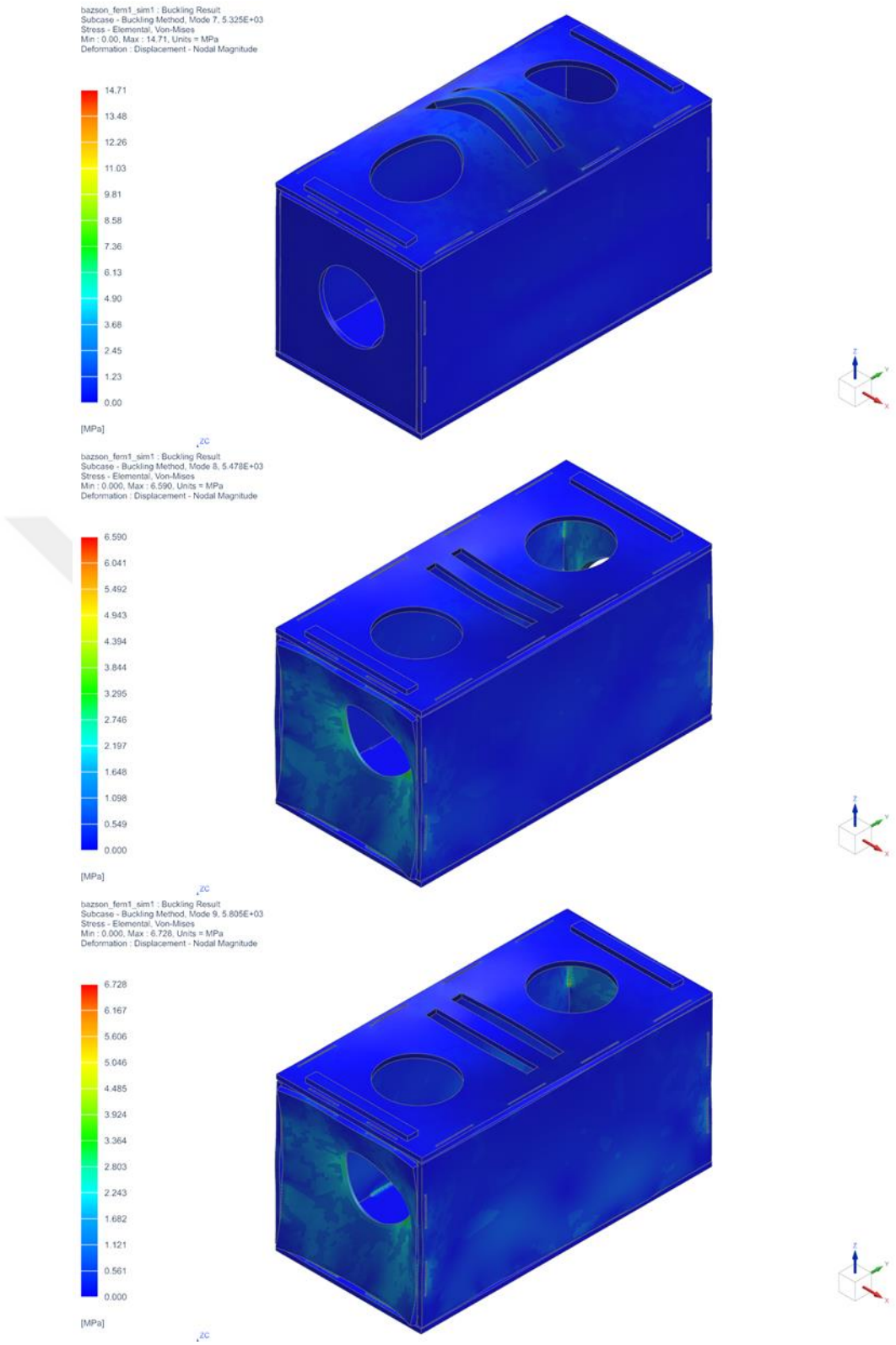

Figure 78C: Critical buckling von Mises analysis under 1 N Force applied from -X direction isometric view (Baz, 2023)

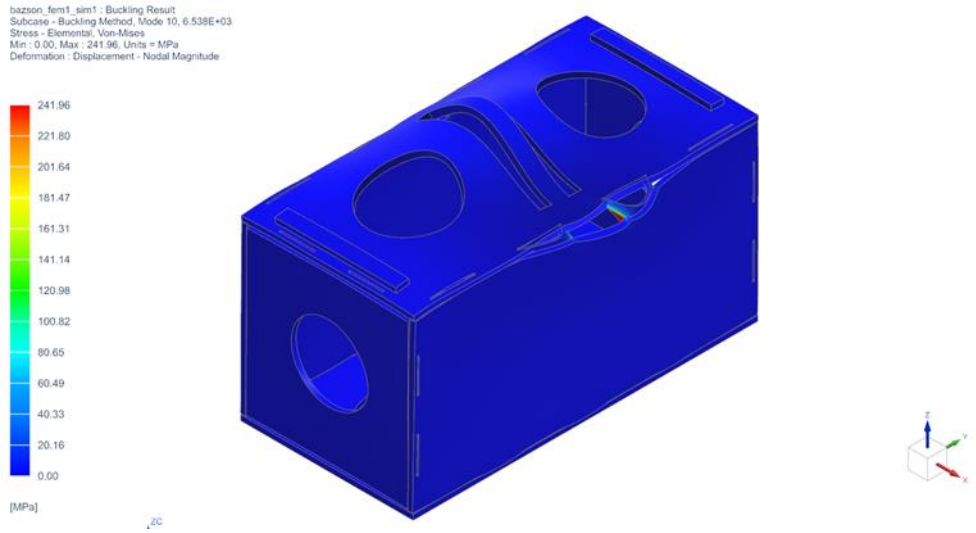

Figure 78D: Critical buckling von Mises analysis under 1 N Force applied from -X direction isometric view (Baz, 2023)

Table 5: Mode Values

	Mode	Value
Displacement and Von Mises mod values under 1 N Force applied from -Z direction	Mode 1	1.884E+03
	Mode 2	1.933E+03
	Mode 3	4.047E+03
	Mode 4	4.341E+03
	Mode 5	4.374E+03
	Mode 6	4.518E+03
	Mode 7	4.935E+03
	Mode 8	5.075E+03
	Mode 9	5.488E+03
	Mode 10	5.573E+03
Displacement and Von Mises mod values under 1 N Force applied from -X direction	Mode 1	1.943E+03
	Mode 2	2.108E+03
	Mode 3	4.262E+03
	Mode 4	4.542E+03
	Mode 5	4.694E+03
	Mode 6	4.991E+03
	Mode 7	5.325E+03
	Mode 8	5.478E+03
	Mode 9	5.805E+03
	Mode 10	6.538E+03

When the critical buckling analysis results are examined, it can be implied that the critical buckling load is the Eigenvalue 1,884E+03, and it is shown in mode 1 in Figure 71 which is the first figure. The NX finite element analysis software obtains this automatically and this result is equal to the critical buckling load of the proposed unit (Görgülüarslan et al., 2015).

3.3 Material

3.3.1 The Bioplastics

The proposed lightweight masonry unit has a raw material which is called bioplastics. These materials are manufactured from materials such as agricultural wastes, vegetable fats, vegetable fats and oils, corn starch, straw, woodchips, sawdust, and food waste. Generally, they are derived from sugar-based materials and their derivatives, which contain cellulose and lactic acids especially. They are different from standard plastics because they are derived from the derivatives of natural gas and petroleum (Amri, Hanifa, et al., 2018).

An aspect is that bioplastics are biodegradable materials, and they can dissolve in the environment with the help of microorganisms easily. They have almost zero hazardous effects on the environment. Because they dissolve totally in the environment in a very short time (Brodin et al., 2017).

They do not consist of any hazardous materials like silicate, aluminum, radon, or asbestos inside because they are organic and just derived from organic compounds (Fras et al., 2014).

As mentioned before, these materials are manufactured by using agricultural wastes or plant-based materials. There are two environmental effects; firstly, it provides a significant decrease in the waste in the environment as it uses them as raw material, so it causes a decrease in the amount of human junk due to daily consumption. Secondly, bioplastics are fully biodegradable that can dissolve in the environment easily.

For the manufacturing process, bioplastics provide a decline of waste materials in the environment as it uses human junk as its raw material. This manufacturing process generates new products from reused materials, and this is called recycling. So, can be expected that this process provides a decline in pollution as a positive side to the environment.

3.3.2 Graphene Oxide as an Alternative

The proposed lightweight masonry unit is produced using bioplastic, but there are many types of bioplastics. There are studies on improving the yielding stress of bioplastics by using some additives. There is a graph below which shows the tensile

and compression stress of mechanical properties of bioplastics of type CPR-M2. Also, when graphene oxide is added almost to all types of bioplastics, it provides an incline in yielding stress. It strengthens the bounds, when it reacts with the cellulose (Brodin et al., 2017). The graph in Figure 79 shows that the tension can reach almost 15 MPa for a bioplastic. When the studies about additives are examined, it is seen that graphene oxide can be chosen as an additive and a very small amount of it can increase the yield strength remarkably. This is resulting chemically from the molecular bounds. This chemical reaction is explained as follows;

"The increase in tensile strength due to the addition of graphene oxide is caused by the strong interaction between the bioplastic compiler molecules with graphene oxide layers. In more detail, it is associated with the interaction between the hydroxyl (OH) group, either from the bioplastic matrix or from the graphene oxide to form an oxygen bridge. The stirring time affects the process of mixing between the composite matrix and the filler graphene oxide. This stirring time corresponds to the filler particle distribution in the matrix cavity." (Amri, Ekawati, et al., 2018, pp. 5)

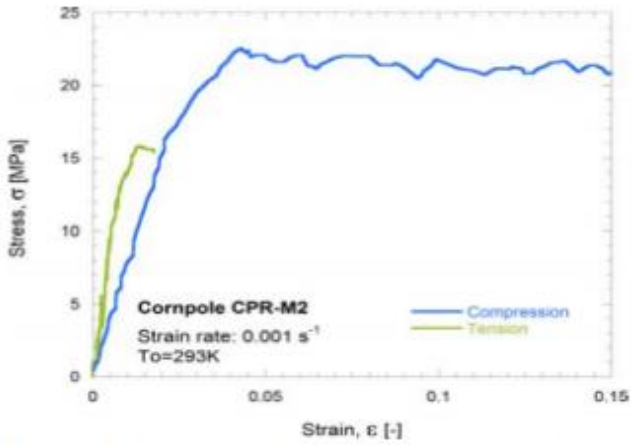

FIG. 3. CPR-M2. Results of tension and compression tests.

Figure 79: Tension and compression results of a bioplastic (Fras et al., 2014)

3.3.3 Lignocellulose as an Alternative

Another additive for the product is lignocellulose which is a recent and remarkably important type of bioplastic. When it is compared with graphene oxide, it is observed that the strength of the lignocellulosic bioplastic is considerably high.

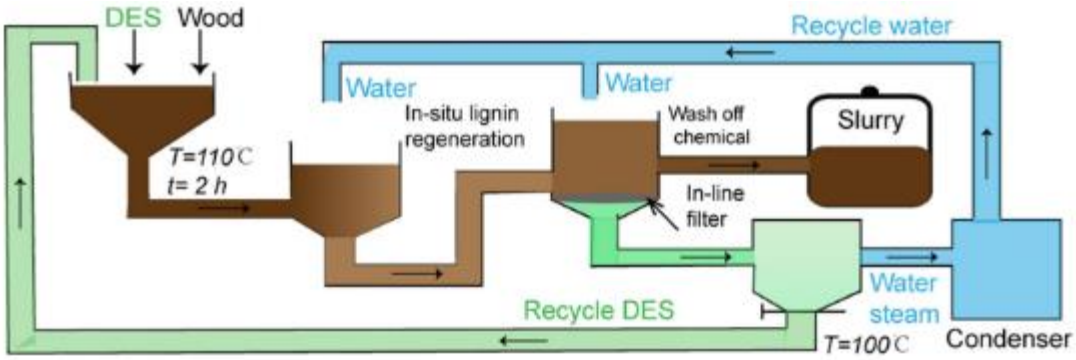

Figure 80: Derivation process of lignocellulosic bioplastics (Xia et al., 2021)

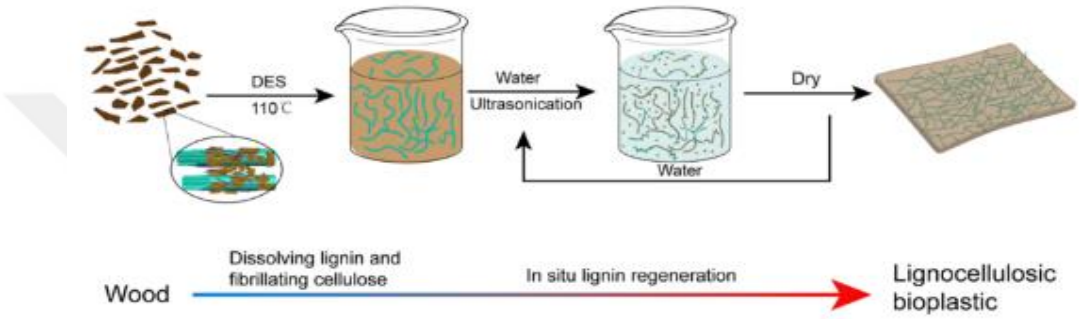

Figure 81: Dissolving process of lignocellulosic bioplastics (Xia et al., 2021)

This material provides benefits from other aspects like thermal conductivity and water absorption as well, and it is more environmentally and cheaper to provide lignocellulose, as it is also an organic compound. The graphic in Figure 81 shows the brief manufacturing process of the lignocellulosic bioplastic.

Figure 82: Degradation phases of lignocellulosic bioplastics in nature (Xia et al., 2021)

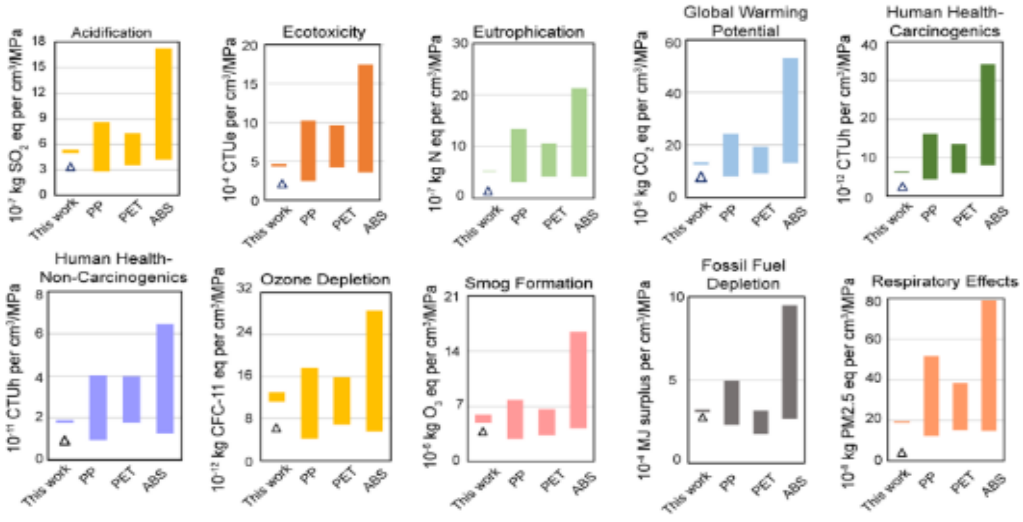

Figure 83: Comparison of lignocellulosic bioplastics with other plastics from different aspects (Xia et al., 2021)

It also dissolves easily in the environment, as it is shown in two different experiments above in Figure 82 and Figure 83.

Figure 84: Lignocellulosic bioplastics' dissolving in nature changing by the derivate material (Xia et al., 2021)

Lignocellulosic bioplastics can be produced by using many different types of organic wastes like wood chips, wheat straw, grass, or bagasse, as shown above in Figure 84. So, it is very easy to produce and very environmentally friendly.

Another important aspect is to understand the chemical properties and working principles of the lignocellulose, while giving this extreme strength to this specific type of bioplastic.

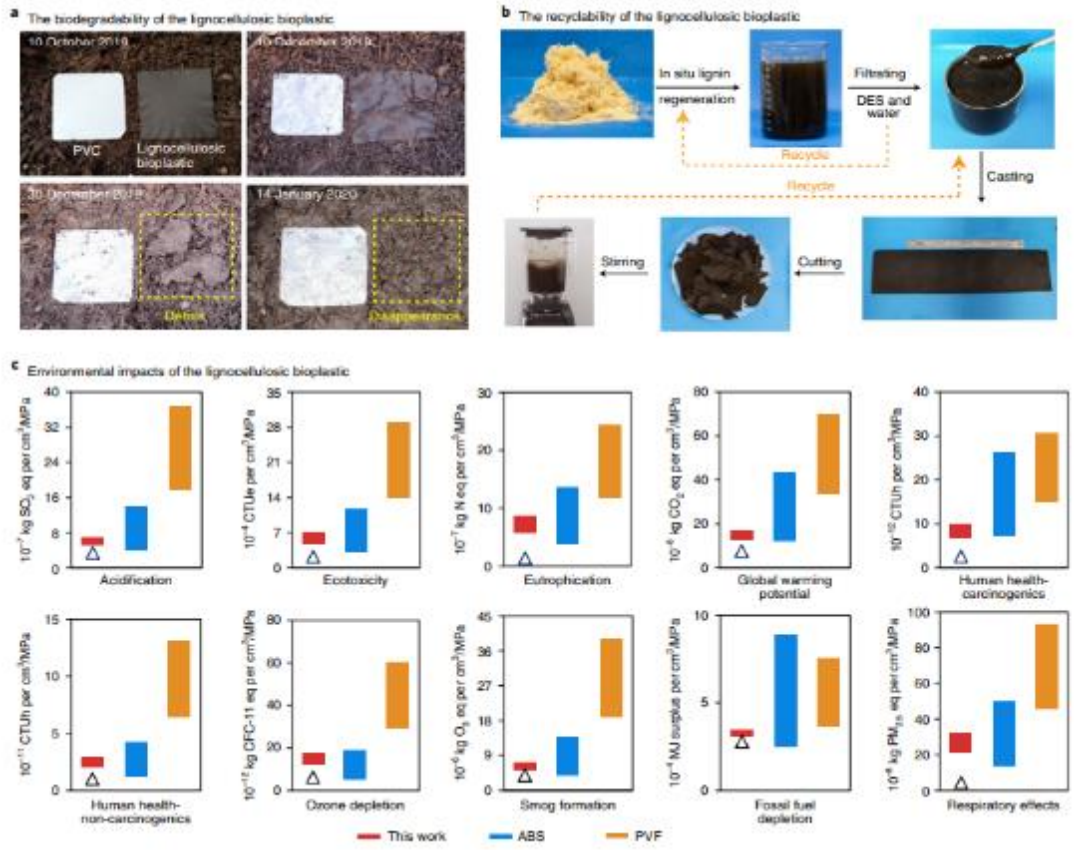

Figure 85: Environmental impacts of lignocellulosic bioplastics (Xia et al., 2021)

Water absorption is another important aspect of its use in the construction industry, so it is also researched elaborately.

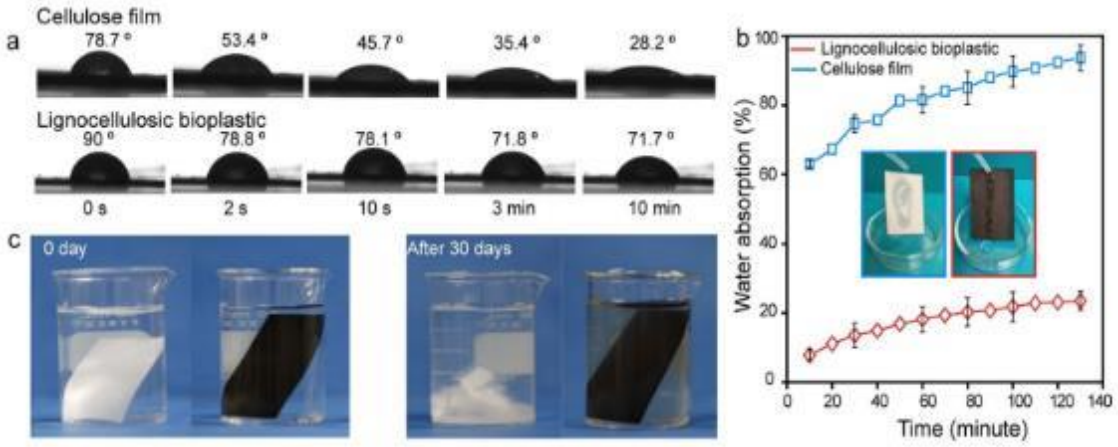

Figure 86: Water absorption capability of lignocellulosic bioplastics (Xia et al., 2021)

For the evaluation of the proposed product's manufacturing opportunity in Turkey, bioplastics are essential. As previously stated, bioplastics are typically produced from

organic detritus. Turkey's population exceeds 80 million, and the population's pollution is considerable. The production of the proposed product reduces waste, providing sustainable waste reduction, which makes its production extremely advantageous and practicable. On the other hand, an additional issue is the additive material, and the most feasible additive is lignocellulose, which is also derived from trees and plants, making it an organic material that can be easily obtained from the environment. However, there is a need for qualified laboratories for deriving lignocellulose and also for producing bioplastic from various types of waste. However, an investment in the laboratory and research process will yield a rapid return in Turkey if manufacturing occurs.

4. EVALUATION OF PROPOSED LIGHTWEIGHT MASONRY UNIT

The pros and cons of the proposed unit will be evaluated and discussed elaborately in this part of the study.

4.1 Strength and Opportunities

Many aspects of the proposal unit can be regarded as its positive sides and the opportunities it can provide.

4.1.1 Weight and Volume Advantage

To illustrate, for AAC and pumice masonry units, when taking a sample with the dimensions of 19 cm by 39 cm by 19 cm. For one store palette, there are about 100 pieces of them and the consumption for 1 sqm is about 12 blocks and so one palette can make almost a 9 sqm wall. One piece of this concrete block is about 8 kg and one piece of this dimensioned AAC is about 5 kg (Url-12). For the masonry unit, if it has been taken as a referent palette that has a volume of 1.4 m3, then one palette weighs about 700 kg for concrete masonry units and 400 kg for the AACs (Israngkura & Ayudhya, 2011).

When the volume is calculated and the mass of the product. The product's pieces can be located one on top of another, and they have a thickness of about 8 mm. 4 modules have an area of 0.074 m2 and 2 pieces have 0.036 sqm. Almost half of them generally can be located one on top of another. For a store palette that has a height of 1.4 m, a depth of 1 m, and a width of 1 m, almost 170 large modules, can be located the height, vertically, and the base of 1 sqm, can be located about 13 times of 170 pieces, horizontally, so can be located to same palette almost 2200 modules as a component which combines the one single concrete block. For one single block, need 4 big pieces and 2 small pieces, these 2200 modules have to be selected considering this rate. Modules can be located, enough for 400 single blocks in one palette, and that palette weighs about 1300 kg.

To make that calculation briefer. The modular surfaces of the proposed bioplastic units (each having a thickness of about 6 mm, 4 modular surfaces having an area of 0.074 sqm, and 2 small modular surfaces having 0.036 sqm) can be piled on top of each other. Almost 170 large bioplastic units can be put in a truck (with a height of 1.4 m, a depth of 1 m, and a width of 1m) vertically in one sqm, and 13 times 170 pieces horizontally, so almost 2200 bioplastic modular surfaces which are equal to 400 bioplastic units in one truck that weighs about 1300 kg.

For 1 sqm of the wall, the number of masonry units to be used is the same as the others. So, with a truckload of standard masonry units can build about 36 sqm of the wall. It can be built 4 times more with the same volume of proposed bioplastic masonry units. On the other hand, as mentioned above, when a pumice concrete block unit weighs about 8 kg and an AAC unit about 5 kg, the proposed bioplastic unit weighs about 2,16 kg.

Table 6: Detailed Mechanical and Physical Properties of Pumice Blocks (Değirmenci & Yılmaz, 2011)

Chemical composition (%)	PA	PC	Physical and mechanical properties of PC	
			Specific weight	
SiO_2	71.10	20.04	Initial setting time (min)	3.15
Al_2O_3	13.50	5.81	Final setting time (min)	150
Fe_2O_3	1.68	3.62	Volume expansion (mm)	185
CaO	1.14	61.52	Specific surface (cm^2/g)	2.00
MgO	0.40	1.43		3516
Na_2O	3.40	0.18	Compressive strength (MPa)	
K_2O	4.05	0.94	2-days	22.0
SO_3	-	2.87	7-days	38.7
Free CaO(%)	-	1.41	28-days	46.8

This comparison shows us how light the product is, compared to the widely used others. This lightness is partly due to its design and partly arises from the bioplastics.

4.1.2 Chemical Structure and Fiber Wrapping

The chart below briefly explains the working principle of lignocellulose. It chemically wraps the molecules and proves the extremely high strength in bioplastics.

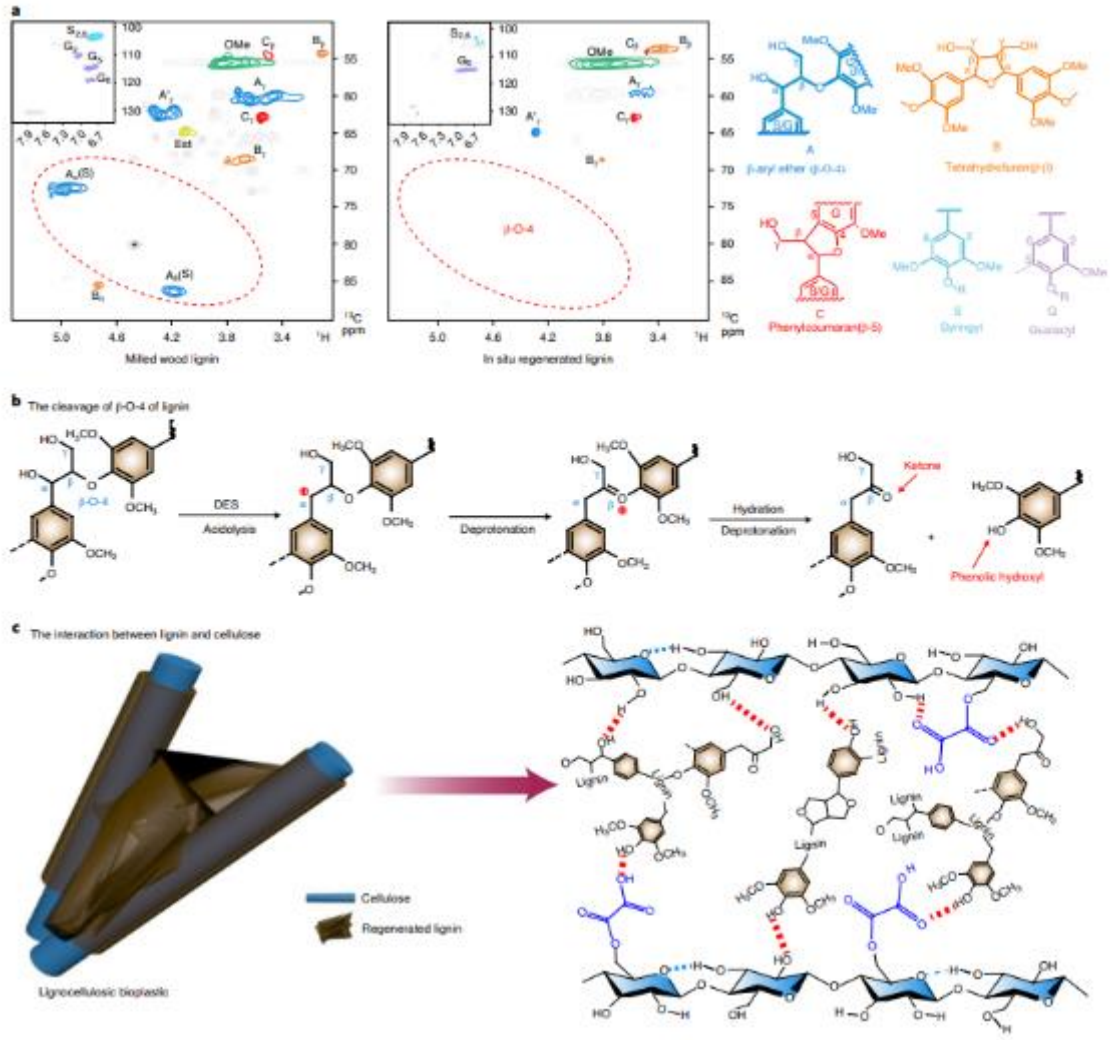

Figure 87: A strong, biodegradable, and recyclable lignocellulosic bioplastic (Xia et al., 2021)

Strength rates are remarkably important while using products in the construction industry. And the charts below show the lignocellulosic bioplastic.

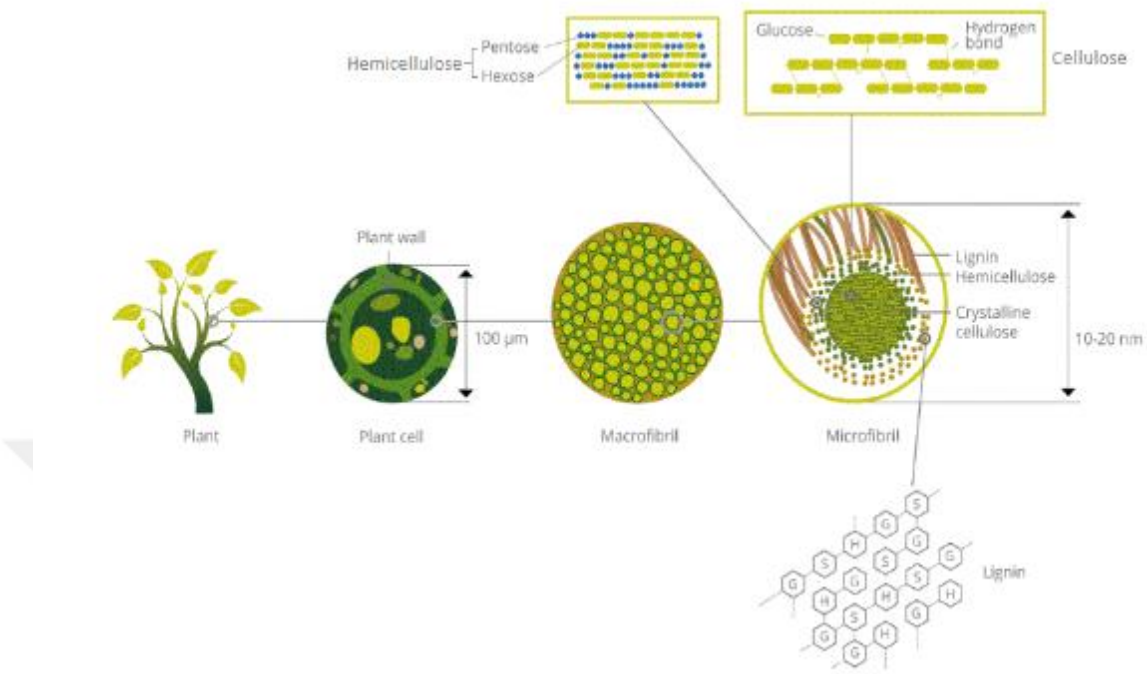

Figure 88: Lignin, Cellulose, and Micro Fibril Structure (Url-13)

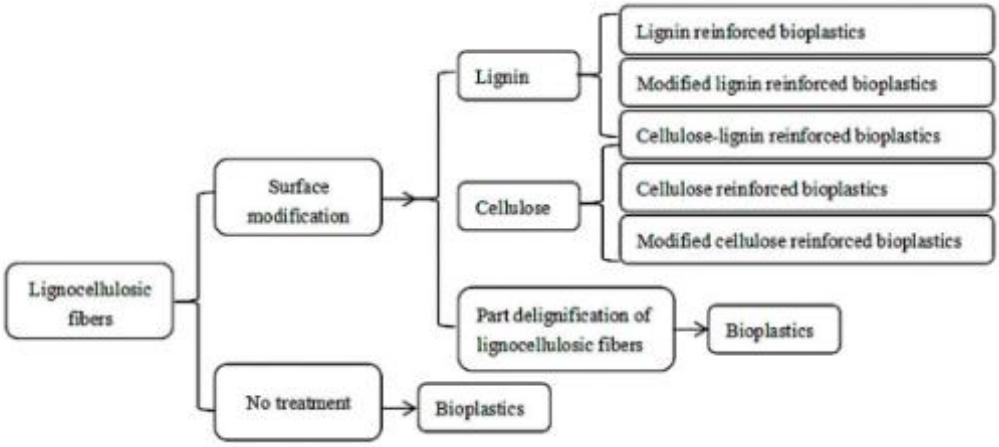

Figure 89: Applications of Lignocellulosic Fibers and Lignin in Bioplastics (Yang et al., 2019)

Lignocellulosic residues containing a significant polysaccharide moiety represent a very interesting source of fillers for bioplastics (Ferrer & Rojas, 2016) The interaction between lignin-containing cellulosic fibers and biopolymers is complex due to the

various compositions of cellulosic fibers. The interaction between jute strips and PLA was evaluated. Five different lignin contents of the wires were added to PLA with a fiber ratio of 30% by weight. A PLA matrix was prepared in a discontinuous extruder and characterized by tensile tests. Macro and micromechanical analysis showed that jute strips with 4% lignin content are most suitable for use as PLA fillers. This phenomenon was mainly attributed to their better interaction and distribution within the PLA matrix and higher intrinsic mechanical properties (Dwivedi, 2017). Lignocellulosic fillers from bioethanol production were blended with Polymers 2019, 11, 751 16/26 PHB. Spectroscopic, thermal, and morphological characterization showed a high polysaccharide content in the filler. The lignocellulosic filler produced an active effect on the physical aging of PHB by acting as a heterogeneous nucleating agent. Infrared spectroscopic data showed that a low interaction between lignocellulosic filler and PHB was observed. In addition, the deterioration of impact and tensile properties in composites has been attributed to this lack of connectivity. On the other hand, bio composites became more resistant to degradation as the lignocellulosic filler concentration increased, possibly due to the antibacterial activity of lignin. Therefore, the use of these agro-industrial residues had great potential to expand the application of PHB, as lignocellulosic fillers improve biopolymer properties in a cost-effective and environmentally friendly way (Angelini et al., 2014: 163-173).

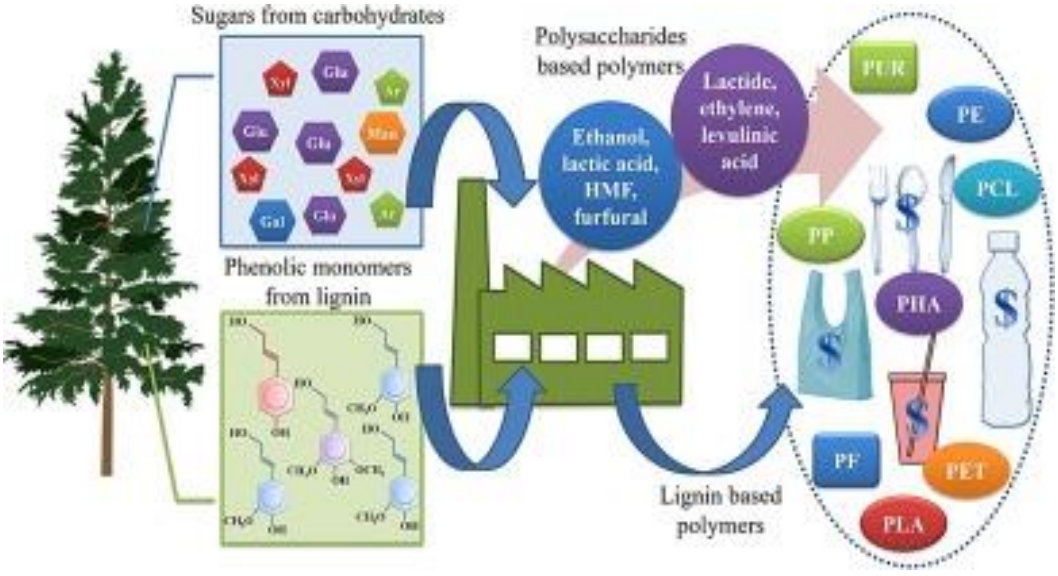

Figure 90: Lignocellulosic as sustainable resources for the production of bioplastics (Brodin et al., 2017)

Lignin-containing cellulose nanofibrils (LCNF) can produce enhanced properties when incorporated into bioplastics. Palm oil residue empty fruit clusters were extracted to obtain lignin-containing cellulose nanofibrils (LCNF) by various separation methods. Different types of LCNF isolated were incorporated into starch bioplastics. Young's modulus and yield stress provided remarkable increases after the incorporation of LCNF. Also, as the LCNF loading increased, the water uptake of the composite bio foams decreased due to the low hydrophilicity of the lignin residues. Starch/LCNF nanocomposites exhibited the same mechanical properties as polystyrene polymers. Therefore, they can be considered as a potential and green alternative in insulation and packaging composites (Ferrer & Rojas, 2016) PLA and varying amounts of LCNF from 5 to 20% by weight were blended to develop composite films by casting and hot pressing. Good interface adhesion between PLA and LCNF was demonstrated due to the presence of lignin and further evidenced by infrared spectroscopy and nanoscale atomic force microscopy characterization results.

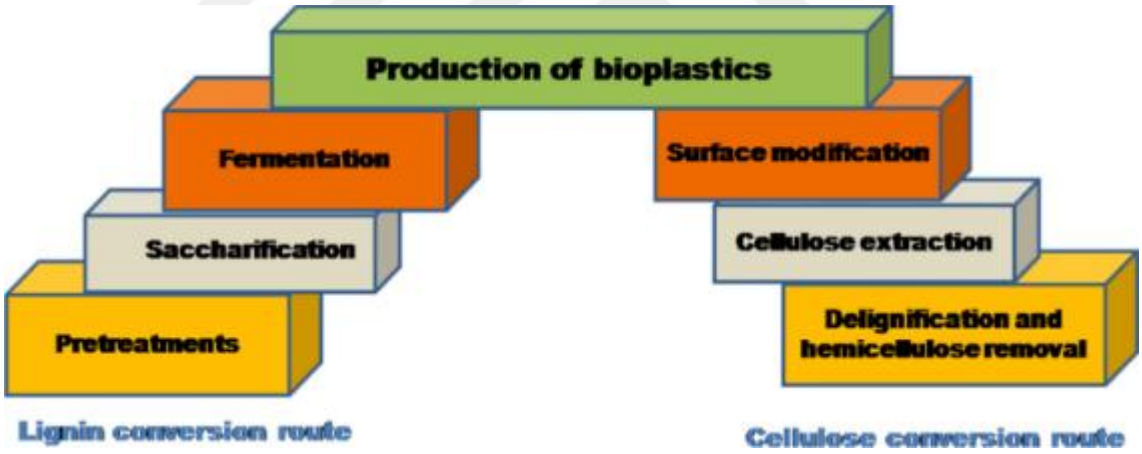

Figure 91: Bioplastic production from renewable lignocellulose feedstocks (Reshmy et al., 2021)

It has been confirmed that the water resistance, thermal and mechanical properties of bioplastics obtained by adding 5-10% by weight of LCNF are significantly improved (Reshmy et al., 2021) Reports of lignin-containing cellulose-reinforced bioplastics are few, but sufficient to indicate promising applications in bioplastics in the future. It can be concluded that they can significantly influence and even determine whether the direct use of lignocellulosic fibers in bioplastics can be achieved. They should be a hot

spot in the future. Lignin-containing cellulose nanofibrils will play an important role in the preparation of bioplastics with lignocellulosic fibers (Yang et al., 2019).

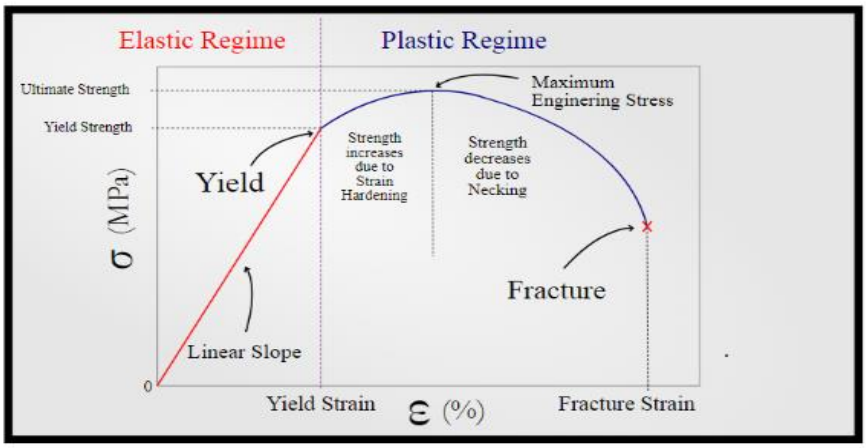

Figure 92: Stress-Strain Diagram (Url-14)

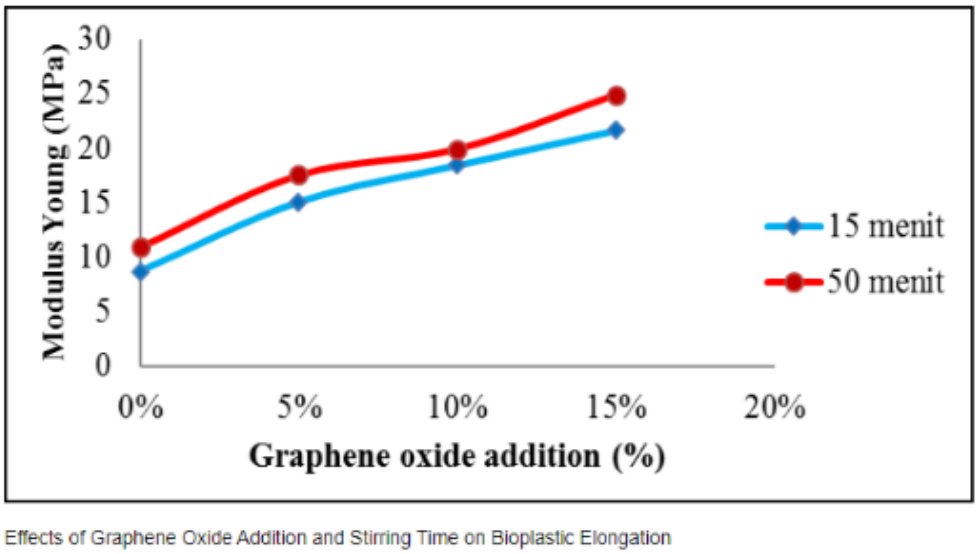

Figure 93: The difference in Young Modulus with graphene oxide addition (Amri, Ekawati, et al., 2018)

As shown above, in Figure 93, lignocellulosic bioplastic provides a tensile strength of up to 120 MPa. On the other hand, standard bioplastic after graphene oxide addition generally observes tensile strength around 5 MPa. Like the AACs strength with the usage of graphene oxide, it can mostly achieve up to that of AACs strength.

Table 7: Effects of Graphene Oxide Addition on Bioplastics (Amri, Ekawati, et al., 2018)

Concentration of GO	Time (minutes)	Sample	Tensile Strength (MPa)	Elongation (%)	Young modulus (MPa)
0%	30	1	1,38	28,09	4,88
	60	2	2,25	25,03	9,00
5%	30	3	2,55	20,62	12,36
	60	4	2,65	18,90	13,99
10%	30	5	2,74	15,35	17,88
	60	6	2,84	14,96	19,00
15%	30	7	3,63	13,45	26,95
	60	8	3,92	13,22	29,66

4.2 Weakness and Threats

There are some weaknesses and threats about the proposed lightweight masonry unit which will be examined as follows.

4.2.1 Durability

However, the study implies that the proposed lightweight masonry unit is as strong as the other common construction units. However, the proposed design proposes not to have a rigid body having many joints and edges with a unique design, different than the others available in the industry.

This issue can result in some strength problems because there occurs an additive process in which the applicator will be in charge and assemble the product in its final shape by bringing the joints together.

When compared with that of other products' their end-shape processes do not include such a process. So that our strong results data can be different a little bit in practical use.

4.2.2 Not Feasible for Every Usage as a Partition Wall

The proposed construction unit cannot be so feasible for every usage area. For example, if the user wants to hang a heavy object, like an LCD TV, a heavy frame, or an item of furniture, on a partition wall built by using the proposed lightweight

masonry units, there can occur some load-bearing problems. The reason is when something is hung on the wall, the load-bearing force becomes that small area that carries the small joint. Due to its design, the proposed lightweight masonry unit is assembled by six separate flat surfaces. The load-bearing part of that small area on the surface can behave weaker and incurable. The load-bearing limits can differentiate depending on the height of the ceiling and the weight of the objects hung on the wall. This can be considered a weakness and/or threat to the proposed lightweight masonry unit. If there is a need for corners generated by the proposed construction block system due to forces of different magnitudes, the joints can be separated from each other, and certain strength problems may arise. So, the wall built by using the proposed construction blocks must be placed between the columns and the beams. In case of a corner location, a supportive L-shaped steel stud, large enough to hold the two perpendicular walls at the corner, will be necessary.

4.2.3 Joint System and Joining with Other Parts of the Construction

Windows and doors require lintel systems to hold the material at the upper part of these openings under the beam and/or the ceiling and carry the load of this part. For commonly used lightweight masonry blocks, generally, steel beams are placed inside the mortar (Smyrou, E., 2016) which carries the load. For the proposed product, mortar is not used between the construction blocks. but for this lintel system, it can be used as the same method just for this lintel system a thin cement-based mortar can be used because the blocks are quite light, and is not resistant to heavy loads. The proposed product has a separately designed lintel system, on the figures below it has shown. It allows the pipeline to pass through inside and carry the blocks. It can be made both from aluminum and iron raw material however the best option is to obtain from bioplastic raw material. This issue needs to be examined in future studies of this project. For the end sides of the walls generated by the proposed block, as for the commonly used blocks, it is used also, their specific foams which are manufactured for compressing the units in construction. that foam can be used at the end of the application. Also, this can be applied between columns, beams, and blocks. When the foam is applied, it starts to expand and then provides compression between columns, beams, and blocks.

Another issue is the opportunity for hanging something on the wall generated by the proposed blocks. Due to the finite element analysis, the blocks can carry up to 200N on a single joint. but for future studies it can be improved by the additive material amount and properties.

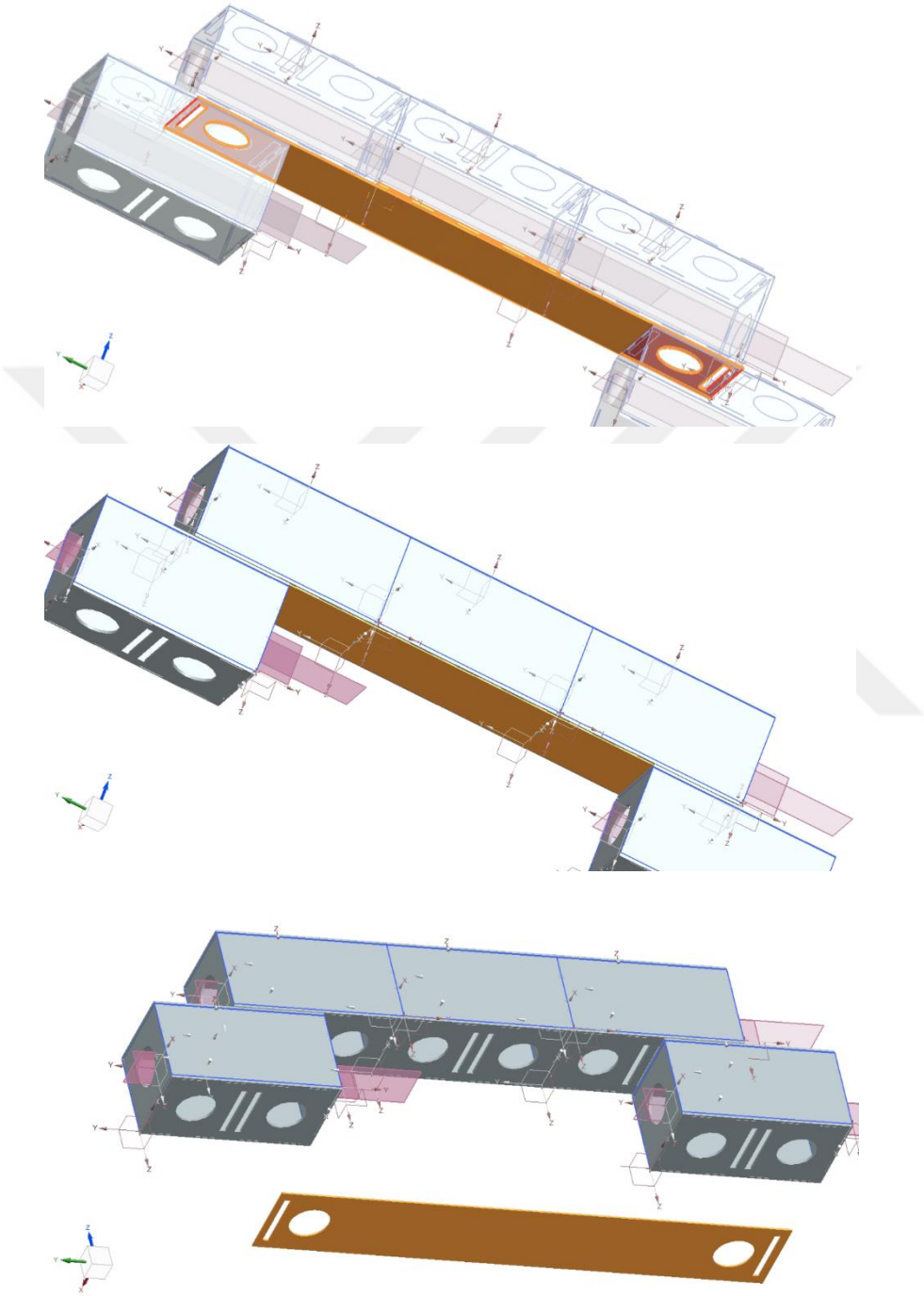

Figure 94A: Lintel Design for the Alternative Block (Baz, 2023)

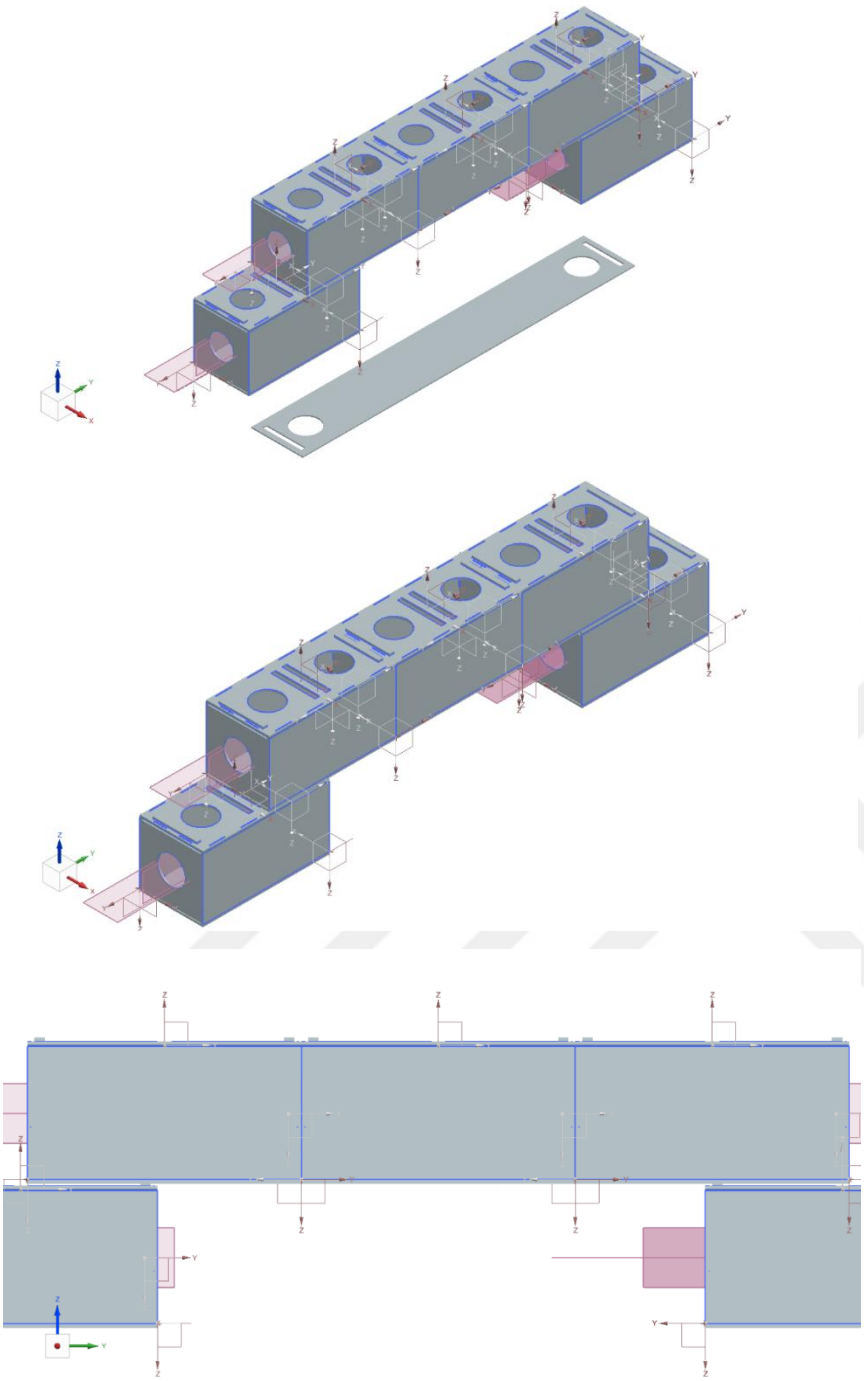

Figure 98B: Lintel Design for the Alternative Block (Baz, 2023)

4.2.4 Coating Alternatives Against Abrasion Risks

The blocks are produced by bioplastic raw materials, which can result in some abrasion problems under different conditions. For this reason, coating alternatives with some chemicals can be proposed to prevent this problem. For sanitary spaces like bathrooms and toilets, different coating materials protect the construction blocks and avoid water contact. A specific example for this is Isonem which is a product that is type of a liquid glass, providing a thin layer on the construction block and protecting it from different possible corrosion-causing effects. Those chemical coatings protect the blocks against fire. generally, there are many chemical companies (like BASF and DuPont) and they are manufacturing those kinds of coating chemicals for construction materials. There are also some alternatives where the user can also add paint inside them. But they are just implemented as alternatives the further studies after prototype manufacturing and tests in real life, will give us more elaborate ideas about possible coating materials.

It is very easy to use them, especially since most of them are used by spraying onto the construction material and correcting with a corrector.

This results in a protection against time issues. Because the lifespan of the block is decreasing over time. So, the coating which will avoid corrosion also pretends the aging of the block so, lengthens its lifespan.

5. CONCLUSION

To conclude, when it is examined the crucial need for being eco-friendly, it can be observed that the construction industry is also responsible for generating new solutions.

The subtheme in this big industry is the blocks which are used very frequently and two main ones are standard concrete masonry units and AAC blocks.

In Table-8 it can bee seen the comparison results for the Pumice, AAC and Proposed Blocks.

Table 8: Comparison Among Standard Blocks (Baz, 2023)

	Pumice Block	**AAC Block**	**Proposed Block**
Weight Advantage	8kgs	5kgs	2,16kgs
Strength (Max. Elongation Under Same Amount Same Directional Force)	2,956E-03mm	0,664mm	1,824mm
Sustainability (Biodegradability in the Environment)	No	No	Yes
Ecofriendly Manufacturing	Not Reducing Pollution	Not Reducing Pollution	Reducing Pollution
Volume Advantage by Modular Design (Number of Pieces in Same Size Palette)	100pcs	100pcs	400pcs
Ranking According to Above Properties	3rd	2nd	1st

Although the AAC block has some positive sides when compared with the standard concrete masonry units, in my opinion, it is not enough to call, it environmentally sustainable. This is the reason for this study to find a new solution. As mentioned before the solution provides a different solution that can be named as environmentally friendly from many aspects. The study has not finished yet and the static tests process is continuing to provide almost the same tensile, compressive, tensional stress resistances with commonly used blocks. Many petroleum-based plastics' stress resistances are more than those commonly used concrete blocks and the bioplastics can surpass those petroleum plastics in many different usage areas that require strength (Amri, A., Ekawati, L. et al., 2018). So that it can be implied that our solution also provides the same resistance and durability as the commonly used concrete blocks. Moreover, the product's resistance and durability level can reach remarkable levels exceeding the concrete blocks' level by additive materials like graphene oxide as mentioned before, a very small amount can be enough to obtain these results (Gironi & Piemonte, 2011).

REFERENCES

Abbas, A. L., Saeed, M. H., *Representation of The Masonry Walls Techniques by Using FEM,* Australian Journal of Basic and Applied Sciences, pp. 39-48, 2017

Abdulla, K.F., Cunningham, L.S., Gillie, M., *Simulating masonry wall behaviour using a simplified micro-model approach,* Engineering Structures, Volume 151, pp. 349-365, 2017.

Al-Chaar, G., Mehrabi, A., *Constitutive Models for Nonlinear Finite Element Analysis of Masonry Prisms and Infill Walls*, 2008.

Amri, A., Ekawati, L., Herman S., Yenti, S., Zultiniar, Y., Aziz, S.P., Bahruddin, U., *Properties Enhancement of Cassava Starch-Based Bioplastics with Addition of Graphene Oxide, IOP Conference Series: Material Science and Engineering*, Volume 345, Issue 1, pp. 012-025, pg.32-45, 2018.

Amri, A., Hanifa, R., Evelyn, E. Awaltanova, E. *The Effects of Graphene Oxide Functionalization on The Properties of Sago Starch-Based Bioplastics,* IOP Conference Series: Materials Science and Engineering, 2018.

Angelini, S., Cerruti, P., Immirzi, B., Santagata, G., Scarinzi, G., Malinconico, M., *From Biowaste to Bioresource: Effect of a Lignocellulosic Filler on the Properties of Poly(3-hydroxybutyrate),* Int. J. Biol. Macromol.,71, pg.163–173, 2014.

Arıbaş, A., Özler, M., *Foldable Brick with Rope Attachments and Detachable Wall Building System,* Patent No: US2016281357A1, 2016.

Bhatti, K., *Modular Block Construction System,* Patent No: US5664387A, 1997.

Brodin, M., Vallejos, M., Opedal, M.T., Area, M.C., Chinga-Carrasco, G., *Lignocellulosics as Sustainable Resources for Production of Bioplastics, Journal of Cleaner Production*, Volume 162, pg. 646-664, 2017.

Caldas, L. R., Pittau, F., Schaeffer, R., Saraiva, A. K. E. B., Paiva, R. L. M., Filho, R. D. T., *Concrete vs. Ceramic Blocks: Environmental Impact Evaluation Considering a Country-Level Approach*, 17 November 2021.

Değirmenci, N., Yılmaz, A., *Use of Pumice Fine Aggregate as An Alternative to Standard Sand in Production of Lightweight Cement Mortar*, Indian Journal of Engineering and Materials Sciences, 2011.

Diaz, J. J. C., Nieto, P. J. G., Rabanal, F. P. A., Martinez-Luengas, A. L., *Design and shape optimization of a new type of hollow concrete masonry block using the finite element method, Engineering Structures,* Volume 33, Issue 1, pp 1-9, Jan 2011

Drazal, L. T., Misra, M., Mohanty, A. K., *SustainableBio-Composites from Renewable Resources: Opportunities and Challenges in The Green Materials World, Journal of Polymers and the Environment*, v.10, April 2002.

Dwivedi, G., *Effect of fiber treatment on flexural properties of natural fiber reinforced composites, Egypt.* J. Pet., 138 Sood, 2017.

Ferrer, A., Rojas, O.J., *Starch-Based bio foams reinforced with lignocellulose nanofibrils from residual palm empty fruit bunches: Water sorption and mechanical strength,* ACS Sustain. Chem. Eng., 4, 5546–5552, 84, 2016.

Fras, T., Nishida, M., Rusinek, A., Pecherski, R., Fukuda, N., *Description of The Yield State of Bioplastics on Examples of Starch-Based Plastics and PLA/PBAT Blends,* Engineering Transactions, 62, 4, pp. 329-354, 2014

Fundi, S.I., Kaluli, J.W., Kinuthia, J., *Finite element modeling of interlocking stabilized laterite soil block walls.* SN Appl. Sci. 3, 225, 2021.

Gironi, F., Piemonte, V., *Bioplastics and Petroleum-Based Plastics: Strengths and Weaknesses, Energy Sources, Part A: Recovery*, Utilization and Environmental Effects, v. 33, issue 21, pp. 1949-1959, 2011.

Görgülüarslan, R. M., Gandhi, U. M., Mandapati, R., Choi, S.K., *Design and fabrication of periodic lattice-based cellular structures, Computer-Aided Design & Applications*, 2015

Grasser, K., Minke, G., *Building with Pumice*, 1990.

Guo, Z., *Principles of Reinforced Concrete, Butterworth-Heinemann*, pp. 89-112, 10.1016/B978-0-12-800859-1.00004-9, 2014.

Hajek, V., Sitar, L., *Building Block and Building Structure Comprising These Blocks*, Patent No: CZ35145U1, 2021.

Hanson, G., Inness K., *Building Block, and Structures Formed Therefrom,* Patent No: US5024035, 1991.

Hibbeler, R. C., *Mechanics of Materials*, Pearson, 2014.

Huarachi, D., A., R., Gonçalves, G., Francisco, A. C., Canteri, M. H. G., Piekarski, C. M., *Life cycle assessment of traditional and alternative bricks: A review, Environmental Impact Assessment Review*, January 2020.

Israngkura, B., Ayudhya, N.A., *Compressive and Splitting Tensile Strength of Autoclaved Aerated Concrete (AAC) Containing Perlite Aggregate and Polypropylene Fiber Subjected to High Temperatures*, Department of Civil Engineering, Faculty of Engineering, Rajamangala University of Technology, Thailand, Received 18 April 2011, Accepted 28 September 2011.

Kattan, P. I., *Matlab Guide to Finite Elements*, Springer, 2008.

Kaya, M., Ranjbar, M., *Finite Element Analysis of an Aircraft Morphing Wing*, 6. 191-196., September 2020.

Lemos, J. V., *Discrete Element Modeling of the Seismic Behavior of Masonry Construction, Reducing the Seismic Vulnerability of Existing Buildings: Assessment and Retrofit*, 10 Feb 2019.

Majdalani, Z., Ajam, M., Mezher, T., *Sustainability in the Construction Industry: A Lebanese Case Study*, 2005.

Mboya, H., Makunza, J., Mwishwa, Y. H. B., *Assessment of Pumice Blocks in Comparison to Cement Sand Blocks and Burnt Blocks 'The Case of Mbeya City – Tanzania*, Journal of Civil Engineering Research and Practice 8, September 2011.

Meyer, C., Prodigue, J., Broux, G., Cantinaud, O., Poussot-Vassal, C. *Ground test for vibration control demonstrator.* Journal of Physics: Conference Series. 744. 012004,2016.

Özdemir, M., H., Özkan, G. *Understanding Defense Industry: A Systems Thinking Perspective,* Received on: 12 May 2021, Accepted on: 17 October 2021.

Pal, van der, M. *Radon Transport in Autoclaved Aerated Concrete,* Technische Universiteit Eindhoven, 2004.

Reddy, J. N., *Introduction to the finite element method,* McGraw-Hill Education, 3th Edition, 2019.

Reshmy, R., Thomas, D., Philip, E.et al., *Bioplastic production from renewable lignocellulosic feedstocks: a review*. Rev Environ Sci Biotechnol 20, pp. 167–187, 2021.

Souza, D., M., Lafontaine, M., Charron-Doucet, F., Chappert, B., Kicak, K., Duarte, F., Lima, L., *Comparative life cycle assessment of ceramic brick, concrete brick, and cast-in-place reinforced concrete exterior walls,* Journal of Cleaner Production, Volume 137, pp. 70-82, 2016.

Seo, S. Y., Jeon, S. M., Kim, K. T., Kuroki, M., Kikuchi, K., *Compression Behavior of Form Block Walls Corresponding to the Strength of Block and Grout Concrete,* International Journal of Concrete Structures and Materials 9, pp. 21-33, 2015.

Simmons, S., Simmons, G. *Modular Building Materials,* Patent No: US6088987, 2000.

Smyrou, E., *Kuşatılmış yığma yapıların deprem davranışı: 2011 Van depremi örneği,* İstanbul, Aralık, 2016.

Sofiah, S., Yuniar,M. A., Melianti, *Mechanical Properties of Bioplastics Product from Musa Paradisica Formatypica Concentrate with Plasticizer Variables*, Journal of Physics: Conference Series,v.1167, pp. 012-048, Palembang, Indonesia, 2018.

Tomaževič, M., Gams, M., *Shaking Table Study and Modelling of Seismic Behavior of Confined AAC Masonry Buildings, Bulletin of Earthquake Engineering,* The Physical Properties of Standard Concrete Masonry Units, 2011.

Wu, X., Shen, G., Gui, X., Ling, Z., Chen, W., *Experimental and analytical behavior of a new type of concrete-filled steel tube tied-arch bridge with trough girder,* 87. 256-267. 10.1002/stab.201810575, Stahlbau, 2018.

Xia, Q., Chaoji, C., Yao, Y., Li, J., He, S., Zhou, Y., Li, T., Pan, X., Yao, Y., Hu, L., A *Strong, Biodegradable and Recyclable Lignocellulosic Bioplastic, Nature Sustainability*. 4. 10.1038/s41893-021-00702-w., 2021.

Yang, J., Chee Ching, Y., Hock Chuah, C., *Applications of Lignocellulosic Fibers and Lignin in Bioplastics, Department of Chemical Engineering*, Faculty of Engineering, University of Malaya, Received on 4 March 2019; Accepted on 6 April 2019; Published: 28 April 2019.

Yılmaz, M., Bakış, A., *Sustainability in Construction Sector, Procedia - Social and behavioral sciences,* Elsevier,v.195, pp. 2253-2262, 2015.

Zabihi, H., Habib, F., Mirsaeedie, L., *Sustainability in Building and Construction: Revising Definitions and Concepts, International Journal of Emerging Science,* pp.570-578, December 2012.

Zimmermann, T., Krawtschuk, A., Strauss, A., Wan-Wendner, R., *Extreme value statistics for the life-cycle assessment of masonry arch bridges,* 941-947. 10.1201/b12352-130, 2012.

Zuhairi, A.H., Ahmed, A. R., *Height-to-Length Ratio Effect on the Response of Unreinforced Masonry Wall Subjected to Vertical Load Using Detailed-Micro Modeling Approach,* International Journal of Science and Research, Volume 7, Issue 1, January 2018.

Internet Sources:

Url-1: https://www.researchgate.net/post/Is_concrete_block_bricks_eco-friendly

Url-2: https://www.hmswashing.com/4-reasons-why-you-must-let-go-of-pumice-now

Url-3: https://media.marshalls.co.uk/image/upload/v1611237240/Environmental-Characteristics.

Url-4: all.biz/tr-tr/gaz-beton-g96891

Url-5: http://www.atekin.com.tr/insaat-malzemesi/bims--tugla-grubu

Url-6: https://www.goudsmit.co.uk/the-benefits-of-finite-element-analysis-fea-in-manufacturing/#:~:text=FEA%20enables%20an%20immediate%20increase,separate%2C%20but%20connected%2C%20piece.

Url-7: https://resources.sw.siemens.com/fr-FR/case-study-obermeyer-nx

Url-8: http://www.homeradontest.com/how_dangerous_is_radon_in_home.php So Just How Dangerous is Radon Gas in Your Home.

Url-9: https://www.epa.gov/radiation/what-radon-gas-it-dangerous "United States Environment Protection Agency, What is radon gas? Is it dangerous?", Access date: 25.11.2020.

Url-10: https://www.civilconcept.com/aac-blocks-specifications/

Url-11: https://omnexus.specialchem.com/selection-guide/acrylonitrile-butadiene-styrene-abs-plastic, Access date: 12.04.2023.

Url-12: https://omnexus.specialchem.com/techlibrary/article/lignocellulosic-biomass-derived-bioproducts-bioplasticsBelénMonje Martínez –Aug. 5, 2021

Url-13: www.ytong.com YTONG Pendik Factory General Manager, Ytong Performance Declaration, Access date:20.11.2020

Url-14: https://msestudent.com/stress-strain-and-the-stress-strain-curve/